NUREG/CR-6426
ORNL-6892
Vol. 1

Ductile Fracture Toughness of Modified A 302 Grade B Plate Materials, Data Analysis

RECEIVED
FEB 18 1997
OSTI

Prepared by
D. E. McCabe, E. T. Manneschmidt, R. L. Swain

Oak Ridge National Laboratory

Prepared for
U.S. Nuclear Regulatory Commission

MASTER

DISTRIBUTION OF THIS DOCUMENT IS UNLIMITED

AVAILABILITY NOTICE

Availability of Reference Materials Cited in NRC Publications

Most documents cited in NRC publications will be available from one of the following sources:

1. The NRC Public Document Room, 2120 L Street, NW., Lower Level, Washington, DC 20555-0001

2. The Superintendent of Documents, U.S. Government Printing Office, P. O. Box 37082, Washington, DC 20402-9328

3. The National Technical Information Service, Springfield, VA 22161-0002

Although the listing that follows represents the majority of documents cited in NRC publications, it is not intended to be exhaustive.

Referenced documents available for inspection and copying for a fee from the NRC Public Document Room include NRC correspondence and internal NRC memoranda; NRC bulletins, circulars, information notices, inspection and investigation notices; licensee event reports; vendor reports and correspondence; Commission papers; and applicant and licensee documents and correspondence.

The following documents in the NUREG series are available for purchase from the Government Printing Office: formal NRC staff and contractor reports, NRC-sponsored conference proceedings, international agreement reports, grantee reports, and NRC booklets and brochures. Also available are regulatory guides, NRC regulations in the *Code of Federal Regulations*, and *Nuclear Regulatory Commission Issuances*.

Documents available from the National Technical Information Service include NUREG-series reports and technical reports prepared by other Federal agencies and reports prepared by the Atomic Energy Commission, forerunner agency to the Nuclear Regulatory Commission.

Documents available from public and special technical libraries include all open literature items, such as books, journal articles, and transactions. *Federal Register* notices, Federal and State legislation, and congressional reports can usually be obtained from these libraries.

Documents such as theses, dissertations, foreign reports and translations, and non-NRC conference proceedings are available for purchase from the organization sponsoring the publication cited.

Single copies of NRC draft reports are available free, to the extent of supply, upon written request to the Office of Administration, Distribution and Mail Services Section, U.S. Nuclear Regulatory Commission, Washington, DC 20555-0001.

Copies of industry codes and standards used in a substantive manner in the NRC regulatory process are maintained at the NRC Library, Two White Flint North, 11545 Rockville Pike, Rockville, MD 20852-2738, for use by the public. Codes and standards are usually copyrighted and may be purchased from the originating organization or, if they are American National Standards, from the American National Standards Institute, 1430 Broadway, New York, NY 10018-3308.

DISCLAIMER NOTICE

This report was prepared as an account of work sponsored by an agency of the United States Government. Neither the United States Government nor any agency thereof, nor any of their employees, makes any warranty, expressed or implied, or assumes any legal liability or responsibility for any third party's use, or the results of such use, of any information, apparatus, product, or process disclosed in this report, or represents that its use by such third party would not infringe privately owned rights.

NUREG/CR-6426
ORNL-6892
Vol. 1

Ductile Fracture Toughness of Modified A 302 Grade B Plate Materials, Data Analysis

Manuscript Completed: September 1996
Date Published: January 1997

Prepared by
D. E. McCabe, E. T. Manneschmidt, R. L. Swain

Oak Ridge National Laboratory
Managed by Lockheed Martin Energy Research Corporation

Oak Ridge National Laboratory
Oak Ridge, TN 37831-6285

S. N. M. Malik, NRC Project Manager

MASTER

DISTRIBUTION OF THIS DOCUMENT IS UNLIMITED

Prepared for
Division of Engineering Technology
Office of Nuclear Regulatory Research
U.S. Nuclear Regulatory Commission
Washington, DC 20555-0001
NRC Job Code B0119

DISCLAIMER

Portions of this document may be illegible in electronic image products. Images are produced from the best available original document.

Abstract

The objective of this work was to develop ductile fracture toughness data in the form of J-R curves for modified A 302 grade B plate materials typical of those used in fabricating reactor pressure vessels. A previous experimental study at Materials Engineering Associates (MEA), Lanham, Maryland, on one particular heat of A 302 grade B plate showed decreasing J-R curves with increased specimen thickness. This characteristic has not been observed in numerous tests made on the more recent production materials of A 533 grade B and A 508 class 2 pressure vessel steels. It was unknown if the departure from norm for the MEA material was a generic characteristic for all heats of A 302 grade B steels or just unique to that one particular plate.

Seven heats of modified A 302 grade B steel and one heat of vintage A 533 grade B steel were provided to this project by the General Electric Company of San Jose, California. All plates were tested for chemical content, tensile properties, Charpy transition temperature curves, drop-weight nil-ductility transition (NDT) temperature, and J-R curves. Tensile tests were made in the three principal orientations and at four temperatures, ranging from room temperature to 550°F (288°C). Charpy V-notch transition temperature curves were obtained in longitudinal, transverse, and short transverse orientations. J-R curves were made using four specimen sizes (1/2T, 1T, 2T, and 4T). The fracture mechanics-based evaluation method covered three test orientations and three test temperatures [180, 400, and 550°F (82, 204, and 288°C)]. However, the coverage of these variables was contingent upon the amount of material provided. Drop-weight NDT temperature was determined for the T-L orientation only.

None of the seven heats of modified A 302 grade B showed size effects of any consequence on the J-R curve behavior. Crack orientation effects were present, but none were severe enough to be reported as atypical. A test temperature increase from 180 to 550°F (82 to 288°C) produced the usual loss in J-R curve fracture toughness. Generic J-R curves and mathematical curve fits to the same were generated to represent each heat of material.

This volume (Vol. 1) deals with the evaluation of data and the discussion of technical findings. Volume 2 is a compilation of all data developed.

Contents

Page

Abstract iii

Figures vii

Tables viii

Acknowledgments ix

1. Introduction 1

2. Material Characterization 9

3. Fracture Mechanics Data 15

4. J-R Curve Characteristics of Seven Heats of Modified A 302 Grade B Steel 17
   - 4.1 Size Effects 17
   - 4.2 Orientation Effects 17
   - 4.3 Test Temperature Effects 17

5. Comment on Available Test Standards 25

6. Material Variability 29

7. Conclusions 33

8. References 35

Appendix A: Selected J-R Curves Representing Typical Values of T Slope, $J_{0.1}$, and J_{Ic} from Table 7 ..... A-1

Appendix B: Selected J-R Curves Representing Typical Values of T Slope, $J_{0.1}$, and J_{Ic} from Table 8 ..... B-1

Figures

Page

1 J-R curve for two 1T compact specimens tested at 180°F (82°C), showing J-integral by deformation theory J and modified J. *Source*: A. L. Hiser and J. B. Terrell, Material Engineering Associates, Inc., Lanham, Md., *Size Effects on J-R Curves for A302-B Plate*, USNRC Report NUREG/CR-6265 (MEA-2320), January 1989 2

2 J-R curve for one 6T compact specimen tested at 180°F (82°C), showing J-integral by modified J. *Source*: A. L. Hiser and J. B. Terrell, Material Engineering Associates, Inc., Lanham, Md., *Size Effects on J-R Curves for A302-B Plate*, USNRC Report NUREG/CR-6265 (MEA-2320), January 1989 2

3 General Electric-supplied plates of modified A 302 grade B steel: (*a*) Codes Z1 and Z2, (*b*) Codes Z3 and Z4, (*c*) Codes Z5 and Z6, and (*d*) Codes Z7 and Z8 3

4 Schematic of J-R curve plot and measurements taken. Filled data points represent the points used in the power law curve fit 16

5 J-R curves from compact specimens of varied size for the typical modified A 302 grade B steel versus the Materials Engineering Associates plate V50 of A 302 grade B steel 19

6 Load-displacement record of 1/2T compact specimen tested at 180°F (82°C), showing no evidence of pop-in 22

7 Load-displacement record of 1/2T compact specimen tested at 400°F (204°C), showing no evidence of pop-in 23

8 Load-displacement record of 1/2T compact specimen tested at 550°F (288°C), showing a hint of minor instability advances that can be disregarded 23

9 Load-displacement record of 2T compact specimen tested at 180°F (82°C), an upper-shelf temperature with no evidence of pop-in 24

10 Load-displacement record of 2T compact specimen tested at 550°F (288°C), showing clear evidence of pop-in behavior at upper-shelf temperature 24

11 Comparison of the first American Society for Testing and Materials test standard on J_{Ic} in 1981 to the first revision made in 1989 26

12 The 1996 American Society for Testing and Materials method (combined standard): (*a*) third-order polynomial fit and (*b*) adjusted J_R-Δa data to the origin at the known initial physical crack size of the specimen 26

13 Comparison of the 1989 American Society for Testing and Materials J_{Ic} test method revision to the newly proposed 1996 version 27

14 Data scatter of J_{Ic} due to material variability 29

15 Typical J-R curve for comparison to the duplicate test shown in Figure 16 30

16 Typical J-R curve for comparison to the duplicate test shown in Figure 15 30

17 Data scatter of $J_{0.1}$ due to material variability 31

Page

18 J-R curves for modified A302 grade B plates, one vintage A533 grade B class 1 plate (Z8) and a Materials Engineering Associates plate of A302 grade B (V50). Tensile properties and corresponding Charpy V-notch impact upper-shelf energies (ft-lb) are also shown 31

Tables

1 Fracture toughness of modified A 302 grade B – test matrix 7

2 Modified A 302 grade B test materials, heat code, and chemistries 10

3 Tensile properties for seven heats of modified A 302 grade B (Z1-Z7) and one vintage heat of A 533 grade B material (Z8) 11

4 Reference temperature determinations 12

5 Charpy V-notch values for material transition temperature and upper-shelf evaluation 13

6 Evaluation of specimen size on J-R curves of modified A 302 grade B steel [averaged values; T-L (transverse) orientation and 180°F (82°C); all specimens 20% side grooved] 18

7 Directionality of J-R curve fracture toughness at 180°F (averaged values over all specimen sizes; all specimens 20% side grooved) 20

8 Test temperature effect on J-R curve [averaged values over all specimen sizes; T-L (transverse) orientation; all specimens 20% side grooved] 21

Acknowledgments

The authors would like to thank Shah M. Malik, Edwin M. Hackett, and Allen L. Hiser of the U.S. Nuclear Regulatory Commission for their helpful comments in the planning stages of this project. Also, the advice of John G. Merkle of the Engineering Technology Division was invaluable in the planning work. John J. Henry, Jr., of the Fracture Mechanics Group assisted in this work in many ways, and his contribution is hereby acknowledged. We especially acknowledge Tom Caine of General Electric Nuclear Energy, who was instrumental in providing all the steel plates tested in this project. Thanks also to John G. Merkle and Mikhail A. Sokolov for peer review, to Julia L. Bishop for preparation of the manuscript, and to Kathy Spence for editing and quality assurance review.

Ductile Fracture Toughness of Modified A 302 Grade B Plate Materials, Data Analysis*

D. E. McCabe, E. T. Manneschmidt, and R. L. Swain

1. Introduction

Type A 302 plates of pressure vessel steel are currently in service in about 19 nuclear reactor vessels.[1] Of these, eight are grade B, ten are modified grade B, and one is grade A. Type A 302 is an early production version of pressure vessel steel that predates the development of fracture mechanics to a level such that could be applied to ordinary structural steels. Consequently, very little fracture mechanics data have been generated for evaluating the reactor vessels mentioned above. Currently, several reactor vessels are approaching the end of design life, and generic background information is needed to assist with end-of-life and life-extension considerations. This project was initiated to fill this information void by developing J-R curves and the few single-value parameters that can be derived from J-R curves.

A fracture mechanics-based toughness evaluation had been made recently at Materials Engineering Associates (MEA), Lanham, Maryland, that characterized one pedigreed plate of A 302 grade B steel, and these results have at times been used to represent generic A 302 grade B performance for in-service evaluations.[2] The plate was known to have received minimal cross rolling in production, and it was purposely selected for the MEA study because of its low upper-shelf (LUS) fracture toughness in the T-L (transverse) orientation. The plate had typical A 302 grade B chemistry, with the exception that sulfur and vanadium were a little on the high side. It had received the heat treatment that is normally used on production A 302 grade B plate. The Charpy V-notch (CVN) upper-shelf energy (USE) in the T-L orientation was about 48 ft-lb and about 108 ft-lb in the L-T (longitudinal) orientation.[3] The expectation in the MEA experiment was that because of the low toughness, the material would not show J-R curve reduction in 1/2T compact specimens. Compact specimens were made of 1/2T, 1T, 2T, 4T, and 6T sizes. The testing was confined to one orientation (T-L) and one test temperature [180°F (82°C)]. Prior to this experiment, the typical J-R curve behavior of steels of more recent production, such as A 533 grade B and A 508 class 2, showed no differences due to specimen size, with the possible exception of 1/2T-size compacts that tended to show slightly lower J-R curves, viz., conservative results. Unfortunately, the MEA experiment on A 302 grade B plate showed just the opposite behavior. Both 1/2T and 1T compact specimens showed reasonable J-R curve development comparable to other LUS steels (see Figure 1). On the other hand, the toughness degenerated with increased size to essentially no crack growth resistance increase beyond crack initiation in 6T-size compacts (see Figure 2). Hence, the suggestion is that J-R curves obtained from 1/2T compacts could not be used to represent A 302 grade B generically. This pattern reversal presently stands alone as the characterization of the J-R curve behavior of A 302 steels.

An objective of this experiment was to generate more generic J-R curve data, except in this case, the material chosen was the more frequently used modified A 302 grade B steel. Seven heats of modified A 302 grade B plate were donated to this investigation by General Electric Company of San Jose, California. All were archival materials that were being saved for possible future tests, as needed, for fracture toughness verification purposes. All represent typical production cross-rolling practices. An add-on to the material selection was one early vintage A 533 grade B plate identified as Z8 in Figure 3*(d)*. The pieces sampled are shown in Figures 3*(a)* through *(d)*, with the segments supplied to this project marked either as Oak Ridge National Laboratory (ORNL) or MEA.

The test matrix design for J-R curve development encompassed four levels of specimen size, 1/2T, 1T, 2T, and 4T; three levels of test temperature, 180, 400, and 550°F (82, 204, and 288°C); and three levels of specimen orientation, T-L, L-T, and L-S (short transverse) [see Table 1]. All conditions were tested in duplicate, except for the

*Research was sponsored by the Office of Nuclear Regulatory Research, Division of Engineering Technology, U.S. Nuclear Regulatory Commission, under Interagency Agreement DOE 1886-8011-9B with the U.S. Department of Energy under Contract DE-AC05-96OR22464 with Lockheed Martin Energy Research Corporation.

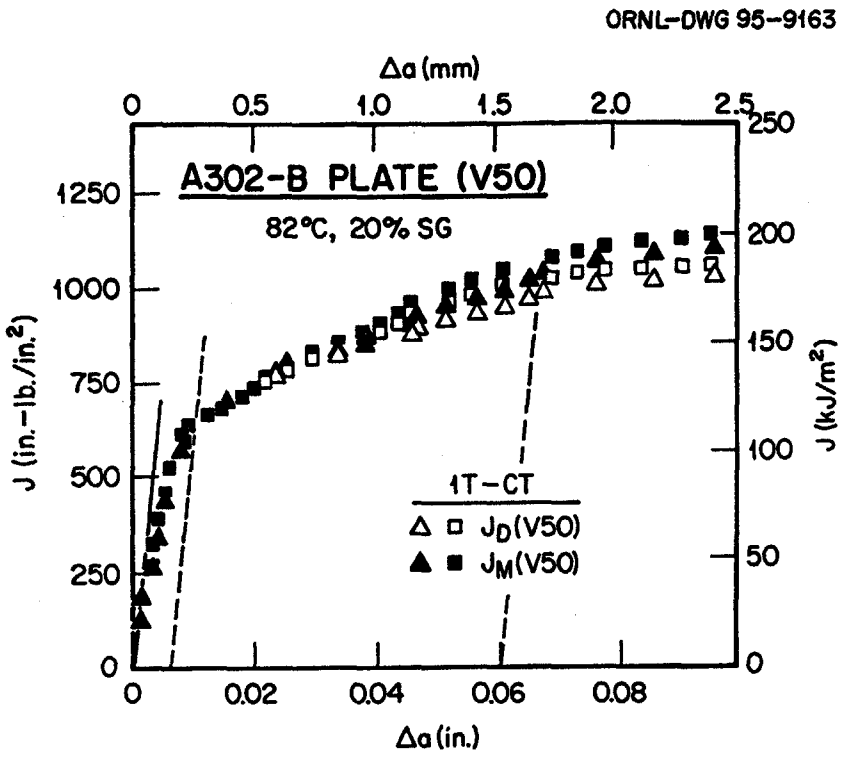

Figure 1. J-R curve for two 1T compact specimens tested at 180°F (82°C), showing J-integral by deformation theory J and modified J. *Source*: A. L. Hiser and J. B. Terrell, Material Engineering Associates, Inc., Lanham, Md., *Size Effects on J-R Curves for A302-B Plate*, USNRC Report NUREG/CR-6265 (MEA-2320), January 1989.

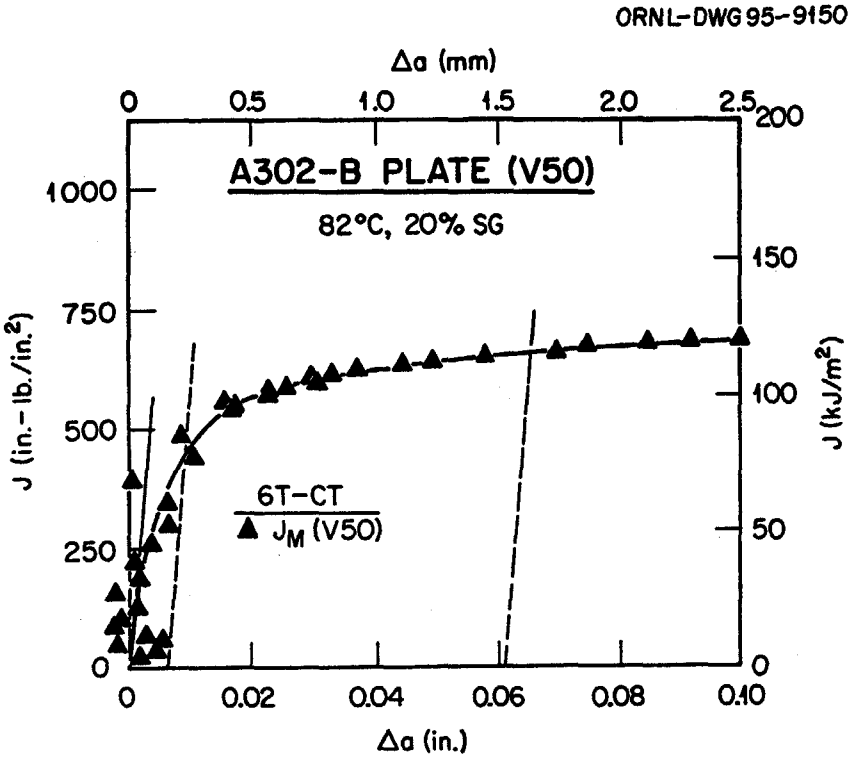

Figure 2. J-R curve for one 6T compact specimen tested at 180°F (82°C), showing J-integral by modified J. *Source*: A. L. Hiser and J. B. Terrell, Material Engineering Associates, Inc., Lanham, Md., *Size Effects on J-R Curves for A302-B Plate*, USNRC Report NUREG/CR-6265 (MEA-2320), January 1989.

ORNL-DWG 94-12243

TEST PLATE CUTTING

B3990-2

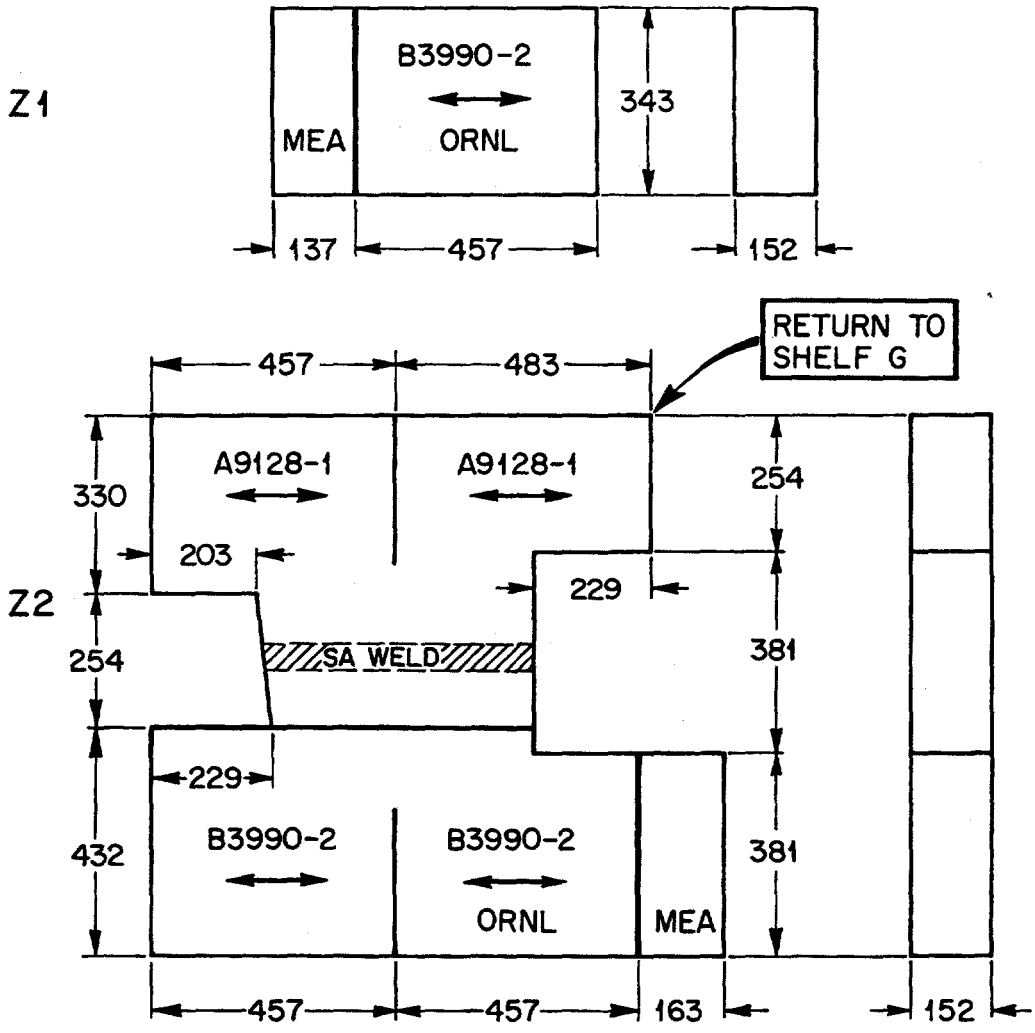

(a)

NOTES:

1. ALL DIMENSIONS ARE IN MILLIMETERS
2. ALL EDGES ASSUMED BURNED

Figure 3. General Electric-supplied plates of modified A 302 grade B steel: (*a*) Codes Z1 and Z2, (*b*) Codes Z3 and Z4, (*c*) Codes Z5 and Z6, and (*d*) Codes Z7 and Z8.

ORNL-DWG 94-12244

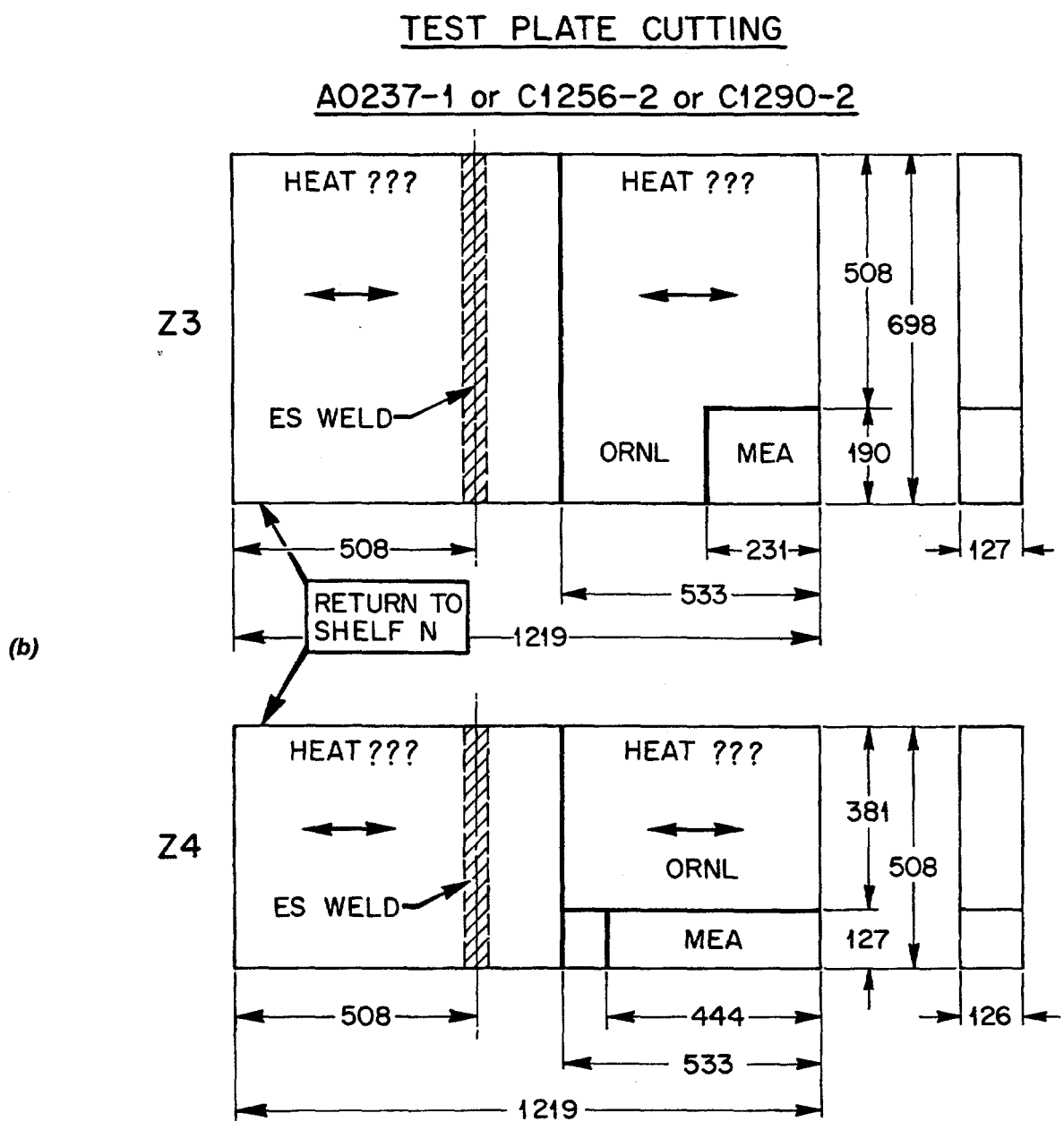

NOTES:

1. ALL DIMENSIONS ARE IN MILLIMETERS
2. ALL EDGES ASSUMED BURNED

Figure 3. (Continued)

ORNL-DWG 94-12245

TEST PLATE CUTTING

P2130-2

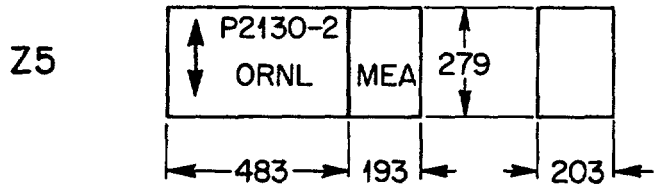

C1079-1 and B5013-2

(c)

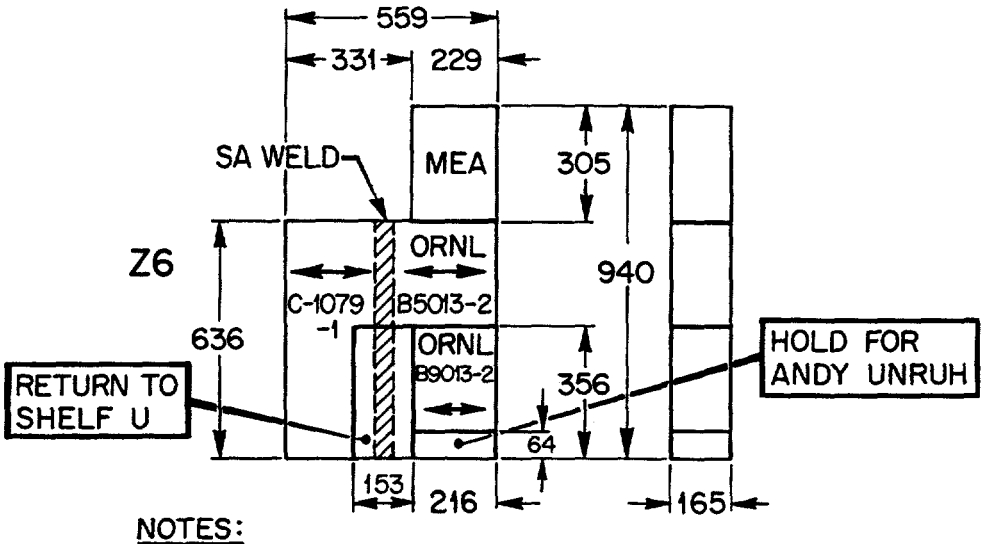

NOTES:

1. ALL DIMENSIONS ARE IN MILLIMETERS
2. EDGES ARE BURN CUT WITH LONG EDGES STAMPED AS QUENCHED EDGES

Figure 3. (Continued)

ORNL-DWG 94-12246

TEST PLATE CUTTING

C2463-1

Z7

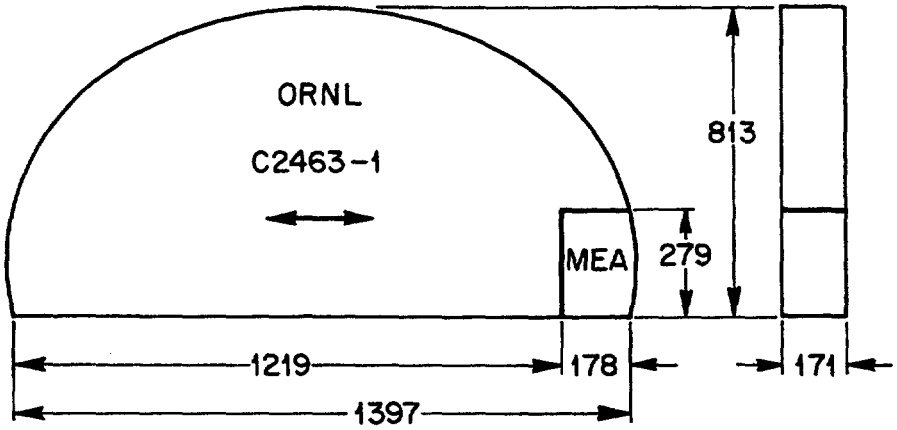

(d)

C2220-2

Z8

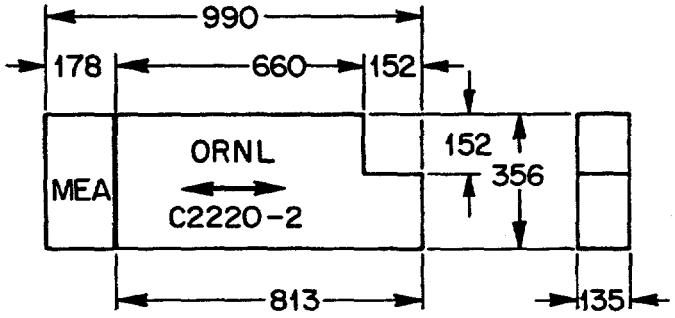

NOTES:

1. ALL DIMENSIONS ARE IN MILLIMETERS
2. ALL EDGES ASSUMED BURNED

Figure 3. (Continued)

Table 1. Fracture toughness of modified A 302 grade B – test matrix

Specimen size	Plate code	Test temperatures (°F)	Orientation[a]	Duplicates	Number of specimens per plate
1/2T C(T)	Z1, Z2	180, 400, 550	T-L, L-S	2	12
	Z3	180, 400, 550	T-L, L-S	2	12
	Z4	180, 400, 550	T-L, L-S	2	12
	Z5	180, 400, 550	T-L, L-S	2	12
	Z6A	180, 400, 550	T-L, L-S	2	12
	Z6B	180, 400, 550	T-L, L-S	2	12
	Z7	180, 400, 550	T-L, L-S	2	12
	Z8	180, 400, 550	T-L, L-S	2	12
Total					96
1T C(T)	Z2	180, 400, 550	T-L, L-S	2	12
	Z3	180, 550	T-L, L-S	2	8
	Z5	180, 550	L-T	2	4
	Z6A	180, 550	T-L, L-S	2	8
	Z6B	180, 550	T-L, L-S	2	8
	Z7	180, 400, 550	T-L, L-S	2	12
Total					52
2T C(T)	Z1	550	T-L, L-T	2	4
	Z2	180, 400	T-L, L-S	2	8
	Z3	180, 550	T-L, L-S, L-T	2	8
	Z4	180, 550	T-L, L-S	2	8
	Z5	180, 550	T-L, L-S	2	8
	Z6A	180, 550	T-L, L-S	2	8
	Z6B	550	T-L, L-S, L-T	2	6
	Z7	180, 400, 550	T-L, L-S, L-T	2	16
	Z8	180, 550	T-L, L-S	2	8
Total					74
4T C(T)	Z2	180, 550	T-L	2	2
	Z3	180	T-L	1	1
	Z4	180	T-L	1	1
	Z7	180, 550	T-L, L-T	3	6
	Z8	180	T-L	1	1
Total					11
Charpy	Z1	*b*	T-L, L-S, L-T	14	42
	Z3	*b*	T-L, L-S, L-T	15	45
	Z4	*b*	T-L, L-S	14	28
	Z5	*b*	T-L, L-S, L-T	14	42
	Z6	*b*	T-L, L-S, L-T	15	45
	Z7	*b*	T-L, L-S, L-T	15	45
	Z8	*b*	T-L, L-S, L-T	14	42
Total					289

[a]T-L = transverse, L-T = longitudinal, and L-S = short transverse.
[b]A full ductile-brittle transition curve to be developed.

4T compact specimens, because of the limited amount of material available. The sampling plan was designed to maximize the information production out of the available materials. Material baseline characterization on all materials included chemical compositions, CVN curves, drop-weight nil-ductility transition (NDT), and tensile tests in the three principal orientations.

2. Material Characterization

The chemical composition of each heat was determined by ABB Combustion Engineering of Chattanooga, Tennessee. The results are presented in Table 2. Plate Z6B had sulfur comparable to the MEA plate, and the vanadium in all heats was about one-sixth of that in the MEA plate. Material chemistry does not appear to be a significant variable in this experiment.

Table 3 has tensile properties that cover the range of orientations and test temperatures of relevance to the J-R curve determinations. The symbols T, L, and S_T represent transverse, longitudinal, and short transverse orientations, respectively. Note that there is a slight reversal in strength loss with increasing test temperature between 400 and 550°F (204 to 288°C). Such behavior could be indicative of dynamic strain aging. Elongation measured in the short transverse orientation indicates that there might be a crack path of low toughness that develops at 550°F (288°C), one that has not been investigated in this study. The suggestion here is that the S-L or S-T crack propagation directions could respond differently. On the other hand, neither of these two crack plane orientations is likely to be of relevance in vessel analysis problems.

Tables 4 and 5 contain data for transition temperature characterization. Table 4 gives the type of CVN data that are used for the establishment of reference temperature, RT_{NDT} (ref. 4), in the American Society of Mechanical Engineers (ASME) *Boiler and Pressure Vessel Code*. Drop-weight NDT values are determined, and the CVN property requirements at NDT + 60°F (+33°C) are evaluated, namely CVN energy > 50 ft-lb (68 J) and lateral expansion > 0.035 in. (0.9 mm). If the CVN criteria are met, then RT_{NDT} = NDT. Failure to meet these two criteria at NDT + 60°F requires the use of Charpy transition curves to establish RT_{NDT}. Plates coded Z6B and Z8 had failed the criteria, and the additional conservatism imposed by the alternate code method can be noted. Table 5 gives additional Charpy information in the form of temperatures of 30 and 50 ft-lb, 50% shear, and the Charpy curve USEs. Of the three orientations, the T-L test direction is the one of lowest toughness in every case. The L-T and L-S orientations show better toughness and at times have about the same USE.

Because the material chemical compositions are so close, the differences in toughness observed here are most likely due to differences in the slabbing, cross-rolling, and heat-treatment practices.

Table 2. Modified A 302 grade B test materials, heat code, and chemistries

Plate code	Heat	Composition (wt %)												
		C	Mn	P	S	Si	Ni	Cr	Mo	V	Nb	Co	Cu	Al
Z1, Z2	B3990-2	0.18	1.35	0.007	0.011	0.23	0.47	0.11	0.44	0.003	0.004	0.011	0.17	0.03
Z3	A0237-1[a]	0.24	1.47	0.008	0.014	0.25	0.52	0.11	0.50	0.002	0.003	0.011	0.11	0.026
Z4	C1290-2[a]	0.22	1.42	0.006	0.013	0.24	0.50	0.11	0.48	0.002	0.003	0.011	0.10	0.027
Z5	P2130-2	0.17	1.16	0.013	0.016	0.17	0.60	0.10	0.50	0.002	0.004	0.012	0.16	0.012
Z6A	C1079-1	0.17	1.35	0.006	0.013	0.23	0.49	0.10	0.45	0.002	0.003	0.012	0.18	0.028
Z6B	B5013-2	0.22	1.39	0.009	0.023	0.20	0.51	0.15	0.48	0.002	0.003	0.017	0.21	0.035
Z7	C2463-1	0.26	1.47	0.008	0.014	0.15	0.53	0.09	0.52	0.002	0.003	0.011	0.16	0.017
Z8	C2220-2	0.27	1.49	0.006	0.015	0.23	0.68	0.12	0.45	0.002	0.003	0.012	0.16	0.016

[a]There was some uncertainty in heat identifications. Values were determined by ABB-Combustion Engineering.

Table 3. Tensile properties for seven heats of modified A 302 grade B (Z1-Z7) and one vintage heat of A 533 grade B material (Z8)

Plate code	Test temperature (°F)	Yield strength[a] (ksi)			Ultimate strength[a] (ksi)			Elongation (%)		
		T	L	S_T	T	L	S_T	T	L	S_T
Z1	75	65.2	64.0	64.2	84.5	84.7	80.1	25.5	25.0	13.5
	180	62.4	64.2	58.1	80.7	80.8	79.0	22.5	23.0	17, 7[b]
	400	57.0	58.8	57.7	79.3	79.7	72.2	21.0	21.5	15, 8[b]
	550	60.3	60.1	58.9	84.8	84.0	57.0	24.5	24.0	8
Z3	75	67.9	67.8	67.0	89.7	90.0	89.3	23.0	27.5	16.5
	180	64.8	64.4	64.0	85.2	85.2	84.7	21.5	23.5	15.0
	400	59.8	59.5	52.9	84.9	84.2	80.5	20.5	23.0	11.0
	550	61.7	61.0	62.2	88.2	89.0	88.3	25.0	25.5	15.0
Z4	75	67.8	68.1	66.5	89.2	89.8	88.2	25.0	24.5	21.5
	180	63.8	64.4	63.5	83.9	84.7	83.6	22.5	23.5	20.5
	400	60.3	*c*	*c*	83.3	*c*	*c*	22.0	*c*	*c*
	550	61.2	61.0	60.4	88.0	87.9	87.1	24.0	26.0	20.0
Z5	75	58.1		55.2	78.1		72.0	24.5		17.5
	180	55.6		52.8	74.4		68.6	22.4		13.5
	400	53.8		49.0	75.8		68.5	21.5		13.0
	550	54.2		49.6	79.8		74.1	23.4		11.5
Z6A	75	61.8	63.7	57.6	81.0	82.4	62.5	28.5	28.0	7.5
	180	57.9	59.1	58.4	70.8	77.0	61.5	16.0	25.0	4.5
	400	55.0	55.6	55.7	76.2	75.8	74.9	21.0	23.5	12.5
	550	55.8	57.7	57.5	81.2	84.0	76.8	21.5	22.0	12.0
Z6B	75	64.9	68.8	62.6	86.3	89.1	77.9	24.5	28.0	9.5
	180	64.5	63.2	61.0	83.6	82.3	78.0	20.5	24.0	11.0
	400	59.3	59.8	57.5	83.7	83.4	69.0	20.5	22.5	4.5
	550	60.7	61.5	60.7	86.2	87.2	64.7	21.5	24.0	5.0
Z7	75	68.5	69.1	68.2	91.7	92.5	92.2	24.5	23.5	17.5
	180	65.5	66.7	66.7	86.7	87.7	87.7	22.5	23.5	17.0
	400	60.1	60.3	61.4	85.6	86.0	86.2	21.5	22.5	13.0
	550	62.3	63.6	62.3	90.0	91.3	90.6	23.4	26.0	11.5
Z8	75	61.9	63.1	61.6	88.2	88.9	87.2	23.5	26.0	17.5
	180	59.8	59.2	58.4	83.4	82.5	81.5	22.5	24.0	17.0
	400	56.7	54.7	55.8	82.7	80.2	80.0	21.0	23.0	14.5
	550	58.0	57.4	54.6	88.2	87.2	84.6	22.5	26.5	11.5

[a]MPa = (ksi) × 6.894.
[b]Unaveraged values.
[c]Omitted because of questionable results.

Table 4. Reference temperature determinations

Plate code	NDT[a] temperature		Charpy properties at NDT[a] + 60°F, T-L (transverse) orientation				RT_{NDT}[b]	
			Energy		Lateral expansion			
	(°F)	(°C)	(ft-lb)	(J)	(in.)	(mm)	(°F)	(°C)
Z1, Z2	–5	–20	93	127	0.063	1.6	–5	–20
Z3	–15	–26	60	82	0.046	1.2	–15	–26
Z4	–15	–26	64	88	0.058	1.5	–15	–26
Z5	–30	–34	56	77	0.048	1.2	–30	–34
Z6A	–30	–34	65	89	0.052	1.3	–30	–34
Z6B	–30	–34	38	52	0.034	0.9	13[c]	–10
Z7	–15	–26	64	88	0.056	1.4	–15	–26
Z8	–20	–29	33	45	0.038	1.0	24[c]	–4

[a]NDT = nil-ductility-transition temperature.
[b]RT_{NDT} = reference nil-ductility-transition temperature.
[c]Determined from Charpy V-notch 50-ft-lb (lower-bound) temperature – 60°F.

Table 5. Charpy V-notch values for material transition temperature and upper-shelf evaluation

Plate code	Orientation[a]	Temperature, °F (°C)						RT_{NDT}[b]		Upper-shelf energy	
		30 ft-lb		50 ft-lb		50% shear		(°F)	(°C)	(ft-lb)	(J)
Z1, Z2	T-L	–33	(–36)	–4	(–20)	25	(–4)	–5	–20	126	173
	L-T	–45	(–43)	–20	(–29)	10	(–12)			160	219
	L-S	–19	(–28)	8	(–13)	30	(–1)			171	234
Z3	T-L	0	(–18)	33	(0)	35	(2)	–15	–26	85	116
	L-T	–37	(–38)	–9	(–23)	25	(–4)			129	177
	L-S	–16	(–27)	21	(–6)	55	(13)			127	174
Z4	T-L	–38	(–39)	11	(–12)	30	(–1)	–15	–26	111	152
	L-S	–56	(–49)	–17	(–27)	35	(2)			130	178
Z5	T-L	–19	(–28)	18	(–8)	20	(–7)	–30	–34	95	130
	L-T	–30	(–34)	–2	(–19)	25	(–4)			153	209
	L-S	–59	(–50)	–41	(–40)	–1	(–23)			171	234
						0					
Z6A	T-L	–17	(–27)	11	(–12)	40	(4.4)	–30	–34	113	155
	L-T	–28	(–33)	–2	(–19)	25	(–4)			129	177
	L-S	–41	(–40)	–10	(–23)	35	(2)			130	178
Z6B	T-L	11	(–12)	60	(16)	40	(4.4)	13	–10	64	88
	L-T	–33	(–36)	–1	(–18)	5	(–15)			117	160
	L-S	–32	(–36)	–5	(–20)	10	(–12)			114	156
Z7	T-L	–21	(–29)	19	(–7)	5	(–15)	–15	–26	96	131
	L-T	–45	(–43)	–12	(–24)	10	(–12)			126	173
	L-S	–50	(–46)	–20	(–29)	0	(–18)			120	164
Z8	T-L	27	(–3)	72	(22)	30	(–1)	24	–4.4	96	131
	L-T	25	(–4)	48	(9)	65	(18)			134	184
	L-S	–5	(–20)	29	(–2)	55	(13)			154	211

[a]T-L = transverse, L-T = longitudinal, and L-S = short transverse.
[b]RT_{NDT} = reference nil-ductility-transition temperature.

3. Fracture Mechanics Data

The test matrix introduced in Table 1 contains about 230 compact specimens for J-R curve tests. The results of each test were carefully evaluated, and any data judged questionable or that might have had a possible orientation identification error will not be reported or used in the present data analysis. Such cases were few and, for the most part, were outside the realm of control of these investigators. Volume 2 will log every test conducted, and all resulting test data, so that both good and questionable data will be available for further use as needed.

Material crack growth resistance is defined by the development rate of J-integral associated with slow-stable crack growth (J-R curves). In this project, crack growth was measured by unloading compliance, following the requirements set forth in American Society for Testing and Materials (ASTM) E 813-87, "Standard Test Method for J_{Ic}, a Measure of Fracture Toughness," and E 1152-89, "Standard Test Method for Determining J-R Curves." J-R curve plots are difficult to compare quantitatively, and it is more convenient to work with single-value parameters that are derived from the J-R curve. One such parameter is the J_{Ic} value, defined as J-integral just after the onset of slow-stable crack growth [after 0.008 in. (0.2 mm) of ductile tearing].[5] The ASTM test practice for J_{Ic} has undergone two revisions since it was first introduced in 1981, and comments on the implication of these revisions on precision and accuracy will be included here as supplementary information. A second single characterization parameter is tearing modulus, T, a dimensionless quantity derived from the J-R curve slope. The third single-value parameter used is the J-integral after 0.1 in. (2.5 mm) of slow-stable crack growth, $J_{0.1}$.

The first-mentioned parameter, J_{Ic}, has been a moving target, undergoing revisions in 1989 and 1995. J_{Ic} was calculated by all three methods, and the 1989 version was chosen as the best of the two new methods for developing material comparisons here. The rationale will be discussed in Sect. 5 of this report. The T-parameter and $J_{0.1}$ J-R curve growth point values are the two material property parameters used in the ASME Code, Sect. XI, Articles K-4220 and K-4331 (ref. 6). It is interesting that the ASTM test methods give no guidance as to how these two design-related parameters are determined. This requires that users of T-modulus and $J_{0.1}$ values must develop their own definitions. Accordingly, for the purposes of this report, the $J_{0.1}$ value will specifically be the J value after 0.1 in. of slow-stable crack growth that includes the blunting line contribution to Δa (see Figure 4). The blunting line contribution is calculated using the following equation:

$$\Delta a = J_{Ic}/(\sigma_{ys} + \sigma_{UTS}) \ . \qquad (1)$$

The T-modulus parameter is defined here as a nondimensional representation of the average J-R curve slope from the J-Δa data that are developed between the two dashed exclusion lines shown. The dashed secant line shown in Figure 4 that extends between the two J-R curve intersection points with the exclusion lines is always close to the average slope determined if a set of tangents were taken along the J-R curve and an average value obtained. Here the secant slope, $(dJ/da)_s$, is used in the following expression:

$$T_{avg} = \frac{E}{\sigma_f^2}\left(\frac{dJ}{da}\right)_s \ . \qquad (2)$$

The value, σ_f, is the denominator in Equation (1) divided by two.

A full J-R curve data plot with extensive growth can be well modeled by an equation of the following form:

$$J = A(\Delta a)^B \exp\left(C/\sqrt{\Delta a}\right) \ . \qquad (3)$$

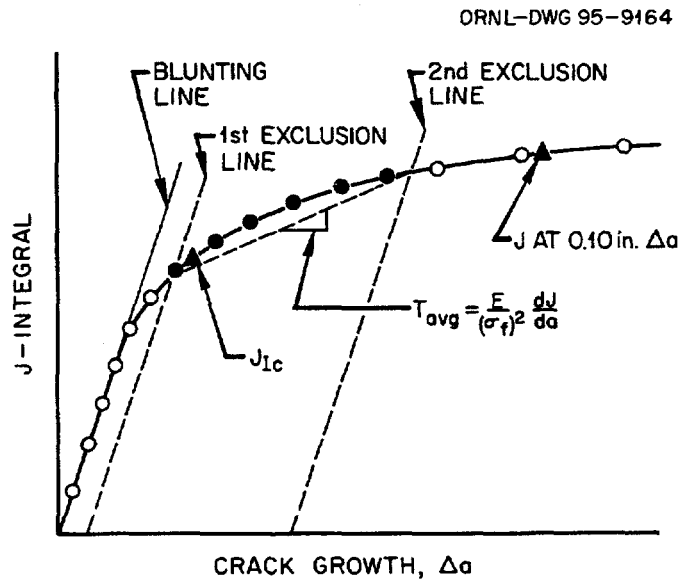

Figure 4. Schematic of J-R curve plot and measurements taken. Filled data points represent the points used in the power law curve fit.

Equation (3) had been introduced by Eason et al. in multivariable modeling of J-R curves for A 533 grade B base metal and various reactor pressure vessel weld metals.[7] In their work they correlate nonfracture mechanics information, such as upper-shelf CVN energy or copper/fluence models, to derive the constants A, B, and C for Equation (3). In this study, Equation (3) is only used to best fit experimentally developed J-R curves, i.e., ones that have been chosen to best represent the materials and test conditions cited in the text matrix.

4. J-R Curve Characteristics of Seven Heats of Modified A 302 Grade B Steel

4.1 Size Effects

Table 6 lists the average T, $J_{0.1}$, and J_{Ic} values from duplicate specimens (single specimens in a few cases) for each specimen size at 180°F (82°C). The same parameters were calculated from the J-R curve plots presented in the MEA report on their plate, V50, of A 302 grade B steel (ref. 2). In that case, only the T-L orientation and one test temperature [180°F (82°C)] had been used to evaluate specimen size effects. Clearly, the MEA result of decreased crack growth resistance with increased specimen size was not reproduced in the modified A 302 grade B materials of this study. In fact, only one heat came close to the low toughness of the MEA V50 plate; this was Z6B and no inversion of size effect between 1/2T to 2T size was shown. Unfortunately, there was not sufficient material of Z6B to make a 4T compact specimen that could have completely settled this size effect issue. On the other hand, plate Z7 was chosen to represent the J-R curve toughness level for the majority of the modified A 302 grade B heats, and the typical J-R curve result is compared to the MEA heat V50 in Figure 5.

A peculiar size effect that can be observed in Figure 5 and in the Table 6 data, however, is that 2T specimens tend to show a slight increased toughness bias in J-R curve performance. One could reasonably doubt this observation if the evidence were available only in terms of J_{Ic} values where high preciseness of compliance-indicated crack growth is needed to determine the minuscule 0.008 in. (0.2 mm) of ductile crack extension. However, the $J_{0.1}$ values are not subject to the high precision need, and the increased toughness behavior in 2T specimens is seen here as well. This J-R curve enhancement is most likely a constraint-based phenomenon, but whether the observation represents increased or decreased constraint remains unproven as of now.

4.2 Orientation Effects

Table 7 shows the crack-plane orientation effect on fracture toughness. The three directions are transverse (T-L), longitudinal (L-T), and short transverse (L-S).[3] Only one test temperature was needed for this evaluation, and because size effects were not particularly overhwelming, the values of T, $J_{0.1}$, and J_{Ic} have been averaged over all specimen sizes. Additional information is presented in the form of Charpy USEs, and the last three columns of Table 7 list the coefficients needed in Equation (3) to generate the one individual specimen J-R curve that is most representative for the given plate and orientation. The choice of J-R curve was made considering the closeness of fit to the averaged T-modulus, $J_{0.1}$, and J_{Ic} values listed. One J-R curve is given for each orientation. The codes for the specimens selected are listed under the column entitled "Fitting curves," and the curves, plus the J-Δa data used, are shown in Appendix A, Figures A1 through A21.

It is not possible to make an all-encompassing statement about directionality effects on toughness for modified A 302 grade B pressure vessel steels because the directionality characteristics are created in the slabbing and cross-rolling practices used by the steel plant. In this experiment, each heat had been marked for the principal rolling direction, and both the Charpy data and J-R curve tests tended to verify these markings. The T-L orientation consistently showed the lowest toughness of the three orientations sampled. Heat code Z3 seemed to give an inconsistent pattern. This same heat is the one which had the most specimens that were subjected to orientation questions needing verification by metallographic methods.

4.3 Test Temperature Effects

Table 8 shows the effect of test temperature on the J-R curve. Again, as with Table 7, the values of T, $J_{0.1}$, and J_{Ic} are averaged over duplicate tests and over all available specimen sizes. The comparison in this case is limited to one orientation, T-L. Representative J-R curves that come the closest to satisfying the averaged T slope, $J_{0.1}$, and J_{Ic} values can be reproduced from the coefficients listed. These curves, and specific J-R curve data used, are shown in Appendix B.

The trend of decreased crack-initiation toughness, J_{Ic}, and J-R curve crack growth resistance with elevated test temperature is typical for all grades of reactor vessel steels. However, something that may have gone unnoticed in other experiments, which has been apparent in these tests, is that crack pop-in events had developed in specimens

Table 6. Evaluation of specimen size on J-R curves of modified A 302 grade B steel [averaged values; T-L (transverse) orientation and 180°F (82°C); all specimens 20% side grooved]

Plate code	Size (T)	T[a]	$J_{0.1}$[b] (in.-lb/in.^{2})	J_{Ic}[c] (in.-lb/in.^{2})
Z1, Z2	1/2	115	3200	1330
	1	130	3410	1360
	2	120	4030	2050
	4	75	2990	1590
Z3	1/2	85	2615	1230
	1	80	2515	1175
	2	115	3055	1095
	4	95	2755	1310
Z4	1/2	105	3050	1360
	2	95	3200	1600
	4	95	2840	1200
Z5	1/2	55	1655	815
	2	50	1825	1080
Z6A	1/2	80	2370	905
	1	85	2535	1065
	2	55	2070	1075
Z6B	1/2	50	1470	715
	1	45	1505	785
	2	35	1430	930
Z7	1/2	80	2600	1290
	1	95	2995	1210
	2	100	3325	1685
	4	125	3120	1270
Z8	1/2	95	2770	1290
	2	85	2525	1160
	4	70	2800	1740
MEA[d] report on plate V50				
p. 58	1/2	36	1293	600
p. 61	1	36	1129	659
p. 66	2	20.4	863	653
p. 70	4	14.3	704	543
p. 74	6	19.4	686	500

[a] $T = E/\sigma_f^2 (dJ/da)_s$.
[b] J at 0.1 in. of slow-stable crack growth.
[c] J after 0.008 in. of slow-stable crack growth.
[d] MEA = Materials Engineering Associates, Lanham, Maryland.

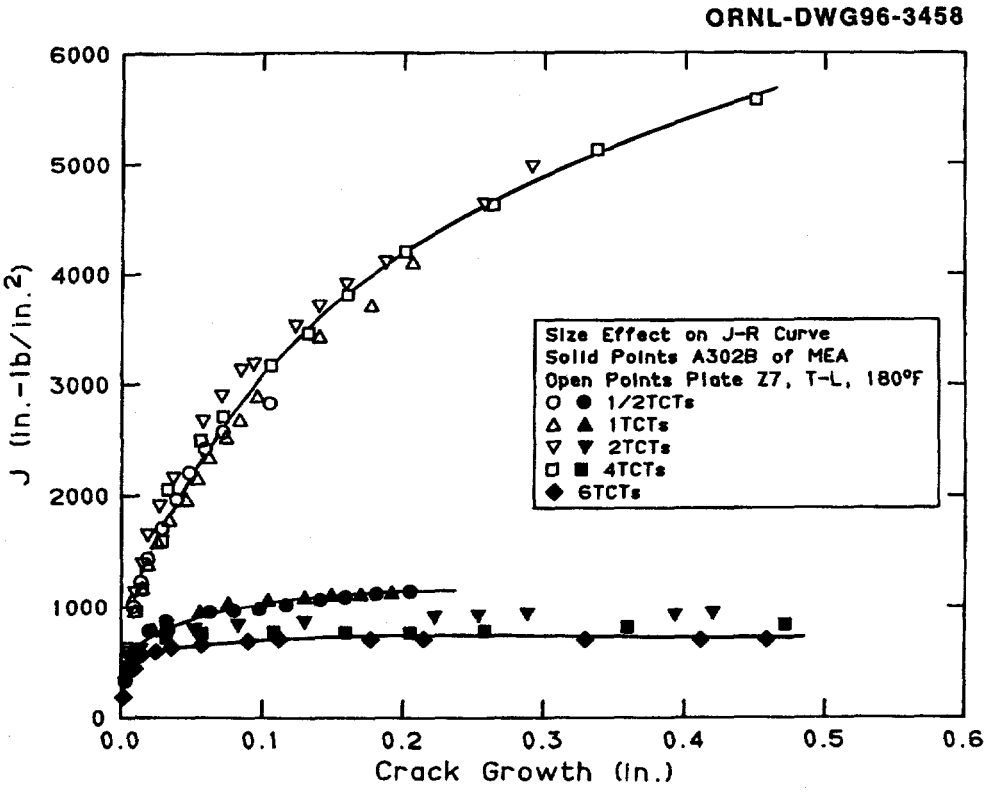

Figure 5. J-R curves from compact specimens of varied size for the typical modified A 302 grade B steel versus the Materials Engineering Associates plate V50 of A 302 grade B steel.

Table 7. Directionality of J-R curve fracture toughness at 180°F (averaged values over all specimen sizes; all specimens 20% side grooved)

Plate code	Orientation[a]	Charpy V-notch upper-shelf energy (ft-lb)	T slope	$J_{0.1}$[b] (in./lb/in.^{2})	J_{Ic}[b] (in./lb/in.^{2})	Fitting curves	$J = A \cdot \Delta a^B \cdot \exp(C/\Delta a^{1/2})$		
							A	B	C
Z1, Z2	T-L	126	120	3300	1350	Z2B2-1T	7.110	0.287	–0.0596
	L-T	160	130	3810	1360	Z2B16-1T	9.513	0.300	–0.0761
	L-S	171	130	3480	1570	Z2B2-1/2T	8.715	0.259	–0.0846
Z3	T-L	85	90	2730	1200	Z310-1/2T	6.030	0.275	–0.0699
	L-T	129							
	L-S	127	70	2000	870	Z34-1/2T	5.633	0.435	–0.0014
Z4	T-L	111	100	3060	1420	Z49-1/2T	6.517	0.226	–0.0368
	L-S	130	130	4080	1880	Z47-2T	13.333	0.446	–0.0246
Z5	T-L	95	45	1630	1075	Z55-2T	3.043	0.177	–0.0329
	L-T	153	90	2640	1225	Z51-1T	6.178	0.318	–0.0348
	L-S	171	160	3895	1195	Z57-1/2T	15.718	0.567	–0.0199
Z6A	T-L	113	75	2325	1040	Z6A8-1T	6.377	0.410	–0.0131
	L-T	129	115	3570	1570	Z6A1-1T	12.299	0.518	–0.0114
	L-S	130	120	3550	1620	Z6A3-1/2T	8.542	0.267	–0.0752
Z6B	T-L	64	45	1470	810	Z6B9-1/2T	2.407	0.100	–0.0790
	L-T	117	70	2360	1130	Z6B1-1T	5.193	0.341	–0.0140
	L-S	114	85	2730	1183	Z6B8-1/2T	1.340	0.079	–0.0235
Z7	T-L	96	95	3000	1250	Z711-1T	8.742	0.446	–0.0279
	L-T	126	140	4500	2120	Z78-1T	12.057	0.383	–0.0501
	L-S	120	145	4405	2045	Z71-1/2T	10.637	0.326	–0.0780
Z8	T-L	96	85	2715	1245	Z83-1/2T	4.963	0.218	–0.0514
	L-T	134							
	L-S	154	145	4190	1860	Z816-1/2T	12.594	0.378	–0.0566

[a]T-L = transverse, L-T = longitudinal, and L-S = short transverse.
[b]To obtain J in units of kPa·m, multiply by 0.175.

Table 8. Test temperature effect on J-R curve [averaged values over all specimen sizes; T-L (transverse) orientation; all specimens 20% side grooved]

Plate code	Temperature (°F)	T slope	$J_{0.1}$[a] (in./lb/in.^{2})	J_{Ic}[a] (in./lb/in.^{2})	Fitting curves	$J = A \cdot \Delta a^B \cdot \exp(C/\Delta a^{1/2})$		
						A	B	C
Z1, Z2	180 400 550	120 70 60	3300 2310 2056	1350 1100 885	Z2B2-1T[b] Z2B11-1/2T Z2B07-1T	7.110 6.022 5.619	0.287 0.362 0.421	–0.0596 –0.0223 –0.0095
Z3	180 400 550	90 80 45	2730 2130 1635	1200 830 830	Z310-1/2T[b] Z311-1/2T Z39-1/2T	6.030 5.713 3.394	0.275 0.362 0.282	–0.0699 –0.0329 –0.0268
Z4	180 400 550	100 80 60	3060 1995 1950	1420 1020 975	Z49-1/2Tb[b] Z416-1/2T Z42-2T	6.517 4.858 3.252	0.226 0.297 0.204	–0.0368 –0.0318 0.0311
Z5	180 400 550	45 40 35	1630 1475 1135	1075 895 585	Z55-2T[b] Z514-1/2T Z512-1/2T	3.043 2.335 2.267	0.177 0.136 0.233	–0.0329 –0.0600 –0.0188
Z6A	180 400 550	75 55 50	2325 1685 1595	1040 805 825	Z6A8-1T[b] Z6A16-1/2T Z6A15-1/2T	6.377 4.490 3.383	0.410 0.343 0.303	–0.0131 –0.0216 –0.0201
Z6B	180 400 550	45 32 24	1470 1175 885	810 665 530	Z6B9-1/2T[b] Z6B11-1/2T Z6B7-1T	2.407 1.801 1.301	0.100 0.150 0.146	–0.0790 –0.0352 –0.0113
Z7	180 400 550	95 60 50	2995 1995 1855	1255 995 790	Z711-1T[b] Z714-1T Z715-1T	8.742 4.220 3.487	0.446 0.340 0.281	–0.0279 –0.0151 –0.0140
Z8	180 400 550	85 65 50	2715 2095 1685	1250 1070 860	Z83-1/2T[b] Z88-1/2T	4.963 3.889	0.218 0.393	–0.0514 0.0124

[a]To obtain J in units of kPa-m, multiply by 0.175.
[b]Curve can be found in Appendix A.

tested at the upper-shelf temperature of 550°F (288°C). Usually, crack pop-in is associated with cleavage crack instability in the middle to just above the lower shelf of the transition temperature range. This upper-shelf pop-in behavior can be somewhat disguised in small specimens such as 1/2 and 1T compact specimens and, hence, may be overlooked. Figures 6 through 8 represent the small specimen evidence, showing how obscure the pop-in behavior development can be between 180 and 550°F (82 and 288°C). The evidence of crack instabilities in Figure 8 is weak enough to be disregarded. The contrast in load-displacement behavior observable in larger specimens is represented in Figures 9 and 10. Here the development of pop-ins is clear for the larger 2T specimen tested at 550°F (288°C). Each of the large displacement steps was caused by rapid crack propagation and arrest events. Such behavior was found to be chronic in heat Z6B, developing in specimens of all orientations, but almost always at 550°F. The other heats also showed pop-in behavior in tests at 550°F, but generally of less frequency and, again, tending to favor large specimens of T-L orientation. At first, dynamic strain aging was believed to be the cause of the pop-in behavior. On the other hand, the physical evidence seems to suggest otherwise. The pop-in phenomenon tended to favor material of lowest J-R curve slope and almost always occurred in the larger specimens that have the greatest elastic stored strain energy and greatest constraint. The grips of large specimens also have the most elastic stored strain energy. This information suggests, therefore, that these pop-ins are ductile crack instabilities, with the initiations being due to the crack-driving force exceeding the J-R curve resistance of the material. This phenomenon should be evaluated further to confirm the postulated cause. Crack instability from any cause may be sustained in structures that have a susbstantial reserve of elastic stored strain energy.

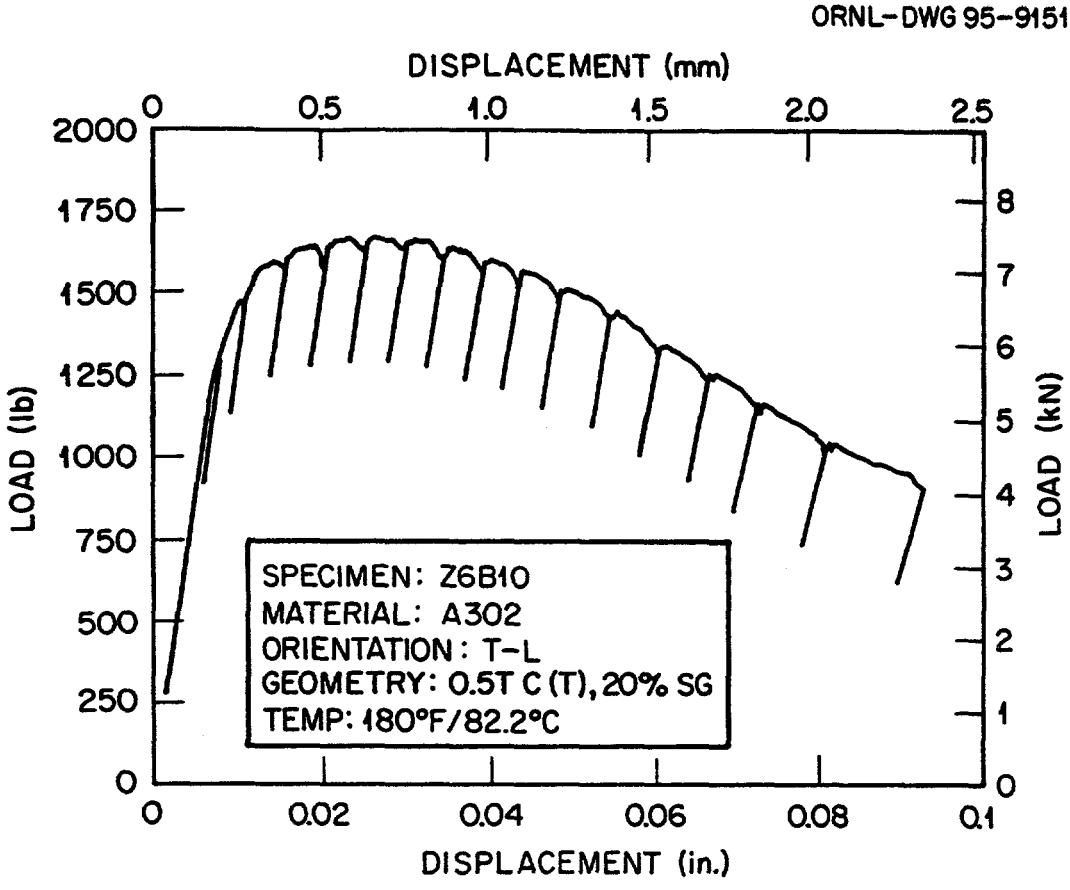

Figure 6. Load-displacement record of 1/2T compact specimen tested at 180°F (82°C), showing no evidence of pop-in.

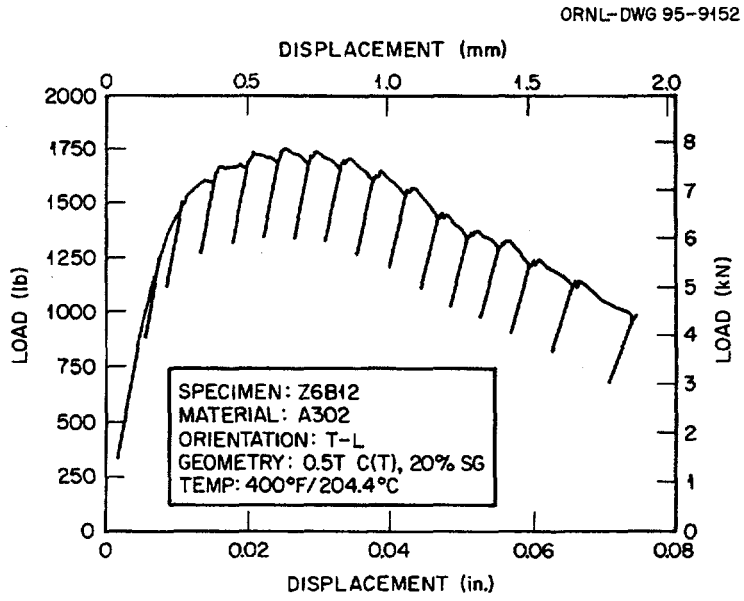

Figure 7. Load-displacement record of 1/2T compact specimen tested at 400°F (204°C), showing no evidence of pop-in.

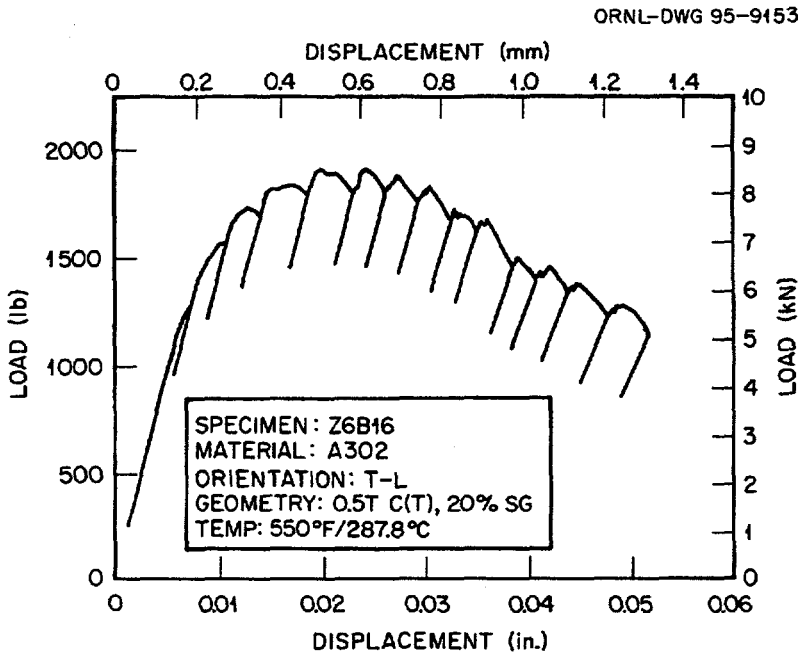

Figure 8. Load-displacement record of 1/2T compact specimen tested at 550°F (288°C), showing a hint of minor instability advances that can be disregarded.

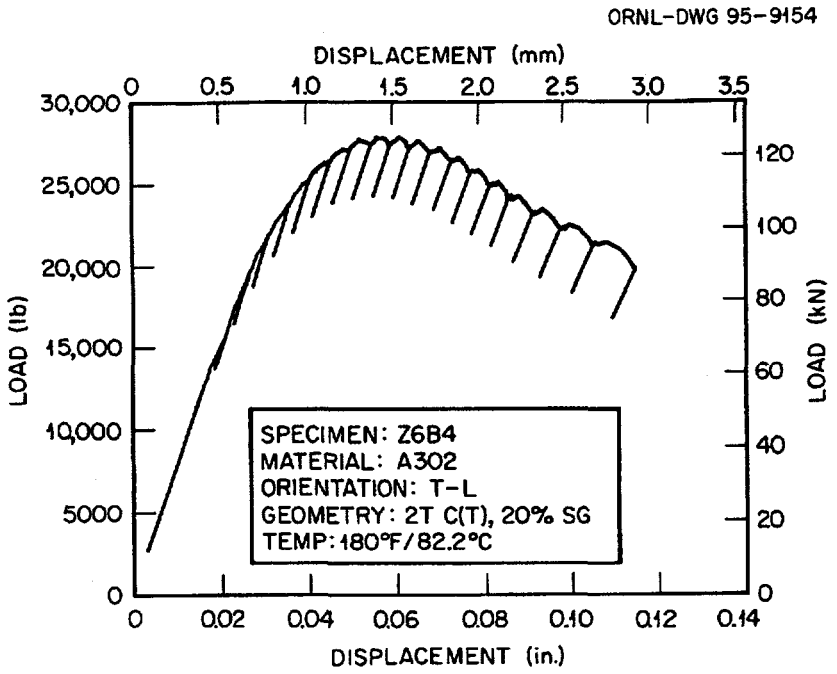

Figure 9. Load-displacement record of 2T compact specimen tested at 180°F (82°C), an upper-shelf temperature with no evidence of pop-in.

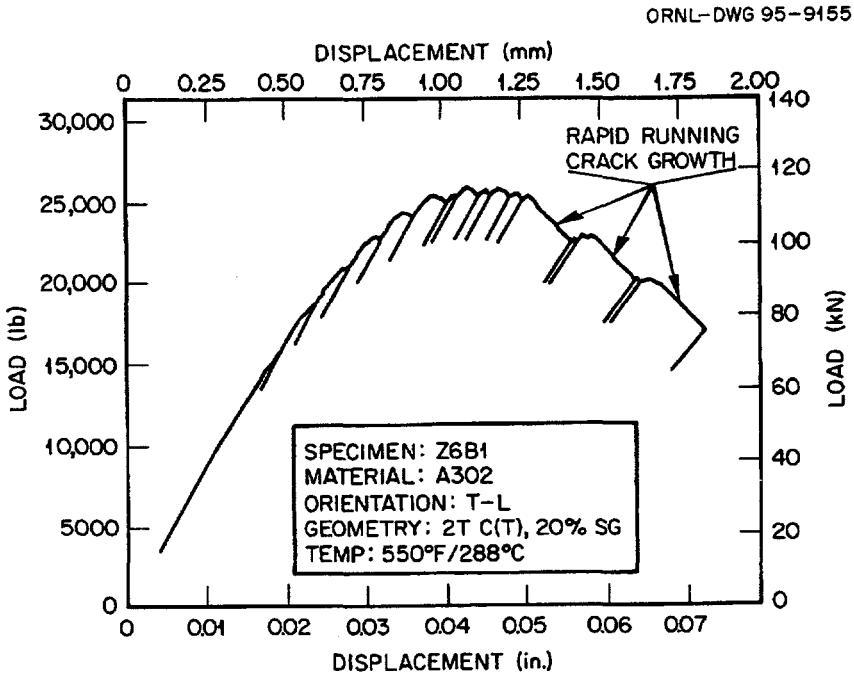

Figure 10. Load-displacement record of 2T compact specimen tested at 550°F (288°C), showing clear evidence of pop-in behavior at upper-shelf temperature.

5. Comments on Available Test Standards

The principal use for an ASTM test method or practice is to establish rules of testing such that independently operating laboratories can produce comparable data. Also, precision among replicate tests must be good enough to fairly compare one material against another. The ASTM test methods related to J_{Ic} determination and J-R curves have been repeatedly evaluated and revised for more than a decade, and this study on modified A 302 grade B steel represents an opportunity to evaluate the progress made.

The first comparison is to evaluate the evolution of analysis procedures for J-integral at the onset of slow-stable crack growth, namely J_{Ic}. Figure 11 compares ASTM E 813-81 to E 813-89 determinations. The 1981 version uses a straight-line fit to J-Δa data exclusively within the exclusion zone indicated in Figure 4. A linear regression line fitted to these data (not shown) is projected to intersect the blunting line where J_{Ic} is defined. This point perhaps slightly underpredicts J at the exact point of onset of ductile tearing. The 1989 version, on the other hand, identifies a point on the J-R curve at 0.008 in. (0.2 mm) of ductile tearing that is advanced forward from the blunting line. This revised definition had been recommended in 1983 in a users experience workshop.[8] A simple power law equation is fitted to the J-Δa data within the exclusion zone. Then J_{Ic} is calculated at 0.008 in. of ductile tearing on this mathematical representation of the J-R curve. Figure 11 suggests that the principal gain from this was an average increase in J_{Ic} of about 7%. The precision of measurement does not seem to have been changed.

The difference between the 1989 and the 1996 versions* for J_{Ic} determination is more subtle than the previous revision. J_{Ic} is still defined at 0.008 in. (0.2 mm) of ductile tearing beyond the blunting line. Also, both versions of the procedure use a power law curve to fit to the data in the exclusion zone and to determine 0.008 in. (0.2 mm) of crack growth. The principal difference is that the 1989 version had used elastic modulus adjustment in the unloading compliance equations to fit the initial part of the J-Δa test data to the calculated blunting line. Any elastic modulus that reasonably characterized the elastic properties of the test material could be used, but the investigator was enabled to apply some subjective judgment to position the data relative to the blunting line. The 1996 version for J_{Ic} uses handbook elastic moduli to develop a J-Δa data set, which is then least-squares fit with a third-order polynomial [see Figure 12(a)]. The point on the polynomial curve at which J is zero identifies the $\Delta a = 0$ point, and all J-Δa data are transposed horizontally so that the polynomial fit curve and the blunting line have the same origin [see Figure 12(b)]. Elastic modulus is removed as a variable, and the 1989 subjectivity allowed for fitting to the blunting line is removed. J_{Ic} results from the two methods plotted against each other are presented in Figure 13. The standard deviation was determined to be about 35 in.-lb/in.^{2} (6 kPa·m). Choosing one method (1989) and comparing variability among replicate specimens (to be covered in Section 6), the standard deviation was typically about 115 in.-lb/in.^{2} (20 kPa·m).

The bottom-line observation about the two revisions to the J_{Ic} method is that both versions contained good information about how to properly apply the compliance technique to slow-stable crack growth measurement. Unfortunately, the attention given to the precision of the analysis procedure can be overwhelmed in materials such as A 302 grade B steel by the variability of J_{Ic} between duplicate specimens.

---

*The 1996 analysis method to determine J_{Ic} is contained in a "combined standard" that has been balloted for the *1996 Annual Book of ASTM Standards*, Sect. 3, Vol. 03.01.

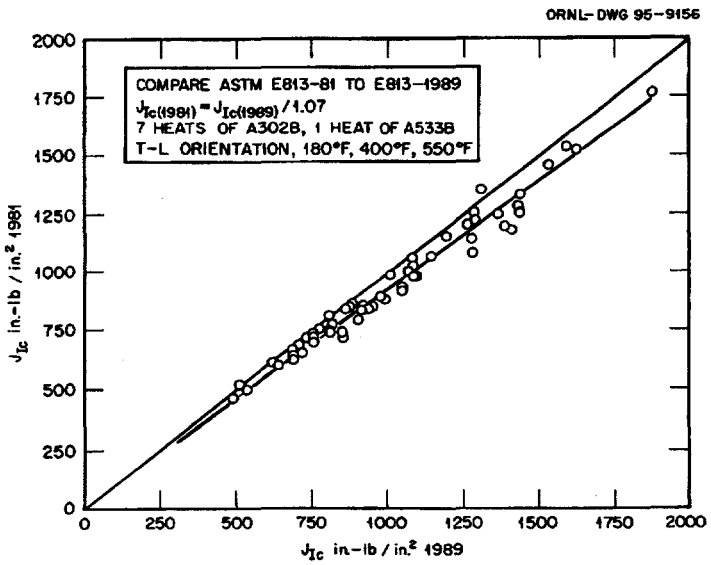

Figure 11. Comparison of the first American Society for Testing and Materials test standard on J_{Ic} in 1981 to the first revision made in 1989.

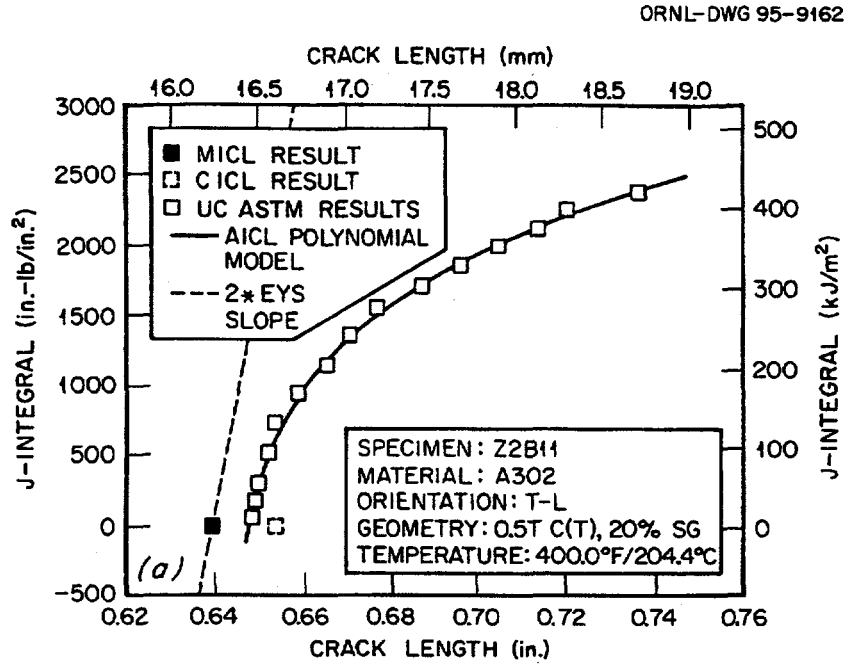

(a)

Figure 12. The 1996 American Society for Testing and Materials method (combined standard): *(a)* third-order polynomial fit and *(b)* adjusted J_R-Δa data to the origin at the known initial physical crack size of the specimen.

(b)

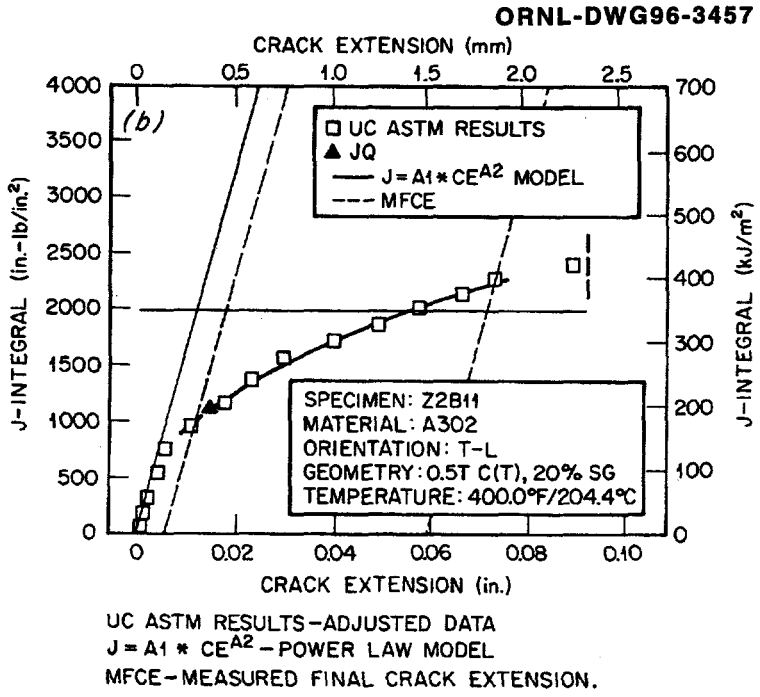

UC ASTM RESULTS–ADJUSTED DATA
$J = A1 * CE^{A2}$ – POWER LAW MODEL
MFCE–MEASURED FINAL CRACK EXTENSION.

Figure 12. (Continued).

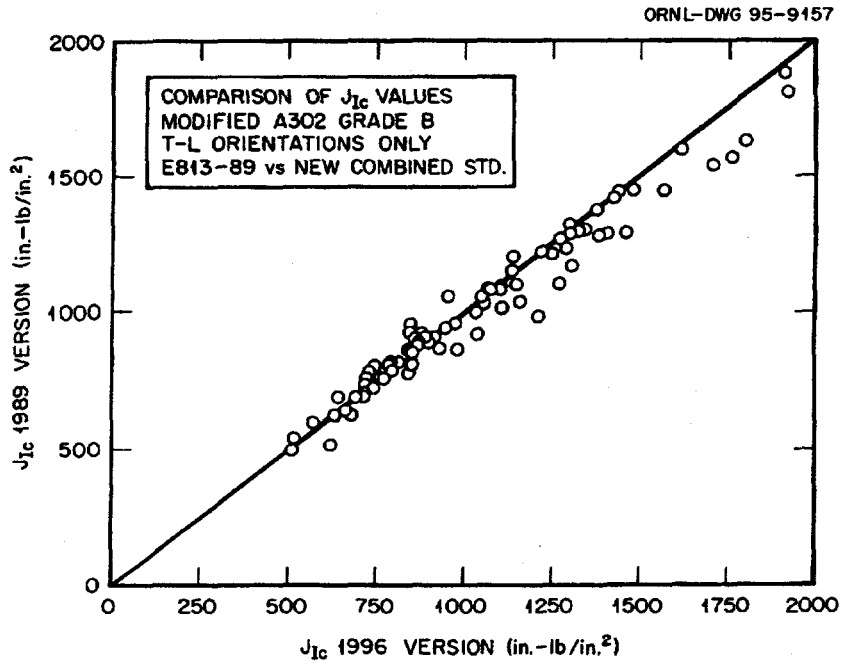

Figure 13. Comparison of the 1989 American Society for Testing and Materials J_{Ic} test method revision to the newly proposed 1996 version.

6. Material Variability

Results from duplicate tests plotted against each other will display variability from all sources. Despite the presumed advantage of measuring J_{Ic} from a defined point on the J-R curve, the precision of analysis seems to be unchanged since 1981. Figure 14 displays J_{Ic} data scatter among duplicate specimens compared to 10% scatter bands parallel to the 1:1 correlation line. The possibility that evaluation methods alone caused the scatter can be dismissed by viewing the two J-R curves for one of the outlier points of Figure 14 (see Figures 15 and 16). Clearly, in this case, the J-R curve data are significantly different, and improvements in the precision of measurements could not remedy this lack of agreement.

The J-R curve fracture toughness parameter of $J_{0.1}$ is inherently less sensitive to the precision of crack growth measurements because this value is obtained on the part of the modified A 302 grade B J-R curves where they are tending toward an upper plateau. Hence, so long as crack growth is not overly extensive compared to the initial remaining ligament size, the $J_{0.1}$ values should provide the most discriminating comparison between duplicate specimens. This comparison is made in Figure 17. The data-pair matchups are the same as those used in Figure 14. Again, the 10% data scatter lines are applied for comparison on an equal basis. Although there are no outliers, as there were for J_{Ic}, it appears that material variability is the dominant factor affecting reproducibility of J_{Ic} and $J_{0.1}$ values.

The extent of J-R curve data scatter indicated in Figures 14 and 17 is relatively manageable from the standpoint of application to design and/or structural integrity analysis. Variability of another kind is demonstrated in Figure 18. This shows the range of J-R curve toughnesses that can be obtained in modified A302 grade B plates and also lists the criteria commonly believed to be related to J-R curve. The plot includes two materials that do not belong to the above stated material identification, codes Z8 (A533 grade B class 1) and the MEA plate of code V50 (A 302 grade B). However, both have the same tensile properties as the modified A302 grade B heats. Specifically, the range of yield strengths and ultimate strengths is covered by 62 ksi (427 MPa) ± 15% and 82.6 ksi (569 MPa) ± 15%, respectively. Total elongations are 21.7 ± 7%. One test temperature (180°F) and one orientation (T-L) were chosen for clarity of presentation. Clearly, tensile tests or tensile properties inferred from hardness determinations could not be used to index these J-R curves. Charpy USEs share this same deficiency to a certain extent as well. However, in the CVN case there is not a complete disconnect in relevance, but it appears that a correlation would contain extremely wide confidence bounds. Apparently, complex deformation mechanisms and responses to microstructural features interact differently between Charpy impact and fracture mechanics tests.

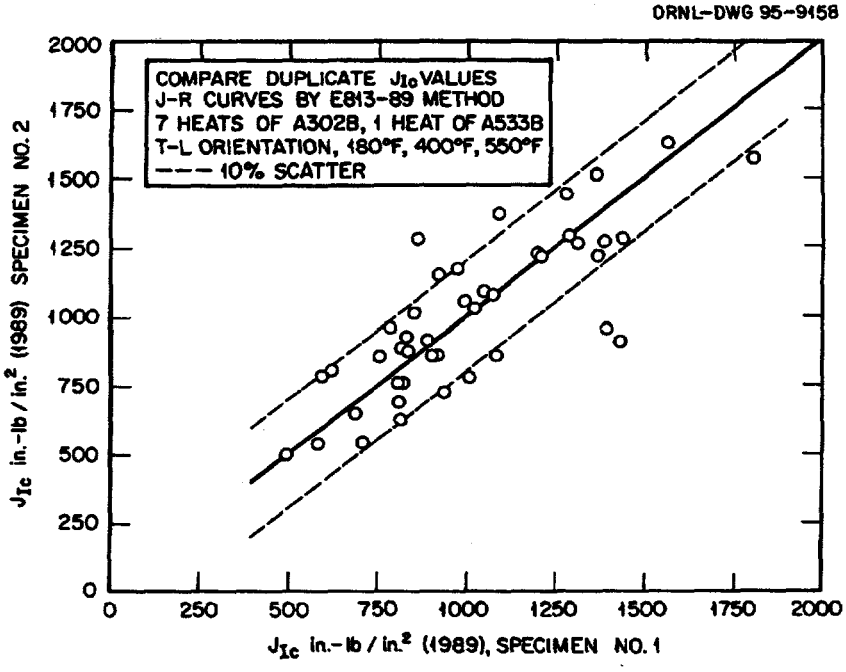

Figure 14. Data scatter of J_{Ic} due to material variability.

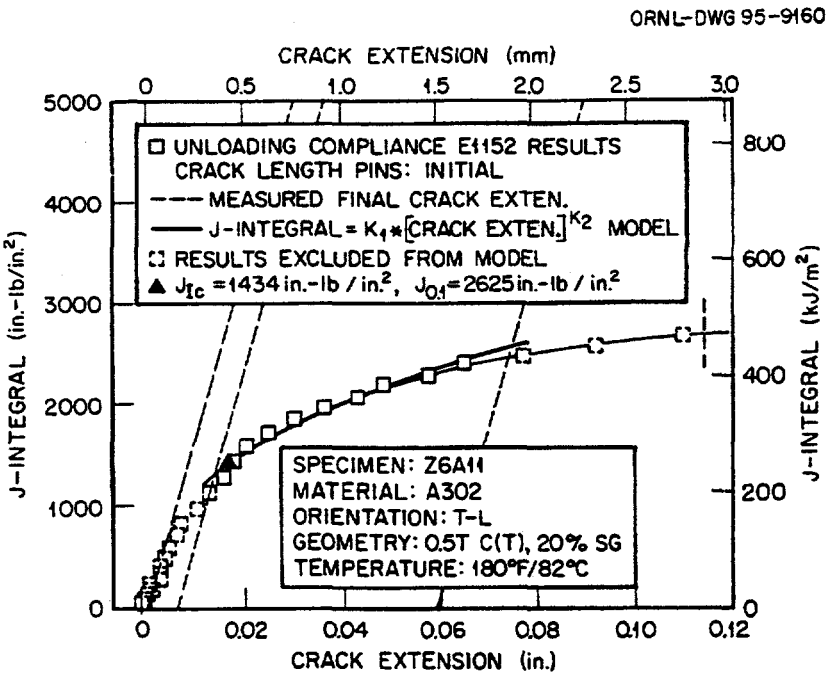

Figure 15. Typical J-R curve for comparison to the duplicate test shown in Figure 16.

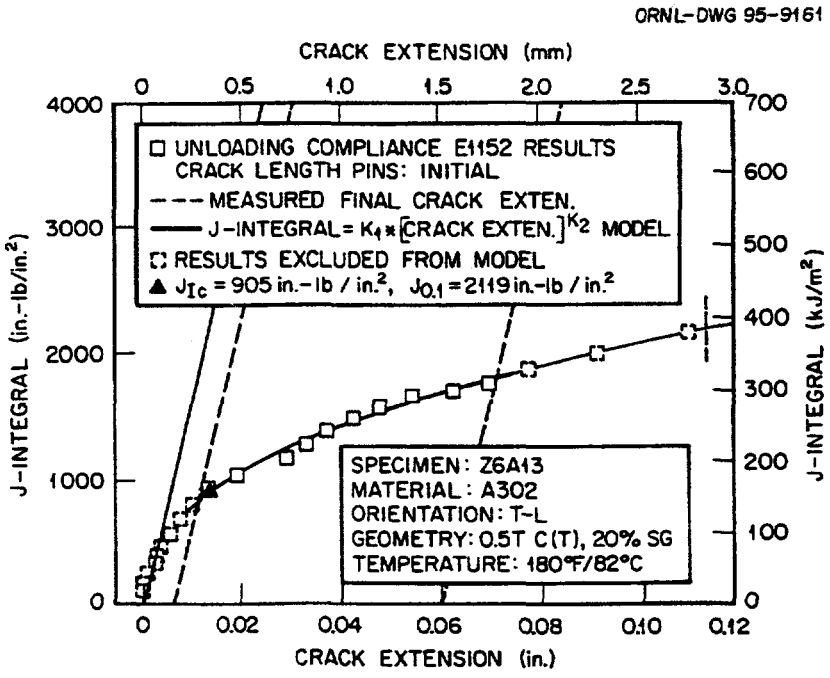

Figure 16. Typical J-R curve for comparison to the duplicate test shown in Figure 15.

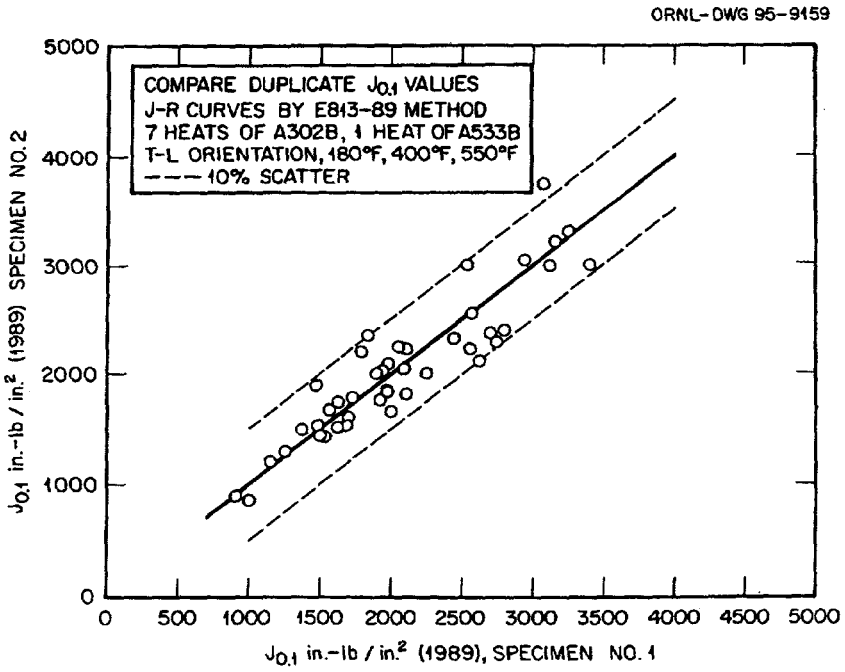

Figure 17. Data scatter of $J_{0.1}$ due to material variability.

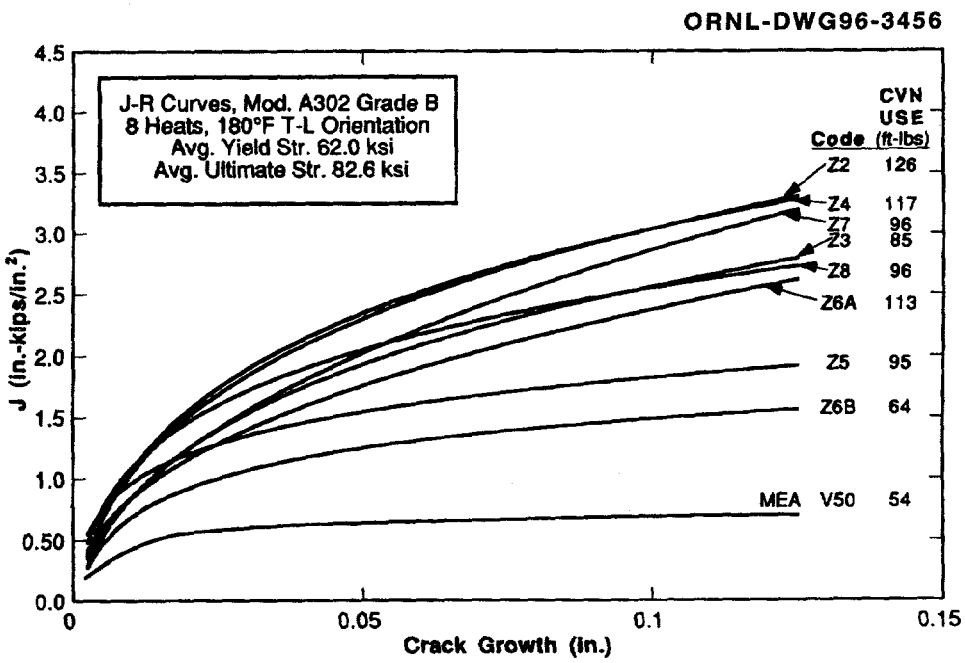

Figure 18. J-R curves for modified A302 grade B plates, one vintage A533 grade B class 1 plate (Z8) and a Materials Engineering Associates plate of A302 grade B (V50). Tensile properties and corresponding Charpy V-notch impact upper-shelf energies (ft-lb) are also shown.

7. Conclusions

Seven heats of modified A 302 grade B plate and one vintage plate of A 533 grade B plate steel were evaluated for upper-shelf fracture toughness in the form of J-R curves. The objectives were to (1) determine if the J-R curve fracture toughness is section size-dependent, (2) develop some generic fracture toughness data on modified A 302 grade B steel for potential use in analyses applications, (3) determine typical orientation effects and test temperature effects, and (4) develop generic CVN and drop-weight NDT data. Over 230 compact specimens of sizes ranging from 1/2T to 4T, 285 CVN, 65 tensile, and 64 drop-weight NDT specimens were tested.

It was determined that the J-R curve toughness of modified A 302 grade B steel of typical production practice does not degrade with increased specimen size. The results from an earlier MEA experiment[2] that showed a significant loss in J-R curve toughness with increased specimen size were not confirmed here. In fact, the fracture toughness of the MEA plate of A 302 grade B was lower than that of any of the modified A 302 grade B steel plates tested in this study, and no significant specimen size effect was observed in materials of improved toughness.

J-R curve data are presented in the form of J_{Ic} values, and J at 0.1 in. (2.5 mm) of crack growth, and T-modulus. The tabulated values were averaged over all specimen sizes. Among the three orientations of transverse (T-L), longitudinal (L-T), and short transverse (L-S), the transverse always showed the lowest toughness. The general pattern for longitudinal and short transverse directions is that both were of higher toughness than transverse, and they tended to be about equal to each other. Representative J-R curves for each orientation of each material are presented in Appendix A, and all were curve-fitted for reproduction purposes. The general pattern of test temperature effects is similarly listed from averaged data, and representative J-R curves were fitted for presentation in Appendix B. The fact that all heats showed J-R curve toughness loss with test temperature increase to 550°F (288°C) is typical.

Drop-weight NDT tests were fairly consistent among heats, ranging from –30 to –5°F (–34 to –20°C). Evaluations for RT_{NDT} showed that two heats, one modified A 302 grade B and the vintage A 533 grade B, had insufficient CVN toughness at NDT + 60°F (33°C) for RT_{NDT} to equal the NDT temperature. The penalty in RT_{NDT} was 43 and 44°F (24°C).

The multiple number of tests on one grade of steel provided an opportunity to evaluate J-R curve and J_{Ic} test methods that have been developed and modified within ASTM. These methods have never been subjected to such a wide range of material characteristics and test conditions. The bottom-line finding from this experiment on the J_{Ic} method revisions made over a decade of development has the following two aspects: The establishment of test practice requirements to obtain crack growth by compliance was useful. On the other hand, the revisions to test record analysis subsequent to the 1981 version of E 813 have made the determination of J_{Ic} unnecessarily complex and hence less useful. The revisions showed no beneficial impact on the precision of J_{Ic} determination for modified A 302 grade B steels.

Two parameters of material crack growth resistance measurement that were useful for comparisons were T-modulus and J at 0.1 in. (2.5 mm) of crack growth. Each required a definition specific to this report, since neither parameter is covered by an ASTM standard analysis procedure.

8. References

1. ASME Section XI Task Group on Reactor Vessel Integrity Requirements, *White Paper on Reactor Vessel Integrity Requirements for Level A and B Conditions*, EPRI TR-100251, Final Report, Electric Power Research Institute, Palo Alto, Calif., January 1993.*

2. A. L. Hiser and J. B. Terrell, Materials Engineering Associates, Inc., Lanham, Md., *Size Effects on J-R Curves for A302-B Plate*, USNRC Report NUREG/CR-6265 (MEA-2320), January 1989.†

3. "Standard Terminology Relating to Fracture Testing," E 616-89, pp. 647-57 in *Annual Book of ASTM Standards*, Vol. 03.01, American Society for Testing and Materials, Philadelphia, 1993.*

4. "Fracture Toughness Requirements for Material," Sect. III, Div. 1, NB-2300, *ASME Boiler and Pressure Vessel Code. An American National Standard,* American Society of Mechanical Engineers, New York, 1994.*

5. "Standard Test Method for J_{ic}, a Measure of Fracture Toughness," E 813-89, pp. 738-52 in *Annual Book of ASTM Standards*, Vol. 03.01, American Society for Testing and Materials, Philadelphia, 1993.*

6. "Evaluation Procedures for Levels A and B Service Loading," Sect. XI, Article K-4000, *ASME Boiler and Pressure Vessel Code. An American National Standard,* American Society of Mechanical Engineers, New York, 1994.*

7. E. D. Eason, J. E. Wright, and E. E. Nelson, Modeling and Computing Services, Boulder, Colo., *Multivariable Modeling of Pressure Vessel and Piping J-R Data*, USNRC Report NUREG/CR-5729 (MCS-910401), May 1991.†

8. G. P. Gibson and S. G. Druce, "Some Observations on J-R Curves," pp. 166-82 in *Elastic-Plastic Fracture Test Methods (The User's Experience), ASTM STP 856*, American Society for Testing and Materials, Philadelphia, 1985.*

*Available in public technical libraries.
†Available for purchase from National Technical Information Service, Springfield, VA 22161.

Appendix A

Selected J-R Curves Representing Typical Values of T Slope, $J_{0.1}$, and J_{Ic} from Table 7

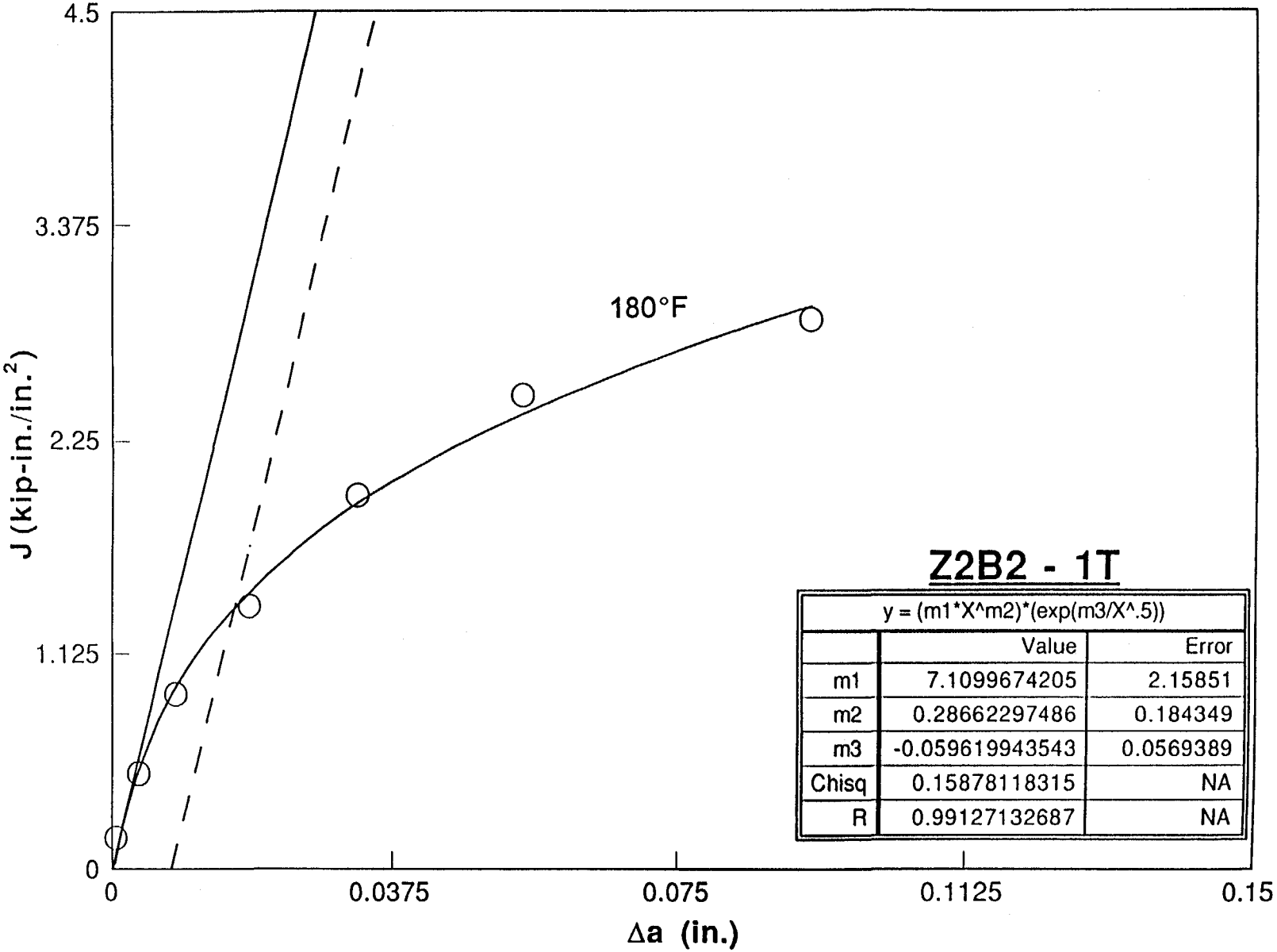

Z2B2 - 1T

y = (m1*X^m2)*(exp(m3/X^.5))		
	Value	Error
m1	7.1099674205	2.15851
m2	0.28662297486	0.184349
m3	-0.059619943543	0.0569389
Chisq	0.15878118315	NA
R	0.99127132687	NA

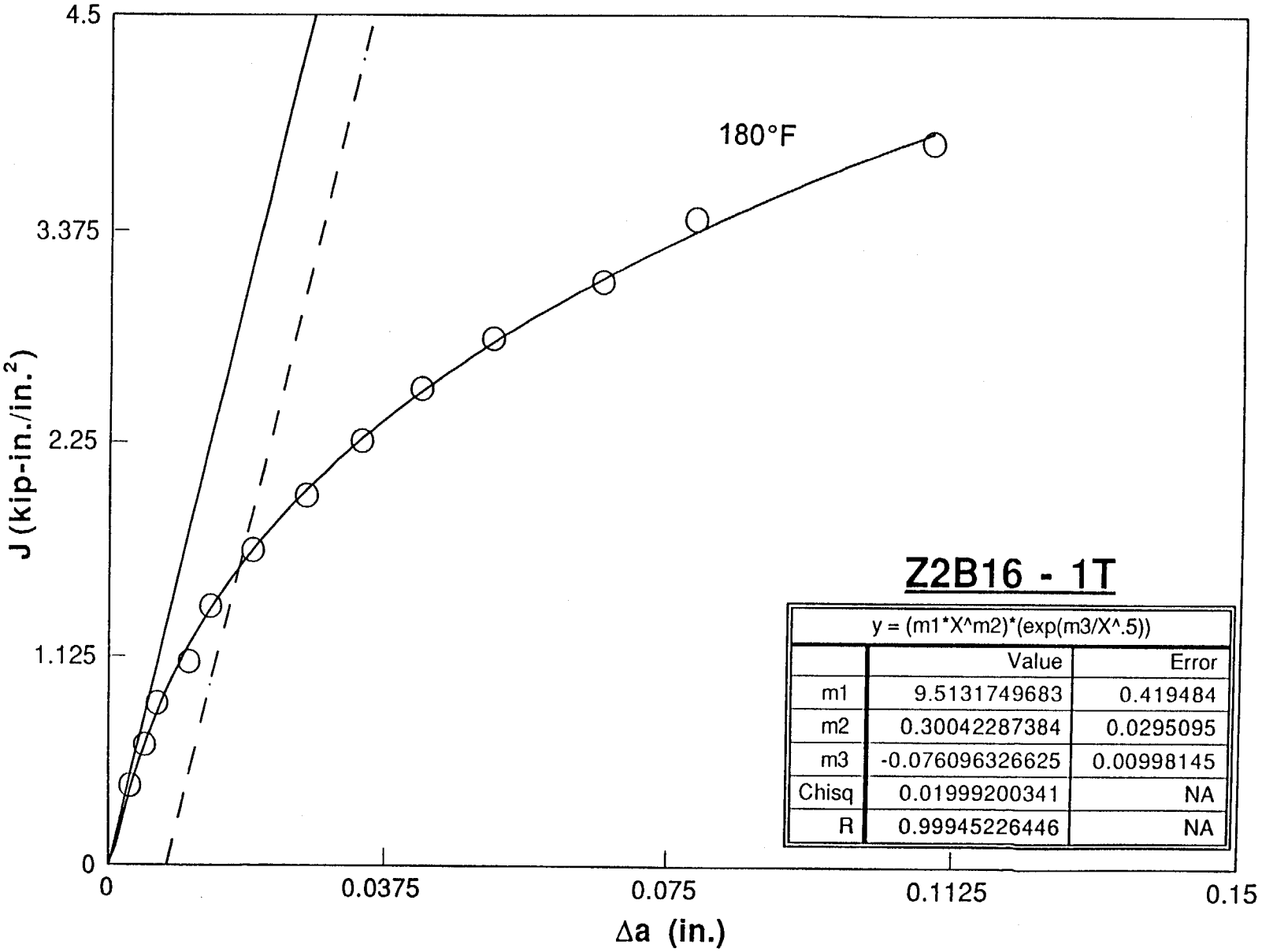
4.5
3.375
2.25
1.125
0
J (kip-in./in.^{2})
0
0.0375
0.075
0.1125
0.15
Δa (in.)
180°F
Z2B16 - 1T
y = (m1*X^m2)*(exp(m3/X^.5))
Value
Error
m1
9.5131749683
0.419484
m2
0.30042287384
0.0295095
m3
-0.076096326625
0.00998145
Chisq
0.01999200341
NA
R
0.9945226446
NA

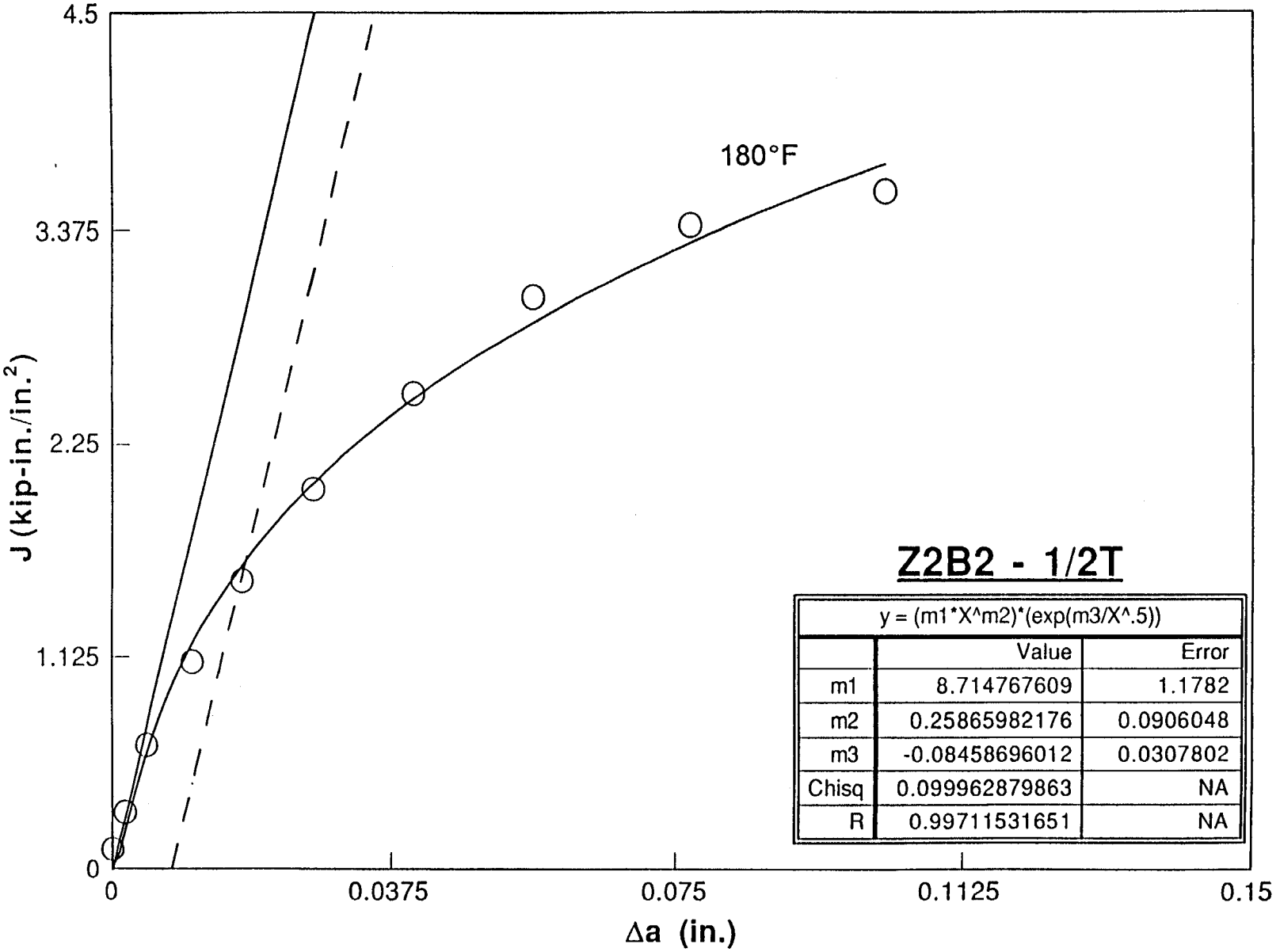

Z2B2 - 1/2T

y = (m1*X^m2)*(exp(m3/X^.5))		
	Value	Error
m1	8.714767609	1.1782
m2	0.25865982176	0.0906048
m3	-0.08458696012	0.0307802
Chisq	0.099962879863	NA
R	0.99711531651	NA

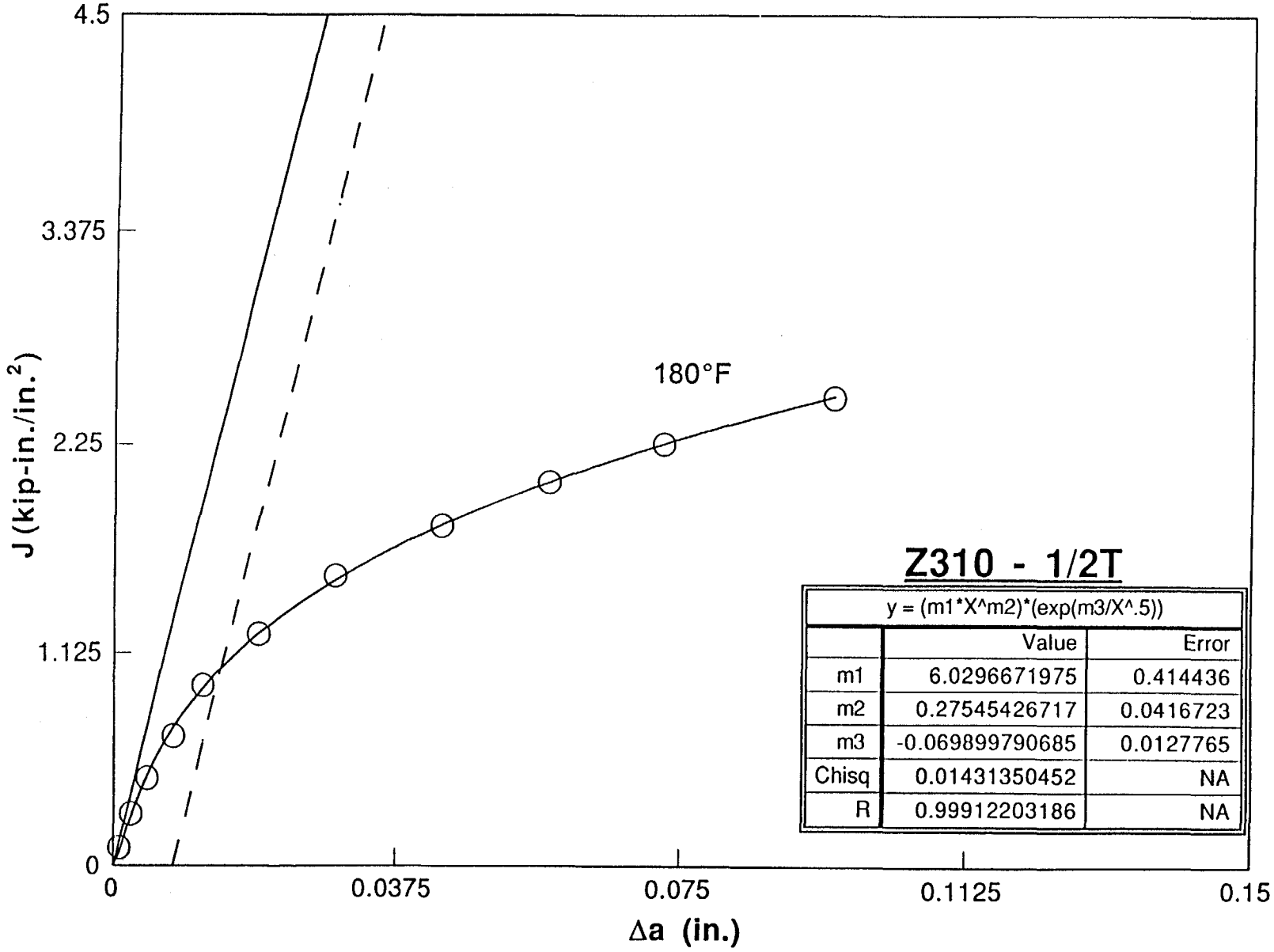
4.5
3.375
2.25
1.125
0
J (kip-in./in.^{2})
0
0.0375
0.075
0.1125
0.15
Δa (in.)
180°F
Z310 - 1/2T
y = (m1*X^m2)*(exp(m3/X^.5))
Value
Error
m1 6.0296671975 0.414436
m2 0.27545426717 0.0416723
m3 -0.069899790685 0.0127765
Chisq 0.01431350452 NA
R 0.99912203186 NA

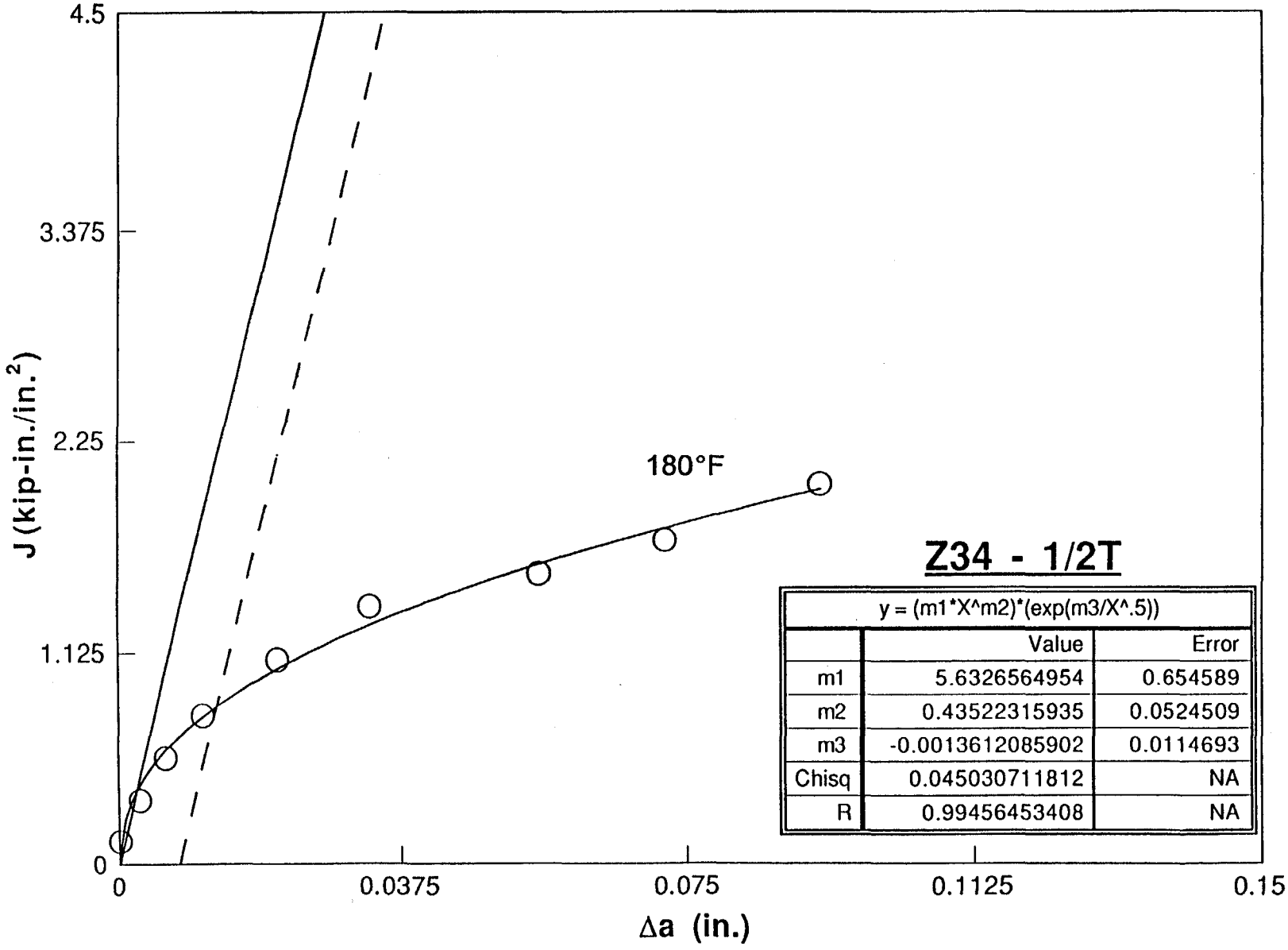
4.5
3.375
2.25
1.125
0
J (kip-in./in.^{2})
0
0.0375
0.075
0.1125
0.15
Δa (in.)
180°F
Z34 - 1/2T
y = (m1*X^m2)*(exp(m3/X^.5))
Value
Error
m1 5.6326564954 0.654589
m2 0.43522315935 0.0524509
m3 -0.0013612085902 0.0114693
Chisq 0.045030711812 NA
R 0.99456453408 NA

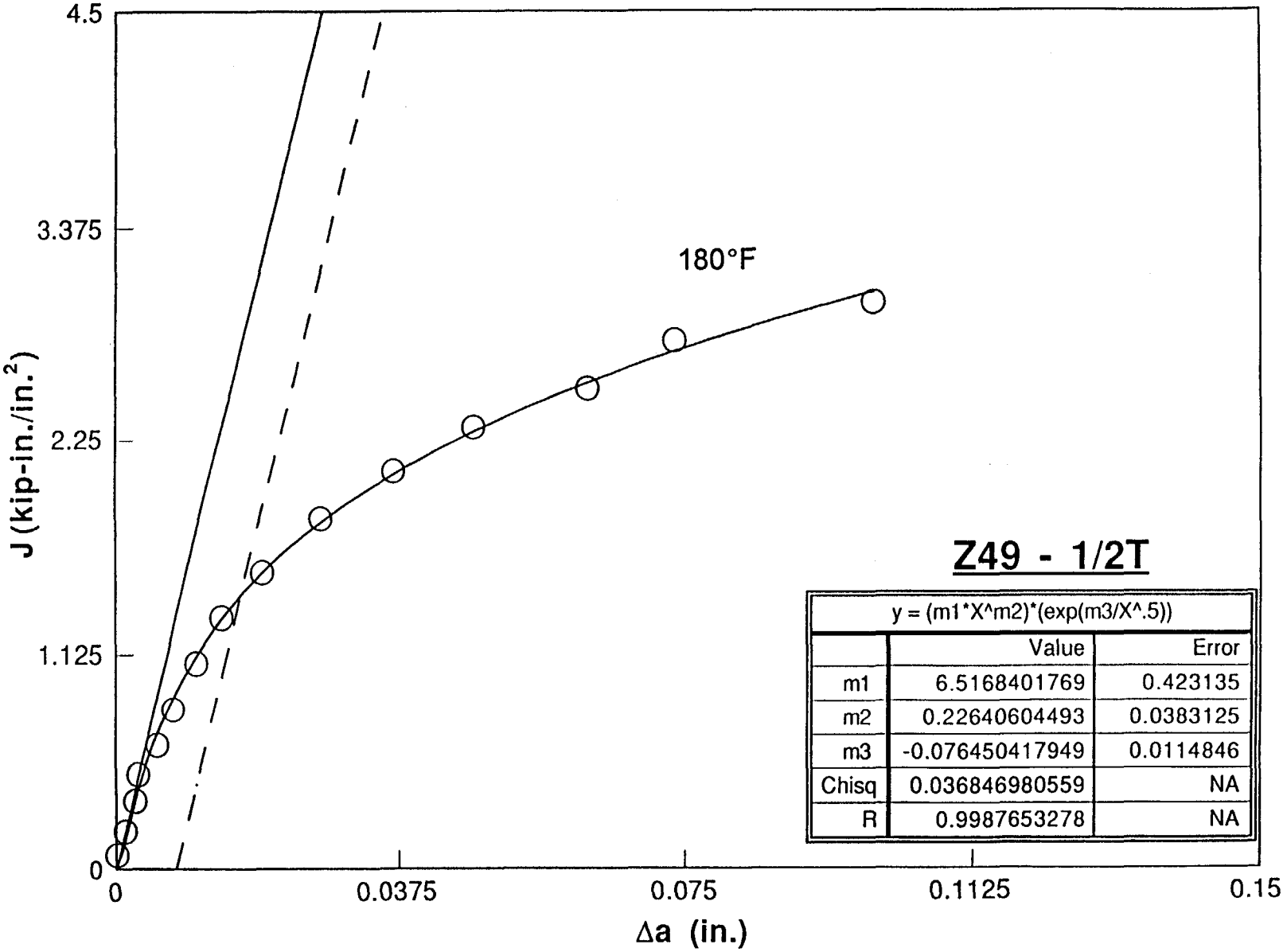
4.5
3.375
2.25
1.125
0
J (kip-in./in.²)
180°F
0
0.0375
0.075
0.1125
0.15
Δa (in.)
Z49 - 1/2T
y = (m1*X^m2)*(exp(m3/X^.5))
Value
Error
m1
6.5168401769
0.423135
m2
0.22640604493
0.0383125
m3
-0.076450417949
0.0114846
Chisq
0.036846980559
NA
R
0.9987653278
NA

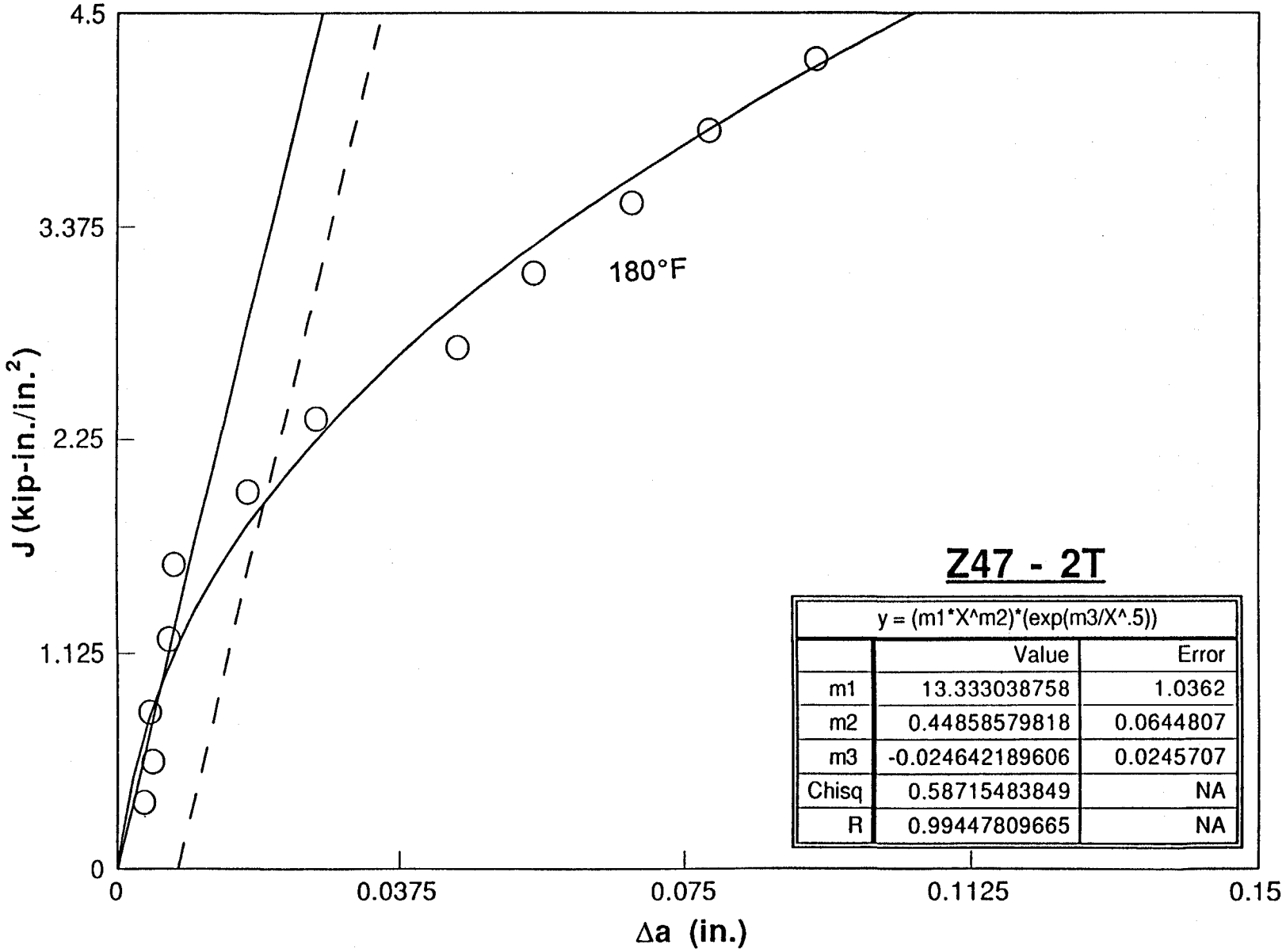
4.5
3.375
2.25
1.125
0
J (kip-in./in.^{2})
0
0.0375
0.075
0.1125
0.15
Δa (in.)
180°F
Z47 - 2T
y = (m1*X^m2)*(exp(m3/X^.5))
Value
Error
m1 13.333038758 1.0362
m2 0.44858579818 0.0644807
m3 -0.02464189606 0.0245707
Chisq 0.58715483849 NA
R 0.99447809665 NA

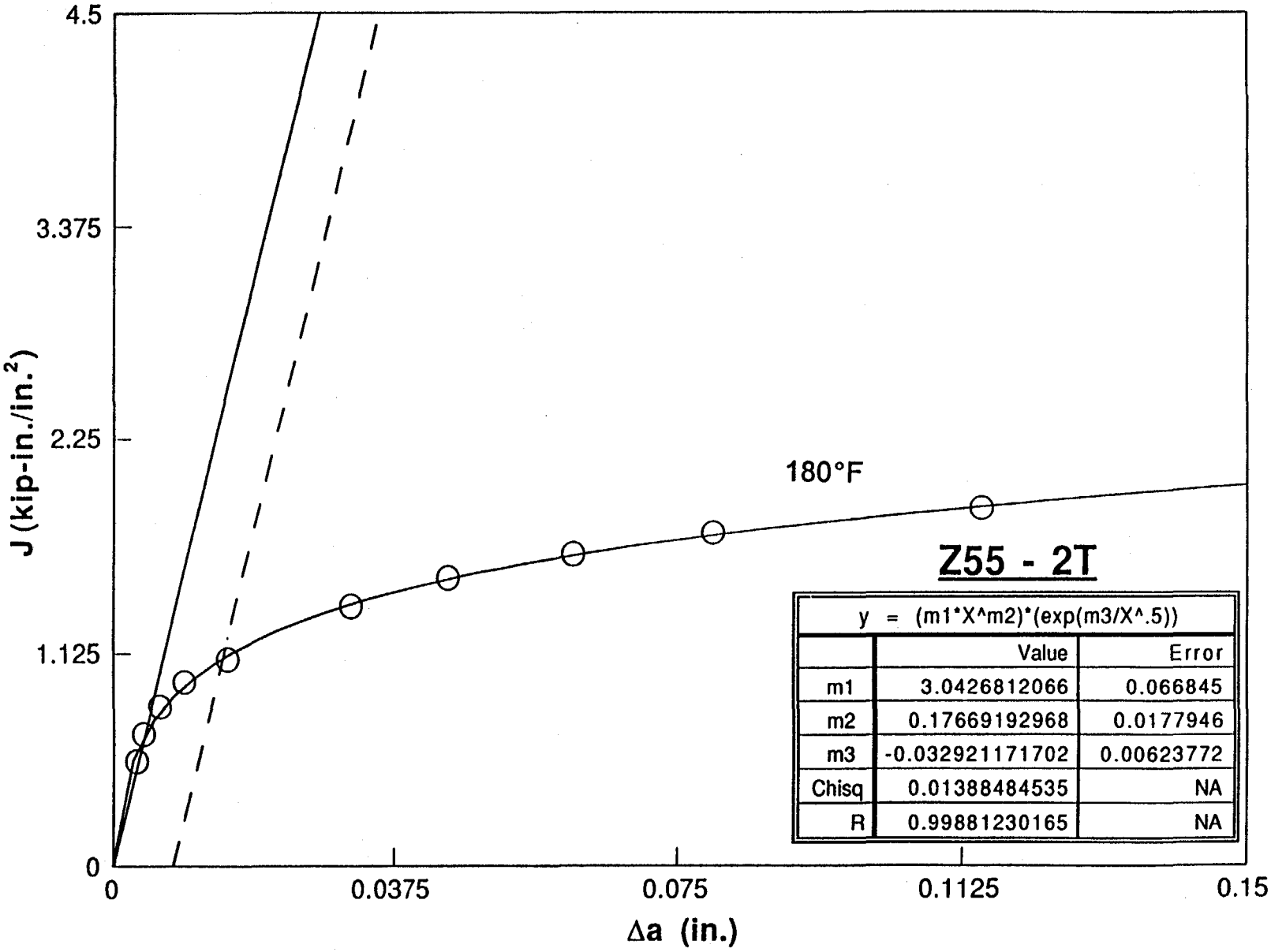
4.5
3.375
2.25
1.125
0
J (kip-in./in.^{2})
0
0.0375
0.075
0.1125
0.15
Δa (in.)
180°F
Z55 - 2T
y = (m1*X^m2)*(exp(m3/X^.5))
Value
Error
m1
3.0426812066
0.066845
m2
0.17669192968
0.0177946
m3
-0.032921171702
0.00623772
Chisq
0.01388484535
NA
R
0.99881230165
NA

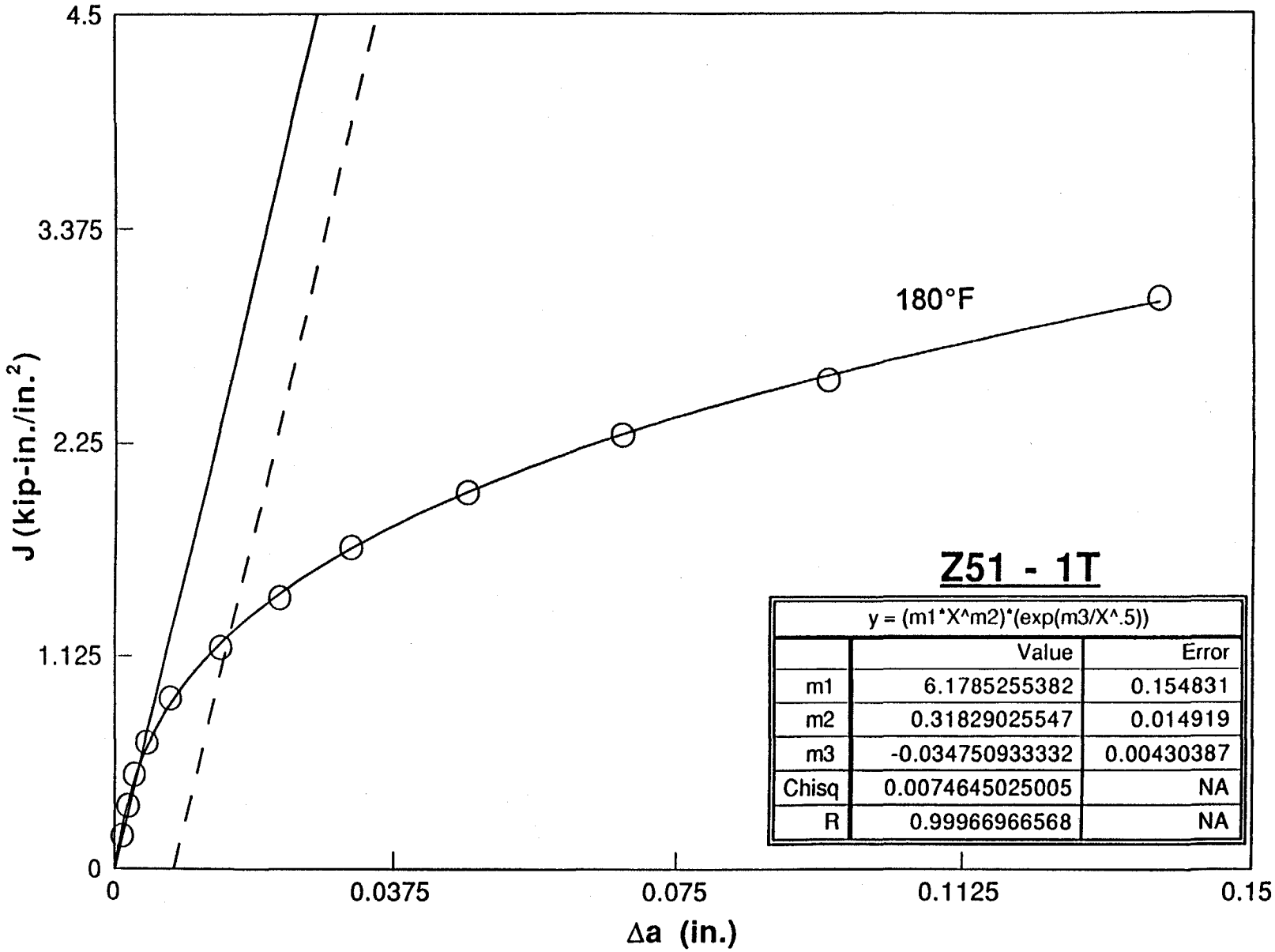
4.5
3.375
2.25
1.125
0
J (kip-in./in.^{2})
0
0.0375
0.075
0.1125
0.15
Δa (in.)
180°F
Z51 - 1T
y = (m1*X^m2)*(exp(m3/X^.5))
Value
Error
m1
6.1785255382
0.154831
m2
0.31829025547
0.014919
m3
-0.034750933332
0.00430387
Chisq
0.0074645025005
NA
R
0.99966966568
NA

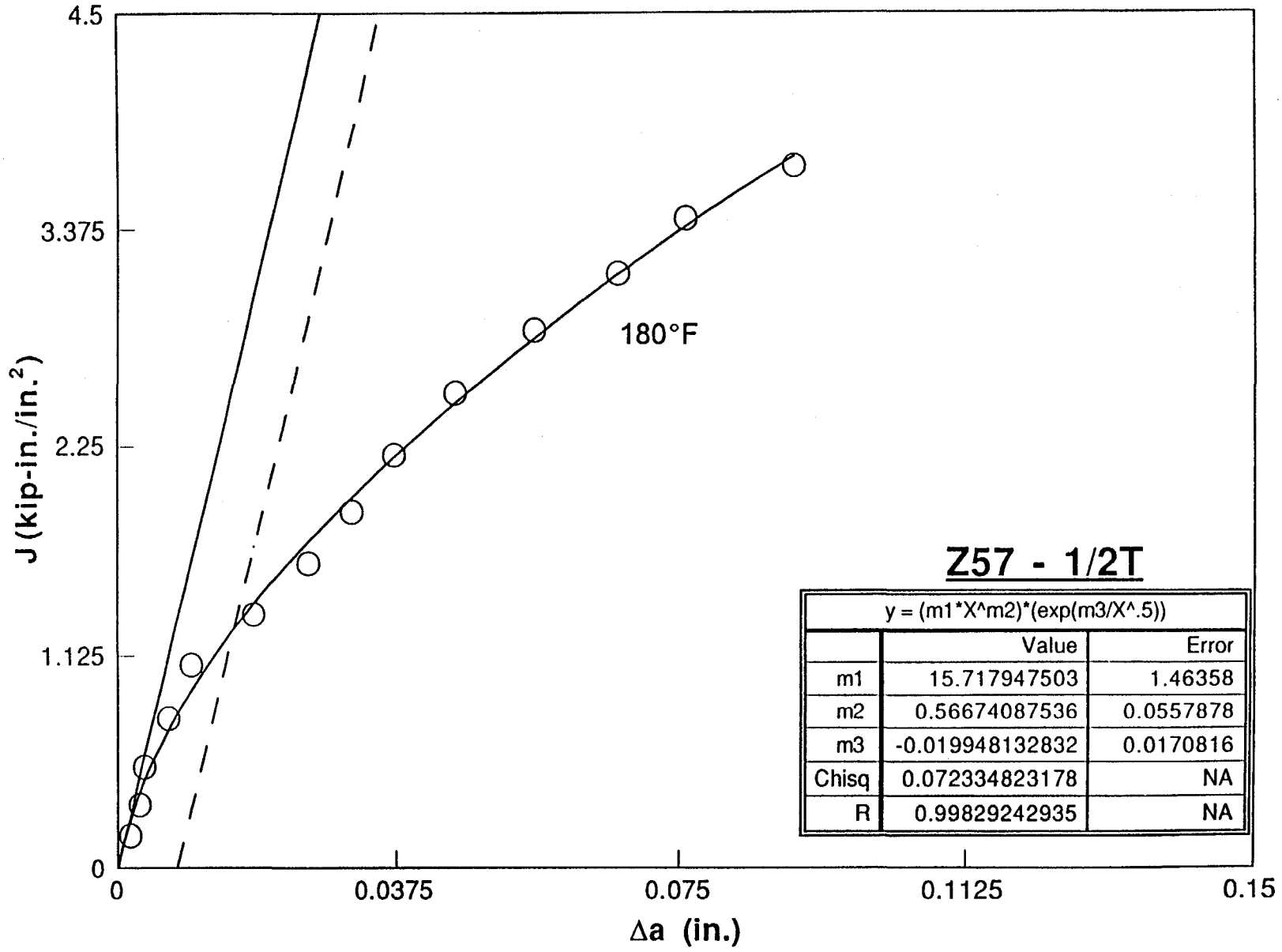
4.5
3.375
2.25
1.125
0
J (kip-in./in.²)
0
0.0375
0.075
0.1125
0.15
Δa (in.)
180°F
Z57 - 1/2T
y = (m1*X^m2)*(exp(m3/X^.5))
Value
Error
m1
15.717947503
1.46358
m2
0.56674087536
0.0557878
m3
-0.019948132832
0.0170816
Chisq
0.072334823178
NA
R
0.99829242935
NA

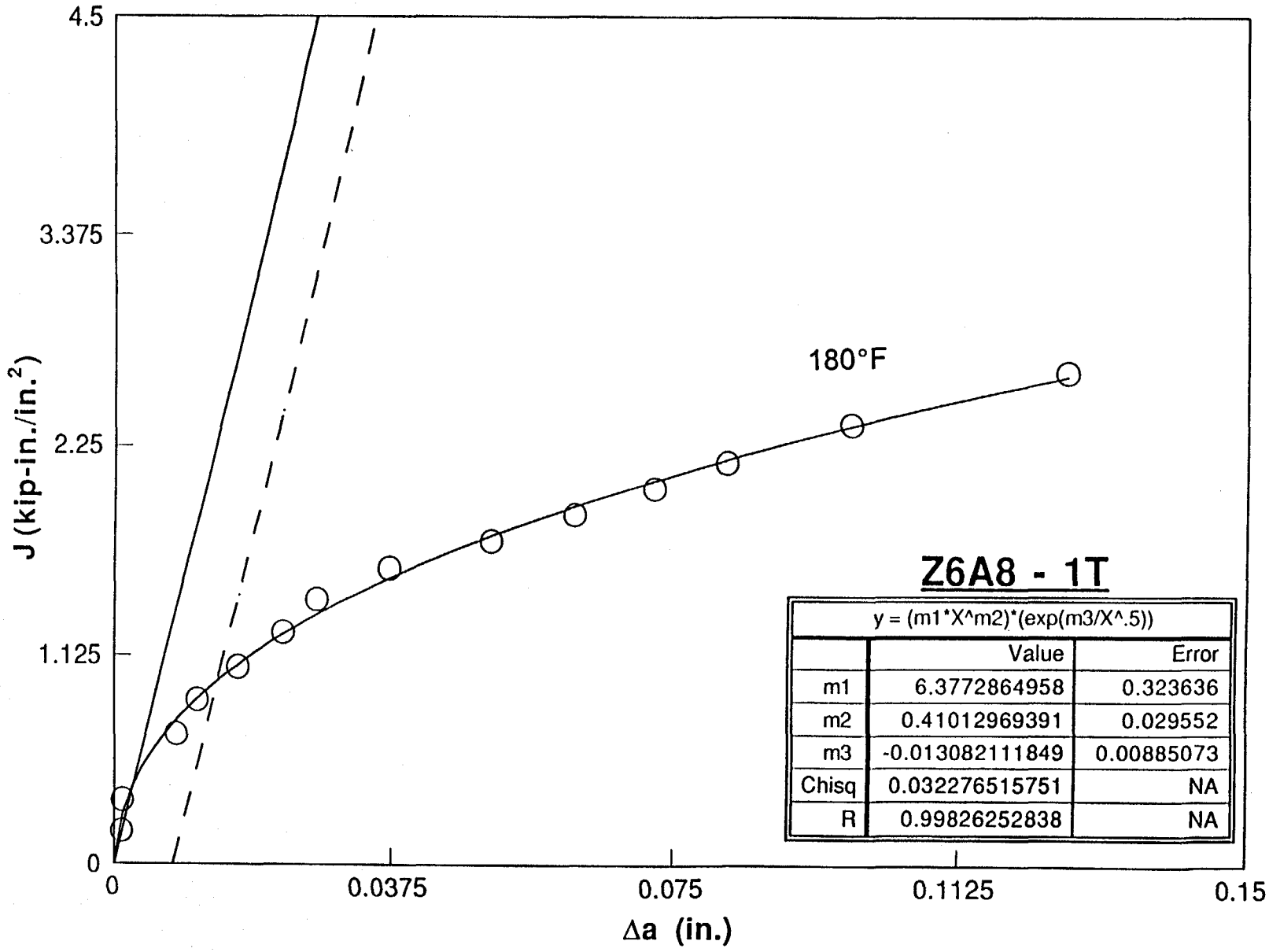
4.5
3.375
2.25
1.125
0
J (kip-in./in.^{2})
0
0.0375
0.075
0.1125
0.15
Δa (in.)
180°F
Z6A8 - 1T
y = (m1*X^m2)*(exp(m3/X^.5))
Value
Error
m1 6.3772864958 0.323636
m2 0.41012969391 0.029552
m3 -0.013082111849 0.00885073
Chisq 0.032276515751 NA
R 0.99826252838 NA

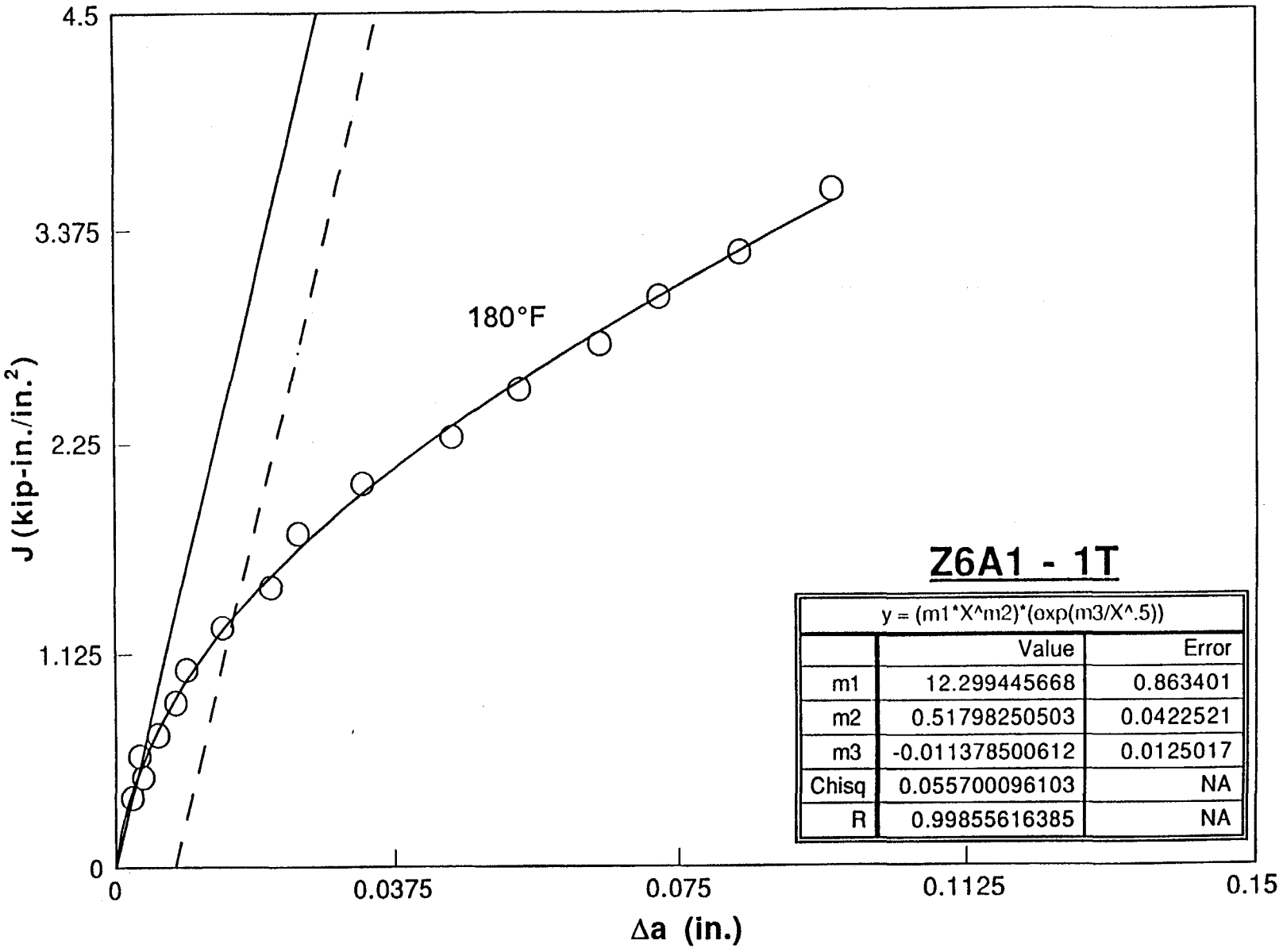
4.5
3.375
2.25
1.125
0
J (kip-in./in.²)
180°F
0
0.0375
0.075
0.1125
0.15
Δa (in.)
Z6A1 - 1T
y = (m1*X^m2)*(exp(m3/X^.5))
Value
Error
m1
12.299445668
0.863401
m2
0.51798250503
0.0422521
m3
-0.011378500612
0.0125017
Chisq
0.055700096103
NA
R
0.99855616385
NA

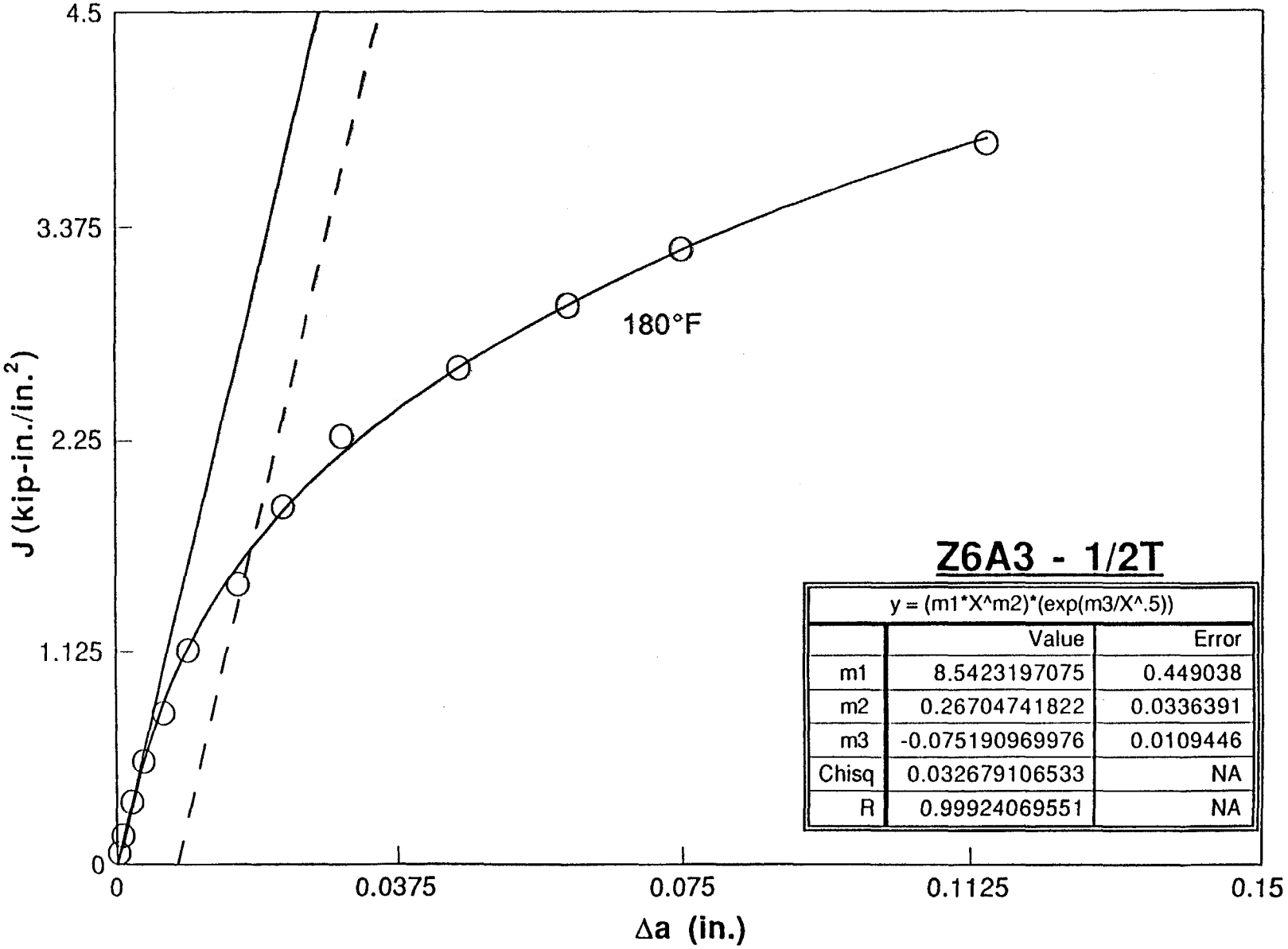

Z6A3 - 1/2T

y = (m1*X^m2)*(exp(m3/X^.5))		
	Value	Error
m1	8.5423197075	0.449038
m2	0.26704741822	0.0336391
m3	-0.075190969976	0.0109446
Chisq	0.032679106533	NA
R	0.99924069551	NA

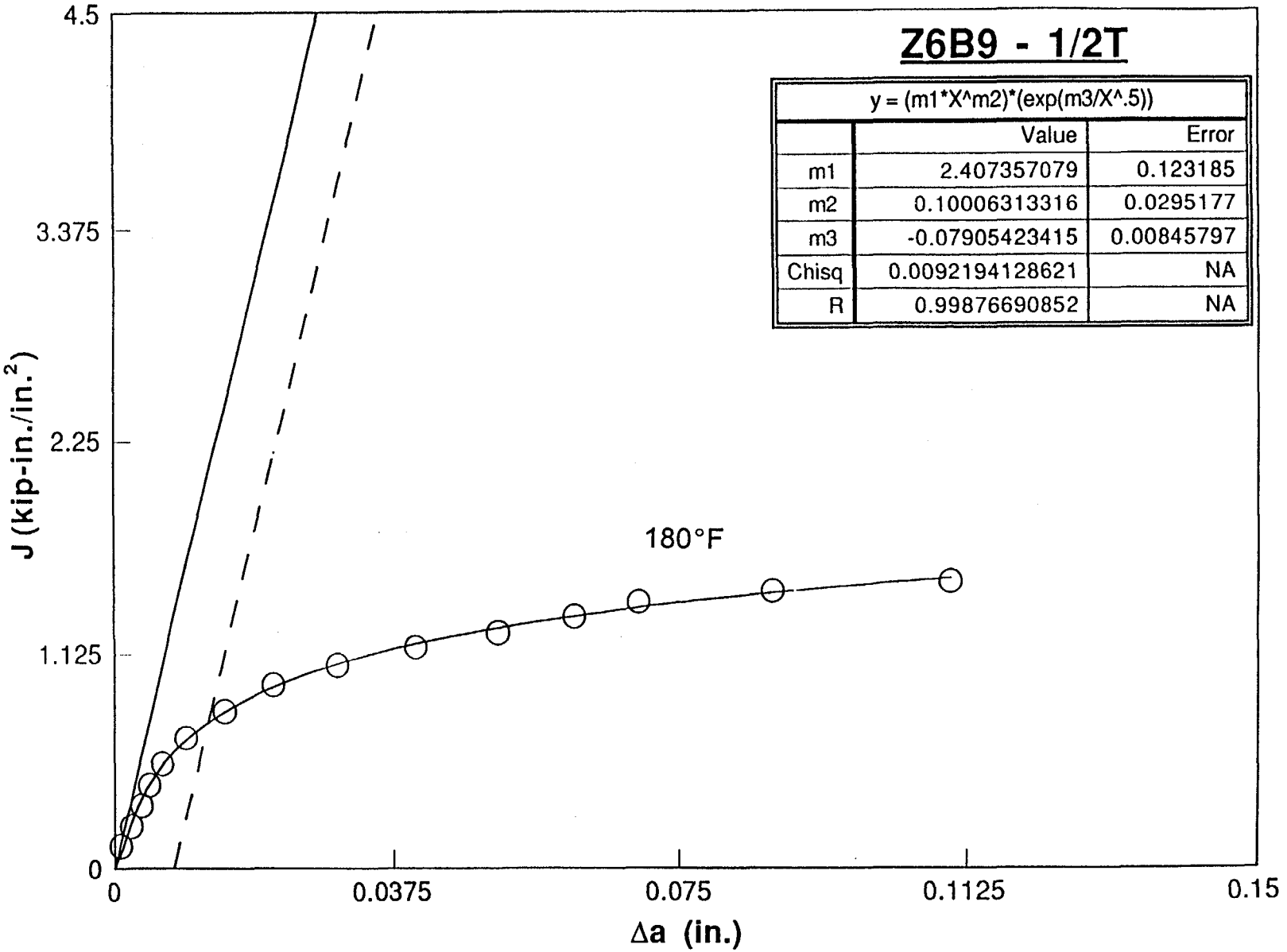
Z6B9 - 1/2T
y = (m1*X^m2)*(exp(m3/X^.5))
Value
Error
m1
2.407357079
0.123185
m2
0.10006313316
0.0295177
m3
-0.07905423415
0.00845797
Chisq
0.0092194128621
NA
R
0.99876690852
NA
180°F
J (kip-in./in.²)
Δa (in.)
4.5
3.375
2.25
1.125
0
0
0.0375
0.075
0.1125
0.15

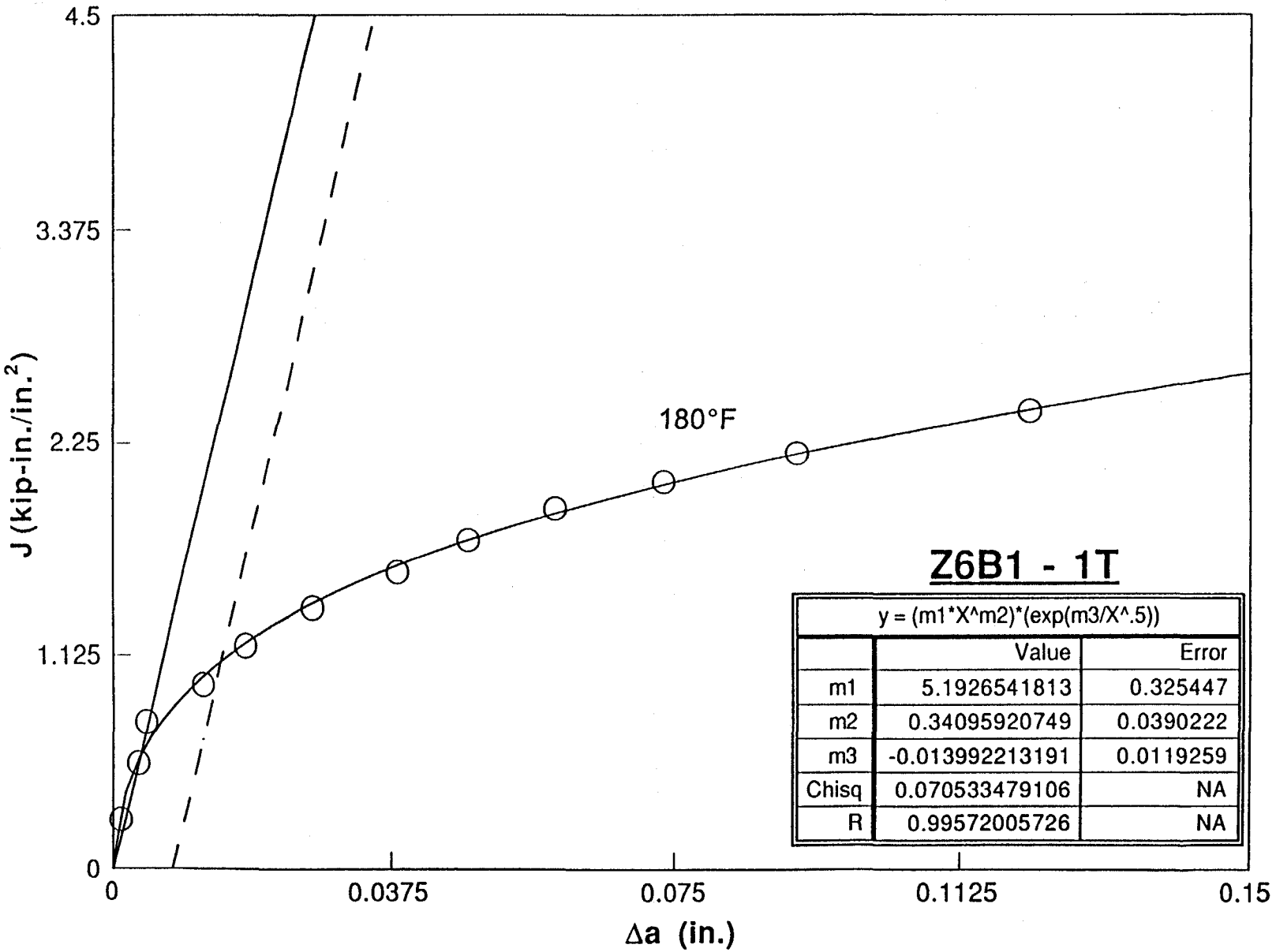
4.5
3.375
2.25
1.125
0
J (kip-in./in.²)
0
0.0375
0.075
0.1125
0.15
Δa (in.)
180°F
Z6B1 - 1T
y = (m1*X^m2)*(exp(m3/X^.5))
Value
Error
m1
5.1926541813
0.325447
m2
0.34095920749
0.0390222
m3
-0.013992213191
0.0119259
Chisq
0.070533479106
NA
R
0.99572005726
NA

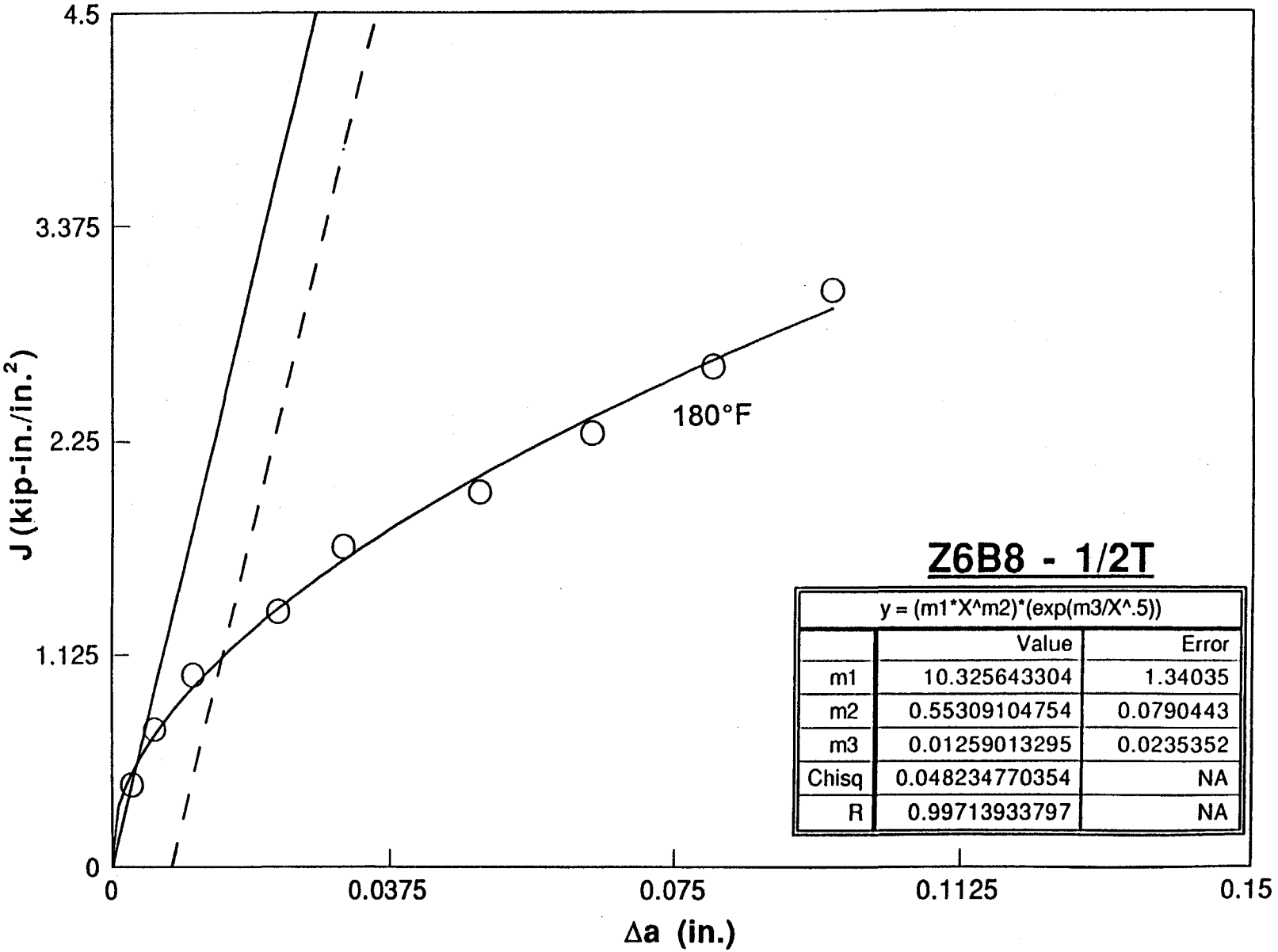
4.5
3.375
2.25
1.125
0
J (kip-in./in.²)
0
0.0375
0.075
0.1125
0.15
Δa (in.)
180°F
Z6B8 - 1/2T
y = (m1*X^m2)*(exp(m3/X^.5))
Value
Error
m1 10.325643304 1.34035
m2 0.5530104754 0.0790443
m3 0.01259013295 0.0235352
Chisq 0.048234770354 NA
R 0.99713933797 NA

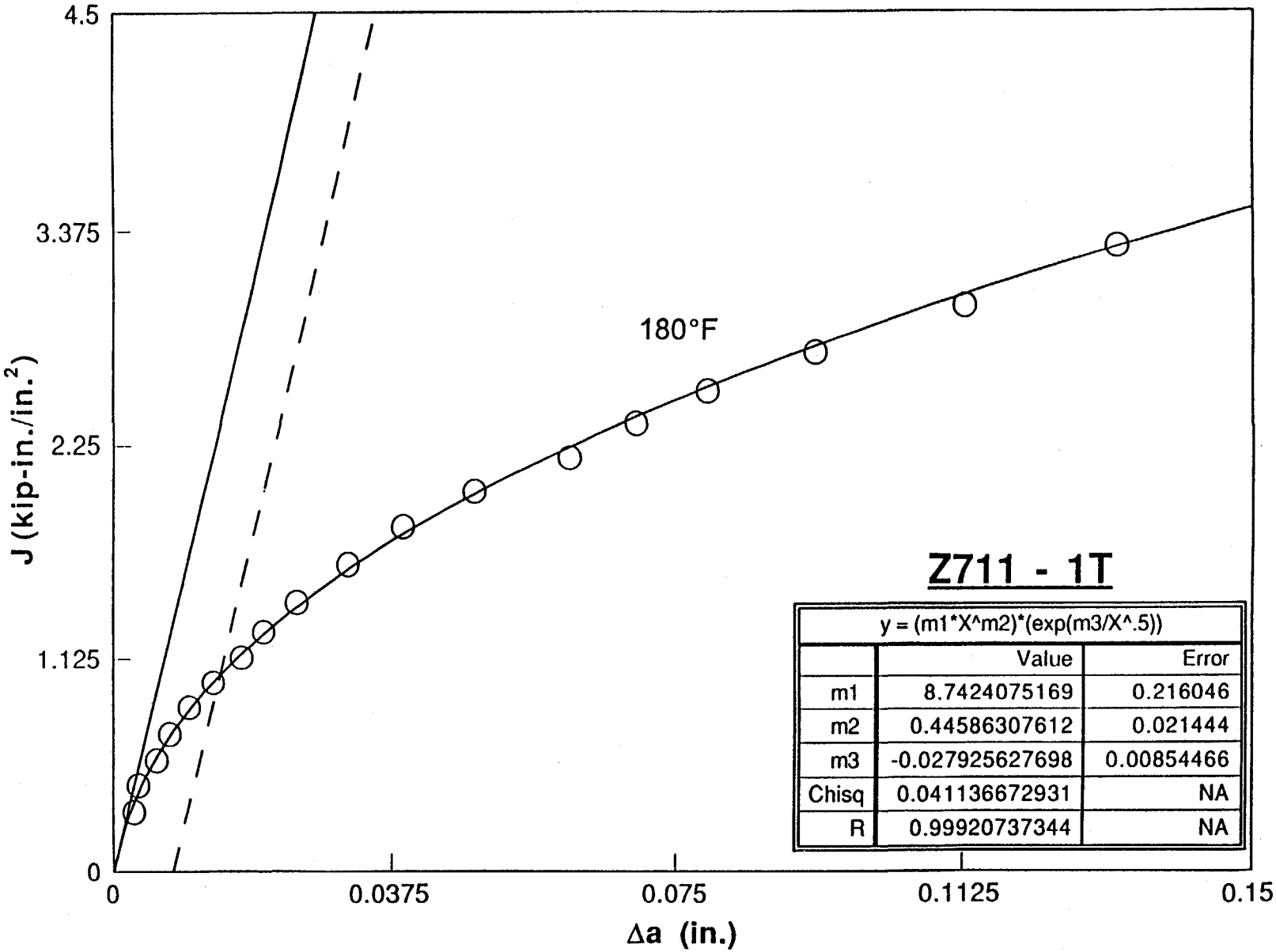
4.5
3.375
2.25
1.125
0
J (kip-in./in.²)
0
0.0375
0.075
0.1125
0.15
Δa (in.)
180°F
Z711 - 1T
y = (m1*X^m2)*(exp(m3/X^.5))
Value
Error
m1 8.7424075169 0.216046
m2 0.44586307612 0.021444
m3 -0.027925627698 0.00854466
Chisq 0.041136672931 NA
R 0.99920737344 NA

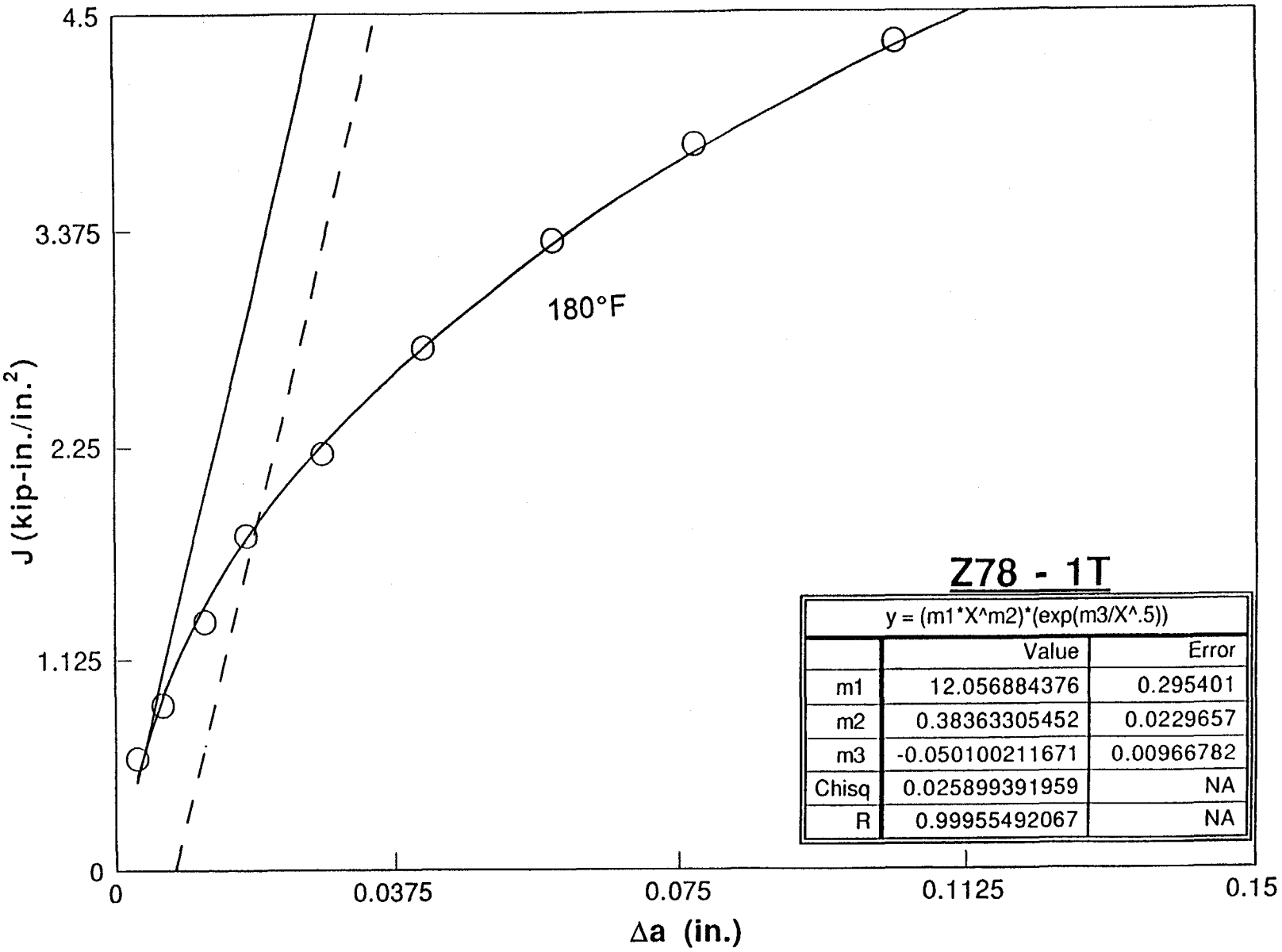
4.5
3.375
2.25
1.125
0
J (kip-in./in.^{2})
0
0.0375
0.075
0.1125
0.15
Δa (in.)
180°F
Z78 - 1T
y = (m1*X^m2)*(exp(m3/X^.5))
Value
Error
m1
12.056884376
0.295401
m2
0.38363305452
0.0229657
m3
-0.050100211671
0.00966782
Chisq
0.025899391959
NA
R
0.99955492067
NA

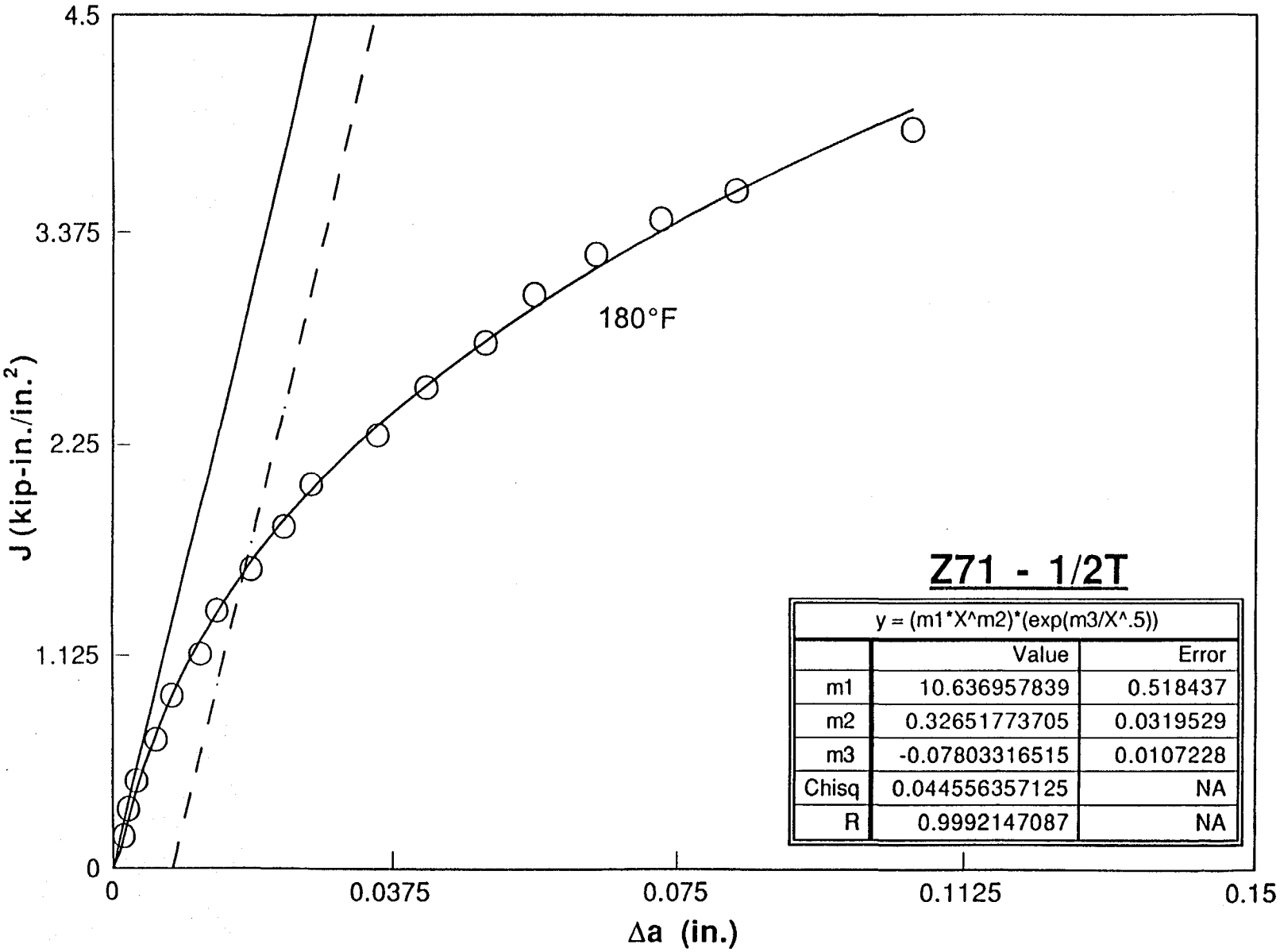

Z71 - 1/2T

y = (m1*X^m2)*(exp(m3/X^.5))

	Value	Error
m1	10.636957839	0.518437
m2	0.32651773705	0.0319529
m3	-0.07803316515	0.0107228
Chisq	0.044556357125	NA
R	0.9992147087	NA

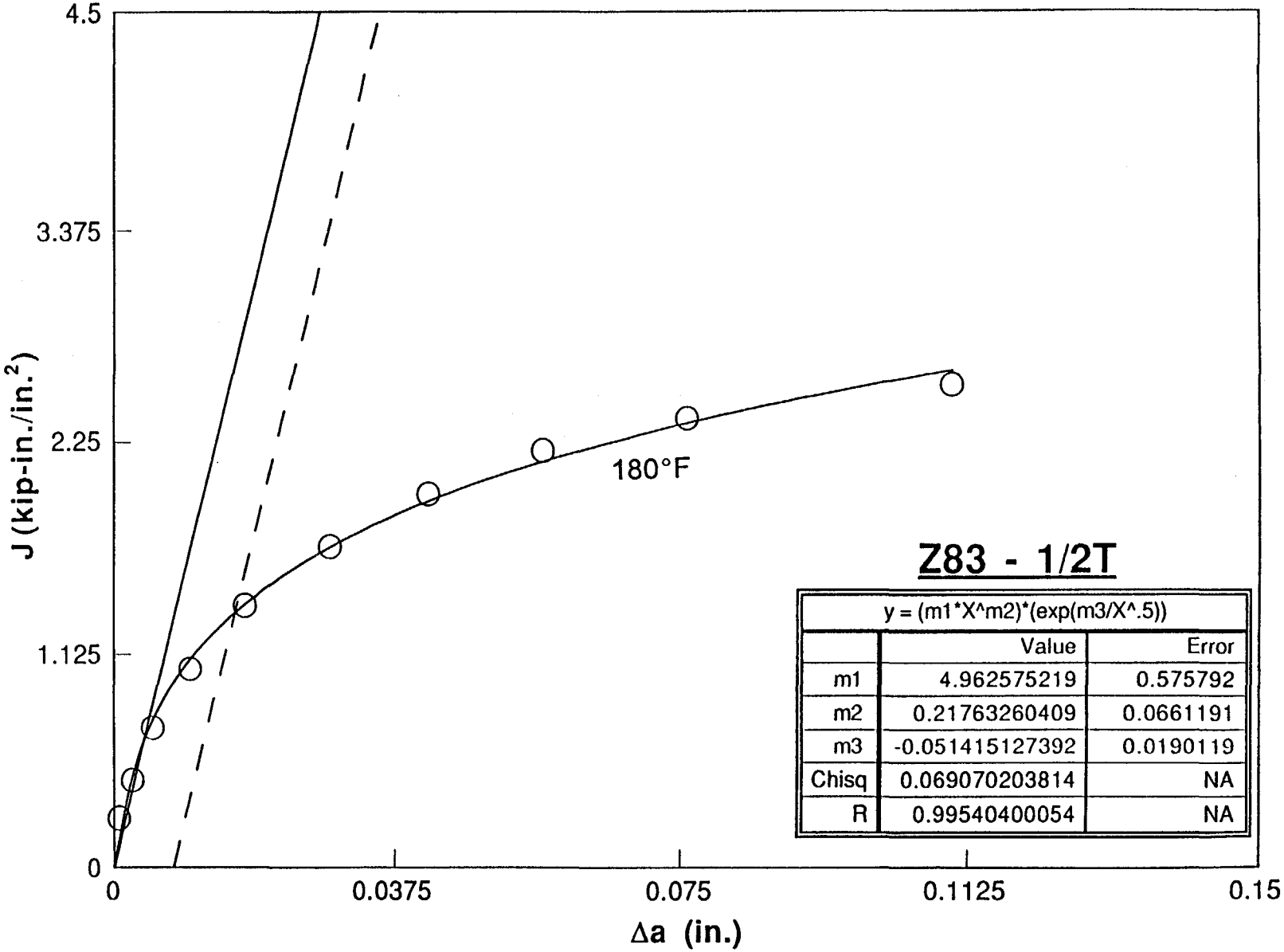
4.5
3.375
2.25
1.125
0
J (kip-in./in.^{2})
0
0.0375
0.075
0.1125
0.15
Δa (in.)
180°F
Z83 - 1/2T
y = (m1*X^m2)*(exp(m3/X^.5))
Value
Error
m1 4.962575219 0.575792
m2 0.21763260409 0.0661191
m3 -0.051415127392 0.0190119
Chisq 0.069070203814 NA
R 0.99540400054 NA

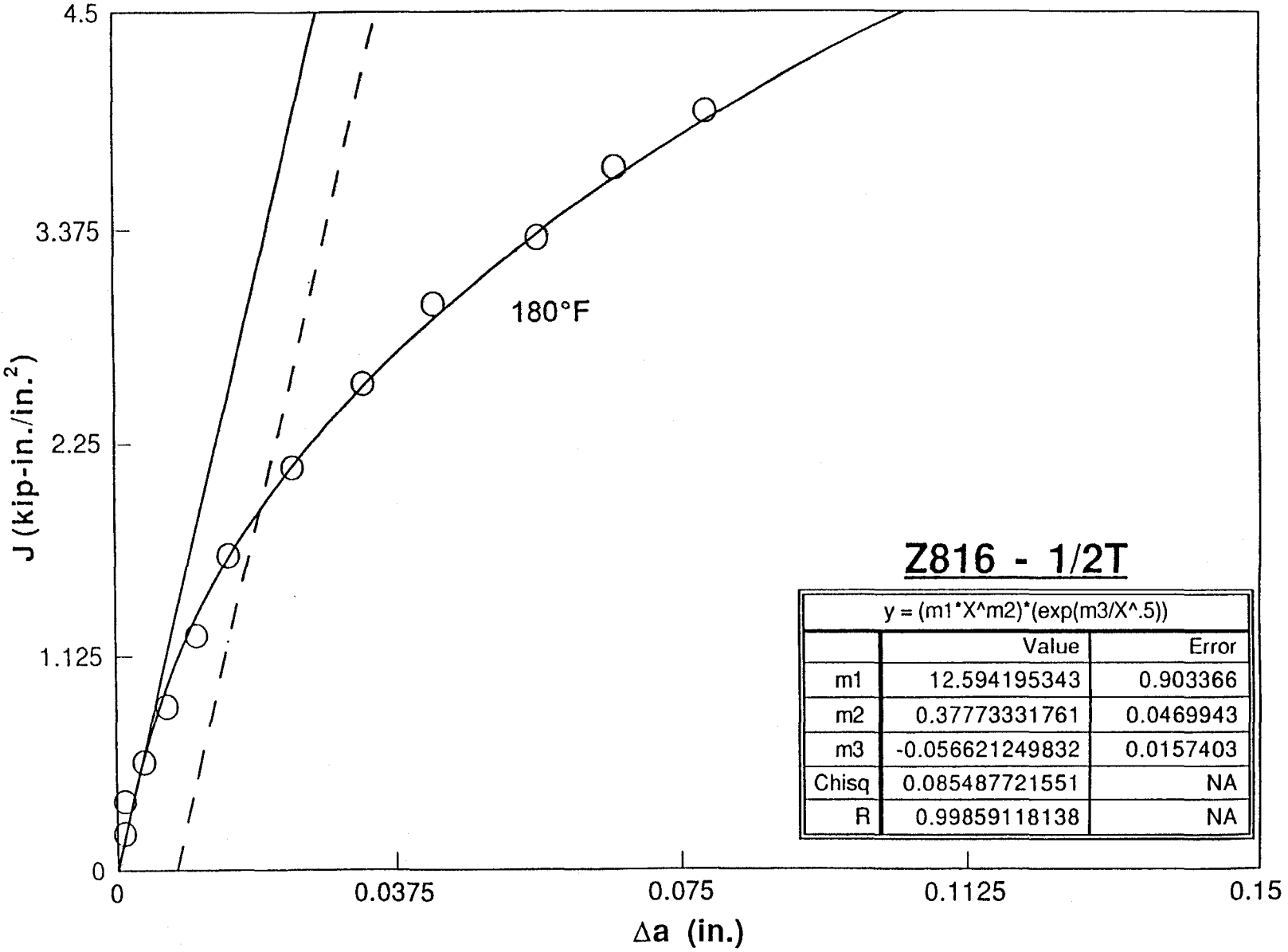

Z816 - 1/2T

y = (m1*X^m2)*(exp(m3/X^.5))		
	Value	Error
m1	12.594195343	0.903366
m2	0.37773331761	0.0469943
m3	-0.056621249832	0.0157403
Chisq	0.085487721551	NA
R	0.99859118138	NA

Appendix B

Selected J-R Curves Representing Typical Values of T Slope, $J_{0.1}$, and J_{Ic} from Table 8

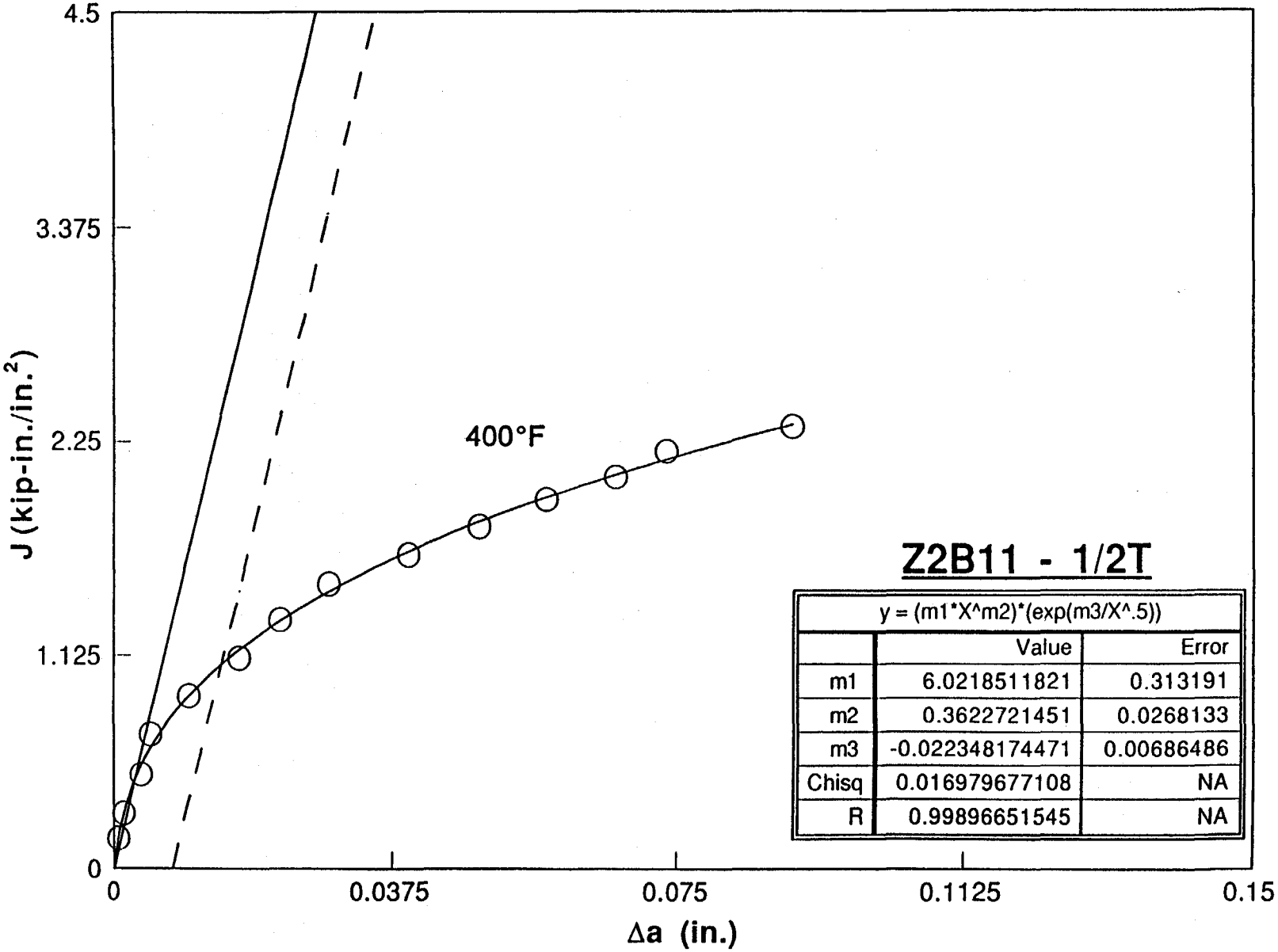

Z2B11 - 1/2T

y = (m1*X^m2)*(exp(m3/X^.5))		
	Value	Error
m1	6.0218511821	0.313191
m2	0.3622721451	0.0268133
m3	-0.022348174471	0.00686486
Chisq	0.016979677108	NA
R	0.99896651545	NA

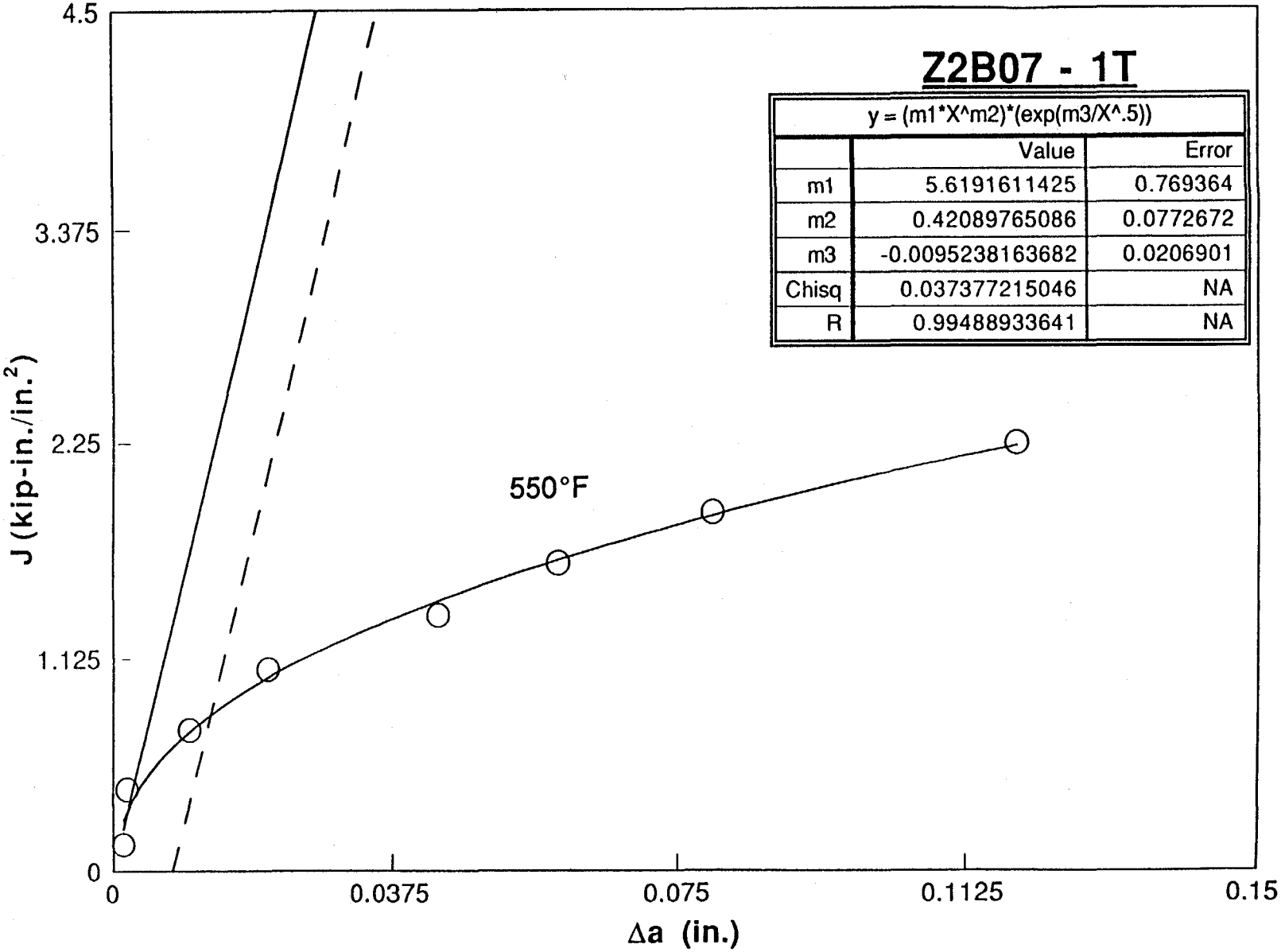
Z2B07 - 1T
y = (m1*X^m2)*(exp(m3/X^.5))
Value
Error
m1
5.6191611425
0.769364
m2
0.42089765086
0.0772672
m3
-0.0095238163682
0.0206901
Chisq
0.037377215046
NA
R
0.99488933641
NA
550°F
J (kip-in./in.²)
Δa (in.)
4.5
3.375
2.25
1.125
0
0
0.0375
0.075
0.1125
0.15

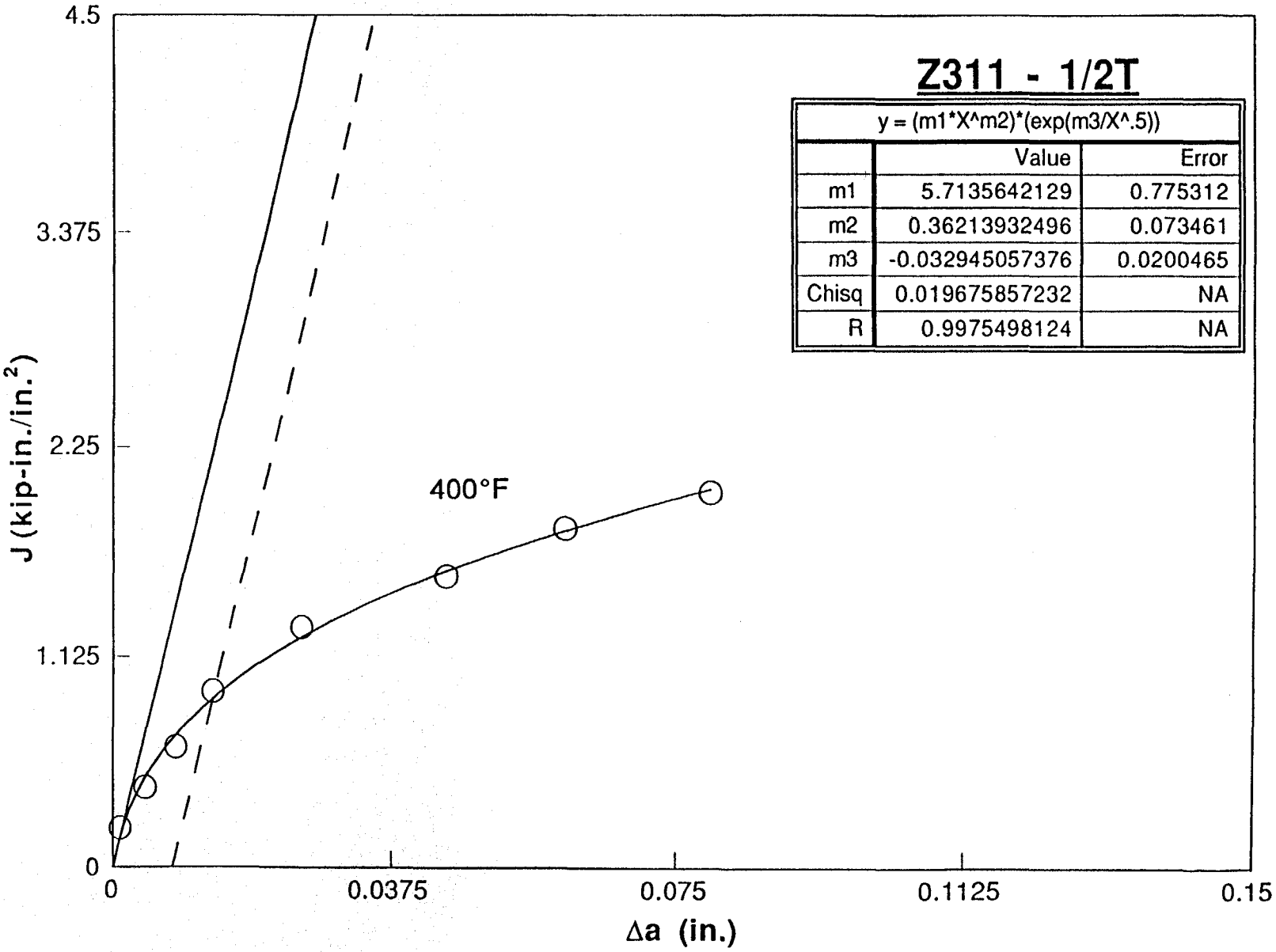
Z311 - 1/2T
y = (m1*X^m2)*(exp(m3/X^.5))
Value
Error
m1
5.7135642129
0.775312
m2
0.36213932496
0.073461
m3
-0.032945057376
0.0200465
Chisq
0.019675857232
NA
R
0.9975498124
NA
400°F
J (kip-in./in.²)
Δa (in.)
4.5
3.375
2.25
1.125
0
0
0.0375
0.075
0.1125
0.15

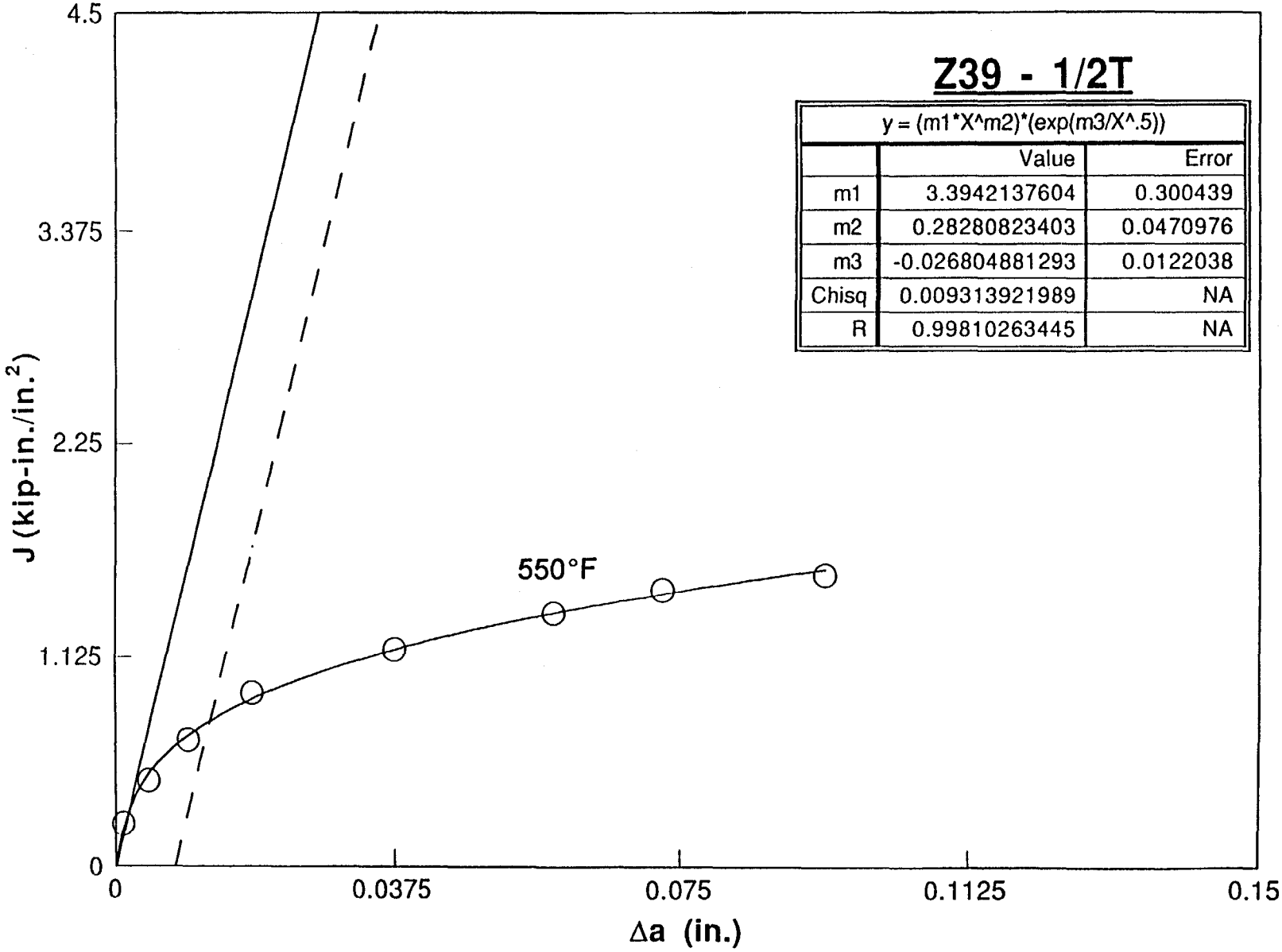
Z39 - 1/2T
y = (m1*X^m2)*(exp(m3/X^.5))
Value
Error
m1
3.3942137604
0.300439
m2
0.28280823403
0.0470976
m3
-0.026804881293
0.0122038
Chisq
0.009313921989
NA
R
0.99810263445
NA
550°F
J (kip-in./in.²)
Δa (in.)
4.5
3.375
2.25
1.125
0
0
0.0375
0.075
0.1125
0.15

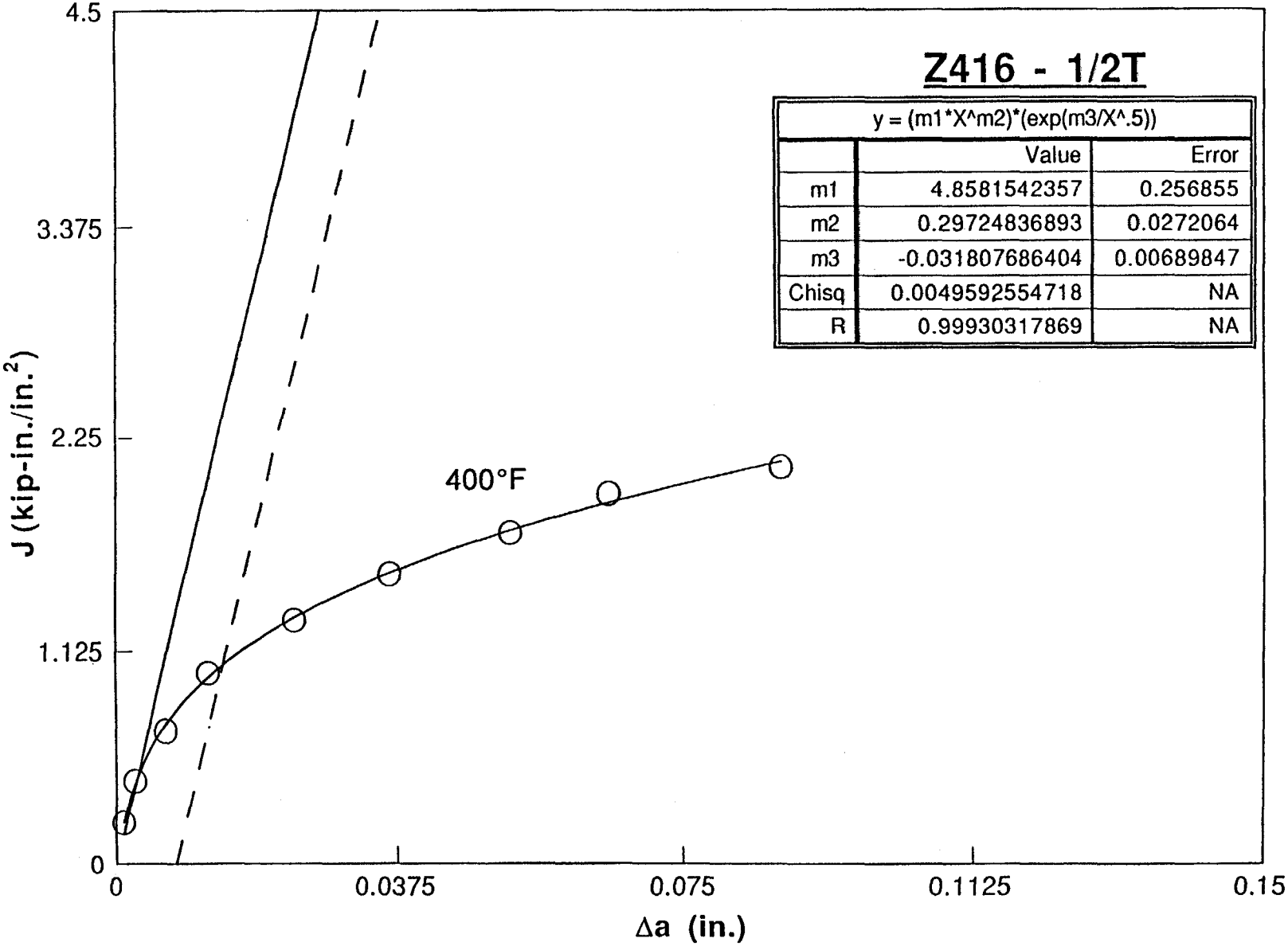
Z416 - 1/2T
y = (m1*X^m2)*(exp(m3/X^.5))
Value
Error
m1
4.8581542357
0.256855
m2
0.29724836893
0.0272064
m3
-0.031807686404
0.00689847
Chisq
0.0049592554718
NA
R
0.99930317869
NA
400°F
J (kip-in./in.²)
Δa (in.)
4.5
3.375
2.25
1.125
0
0
0.0375
0.075
0.1125
0.15

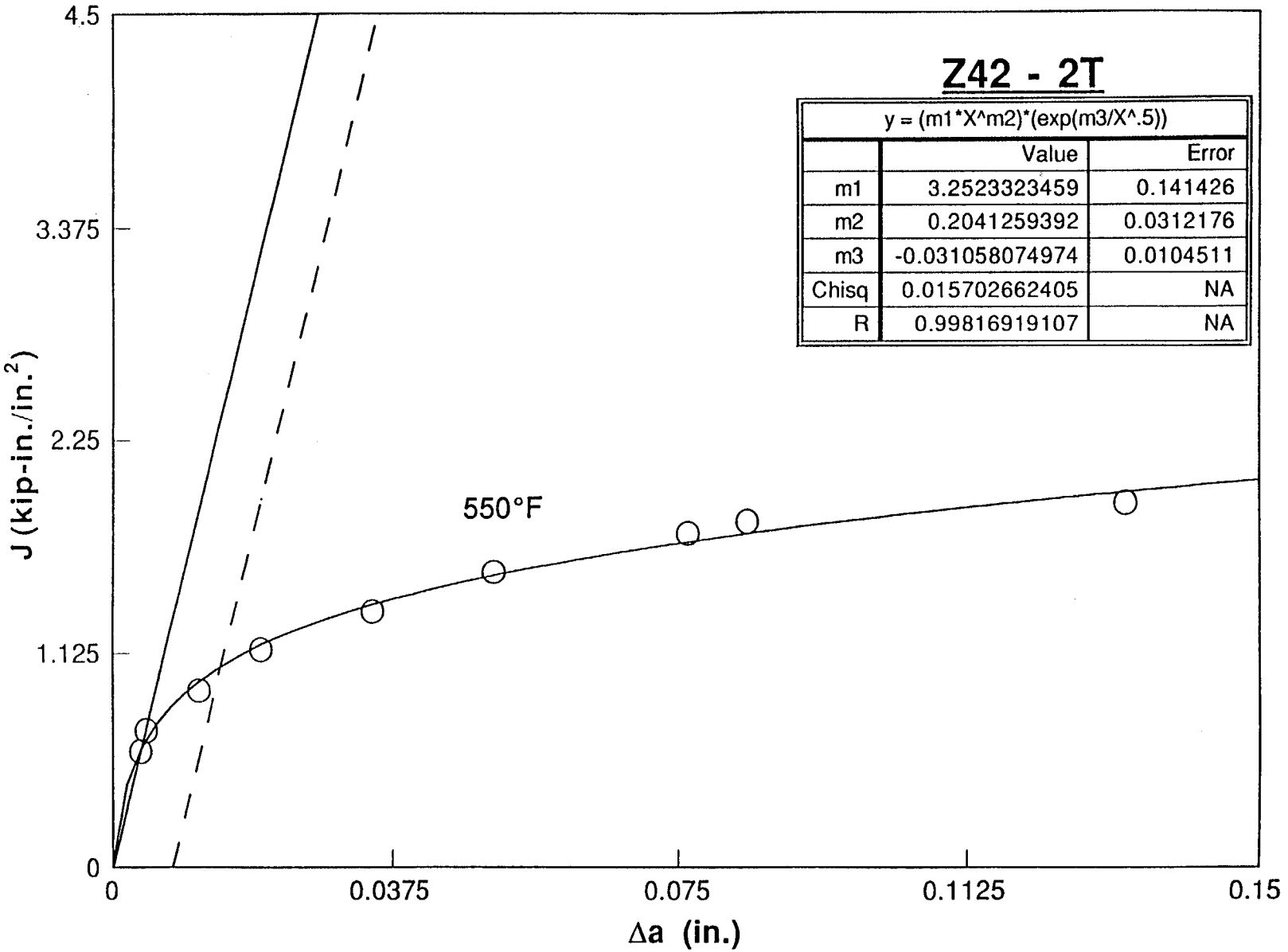
Z42 - 2T
y = (m1*X^m2)*(exp(m3/X^.5))
Value
Error
m1
3.2523323459
0.141426
m2
0.2041259392
0.0312176
m3
-0.031058074974
0.0104511
Chisq
0.015702662405
NA
R
0.99816919107
NA
550°F
J (kip-in./in.^{2})
Δa (in.)
4.5
3.375
2.25
1.125
0
0
0.0375
0.075
0.1125
0.15

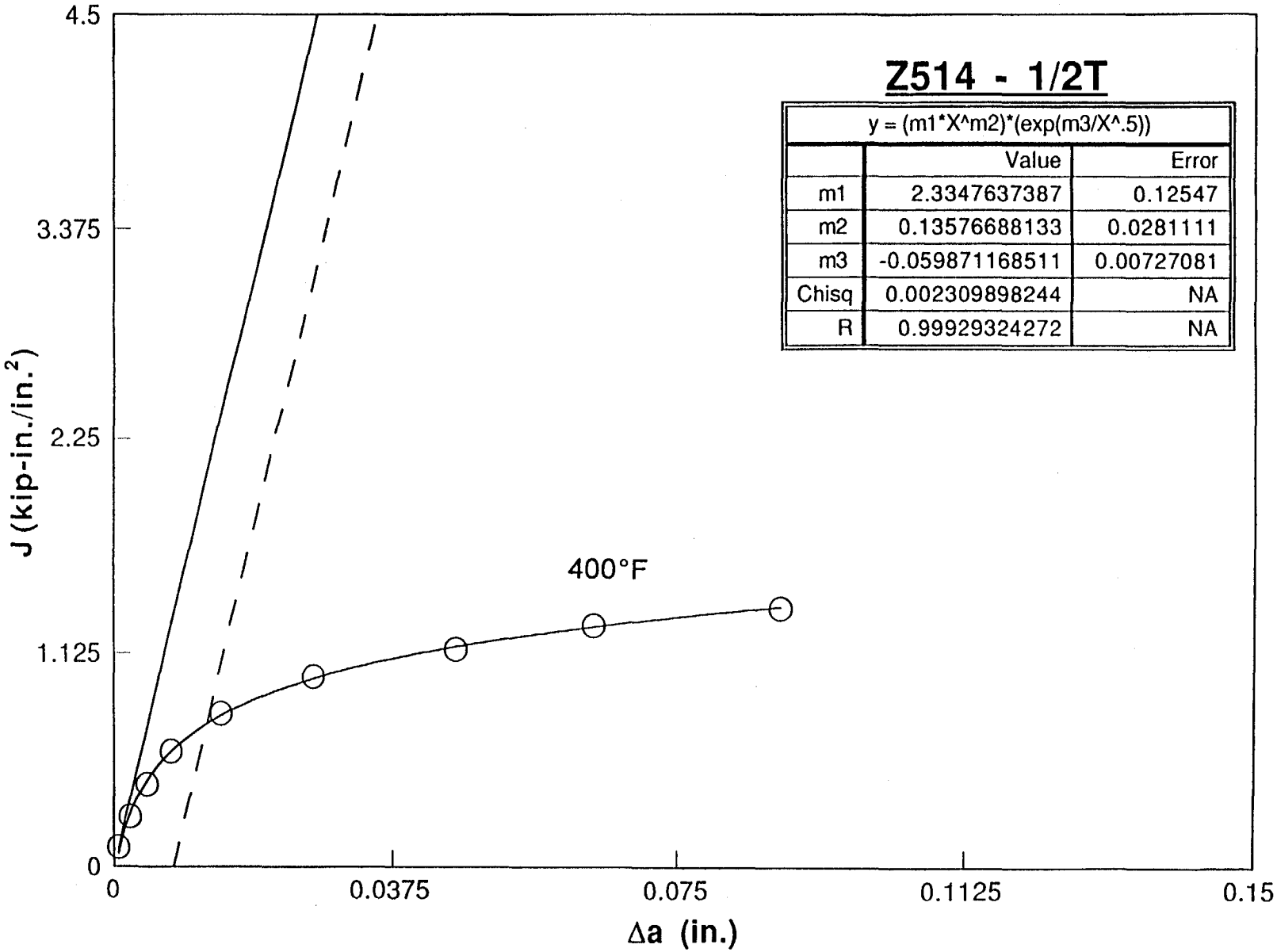
Z514 - 1/2T
y = (m1*X^m2)*(exp(m3/X^.5))
Value
Error
m1
2.3347637387
0.12547
m2
0.13576688133
0.0281111
m3
-0.059871168511
0.00727081
Chisq
0.002309898244
NA
R
0.99929324272
NA
400°F
J (kip-in./in.²)
Δa (in.)
4.5
3.375
2.25
1.125
0
0
0.0375
0.075
0.1125
0.15

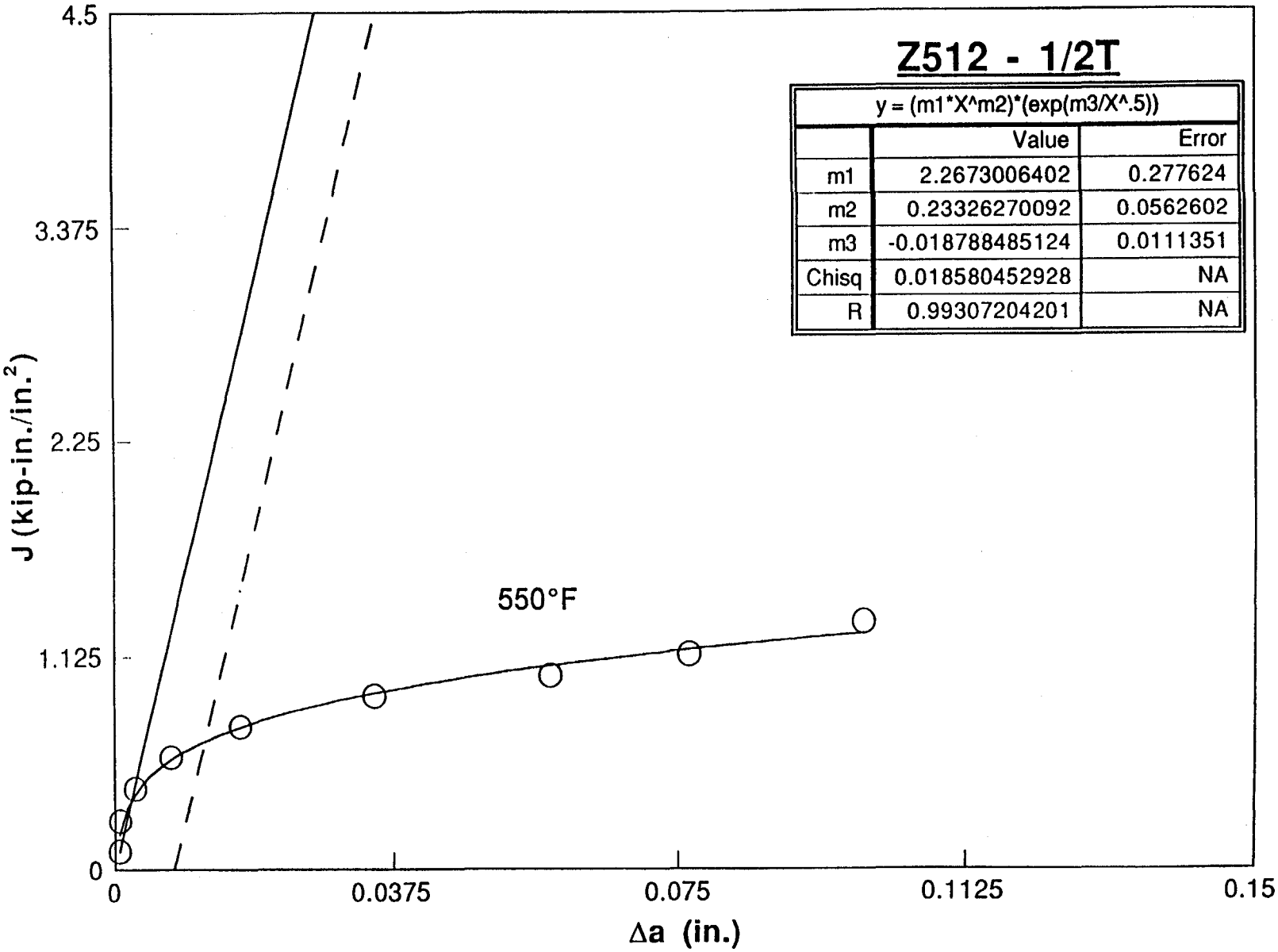
Z512 - 1/2T
y = (m1*X^m2)*(exp(m3/X^.5))
Value
Error
m1
2.2673006402
0.277624
m2
0.23326270092
0.0562602
m3
-0.018788485124
0.0111351
Chisq
0.018580452928
NA
R
0.99307204201
NA
550°F
J (kip-in./in.²)
Δa (in.)
4.5
3.375
2.25
1.125
0
0
0.0375
0.075
0.1125
0.15

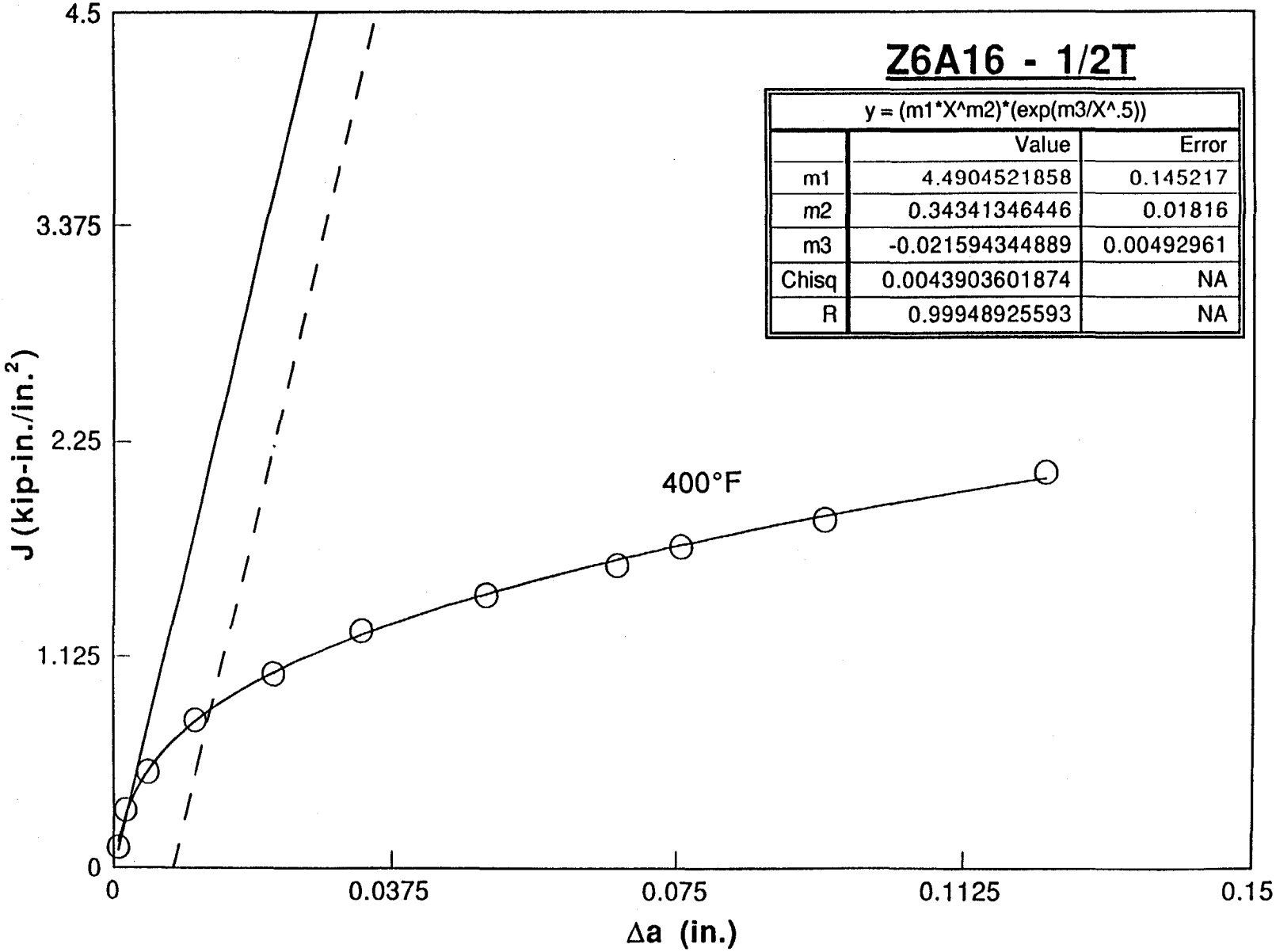
Z6A16 - 1/2T
y = (m1*X^m2)*(exp(m3/X^.5))
Value
Error
m1
4.4904521858
0.145217
m2
0.34341346446
0.01816
m3
-0.021594344889
0.00492961
Chisq
0.0043903601874
NA
R
0.99948925593
NA
400°F
J (kip-in./in.²)
Δa (in.)
4.5
3.375
2.25
1.125
0
0
0.0375
0.075
0.1125
0.15

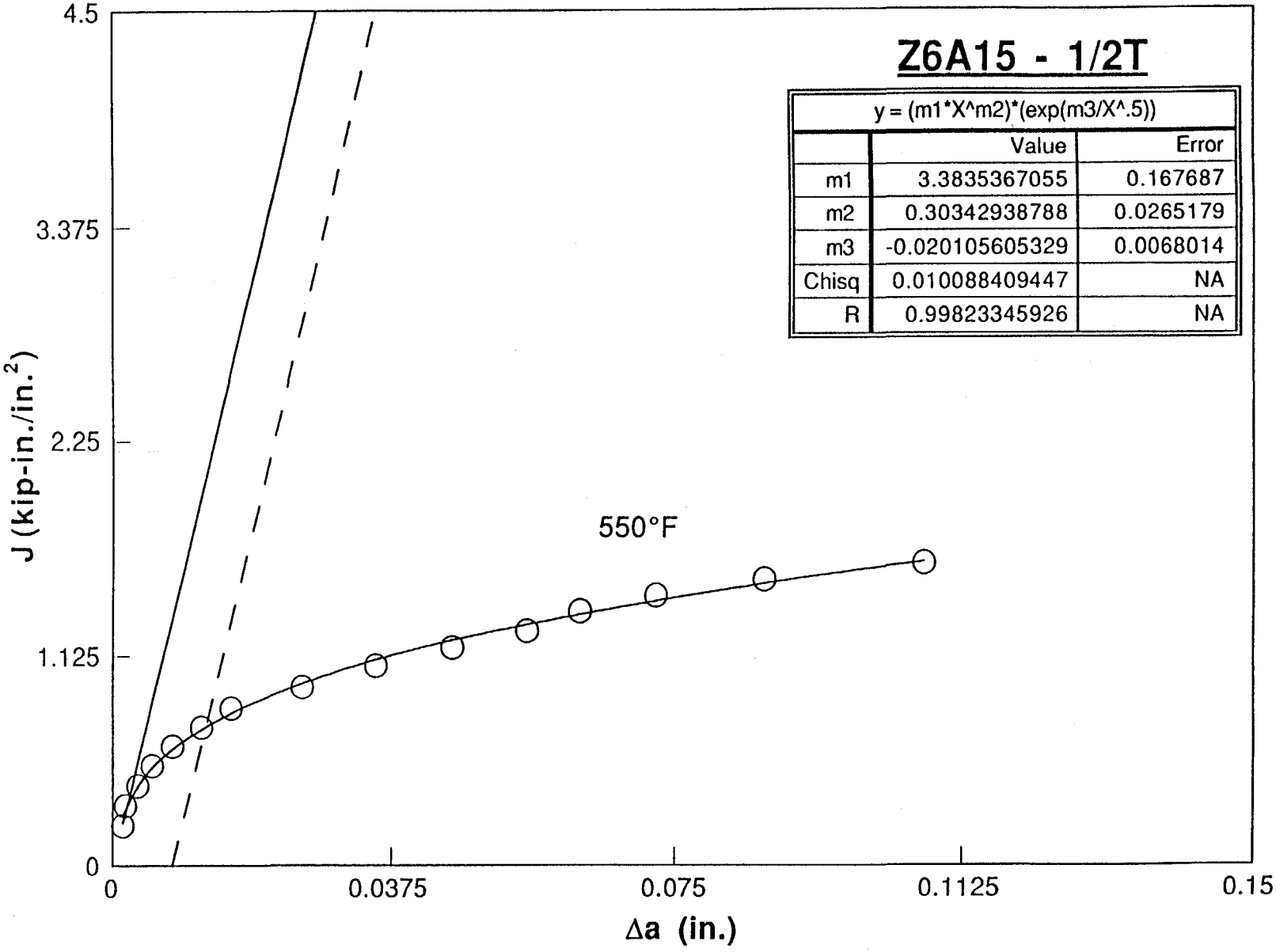
Z6A15 - 1/2T
y = (m1*X^m2)*(exp(m3/X^.5))
Value
Error
m1
3.3835367055
0.167687
m2
0.30342938788
0.0265179
m3
-0.020105605329
0.0068014
Chisq
0.010088409447
NA
R
0.99823345926
NA
550°F
J (kip-in./in.²)
Δa (in.)
4.5
3.375
2.25
1.125
0
0
0.0375
0.075
0.1125
0.15

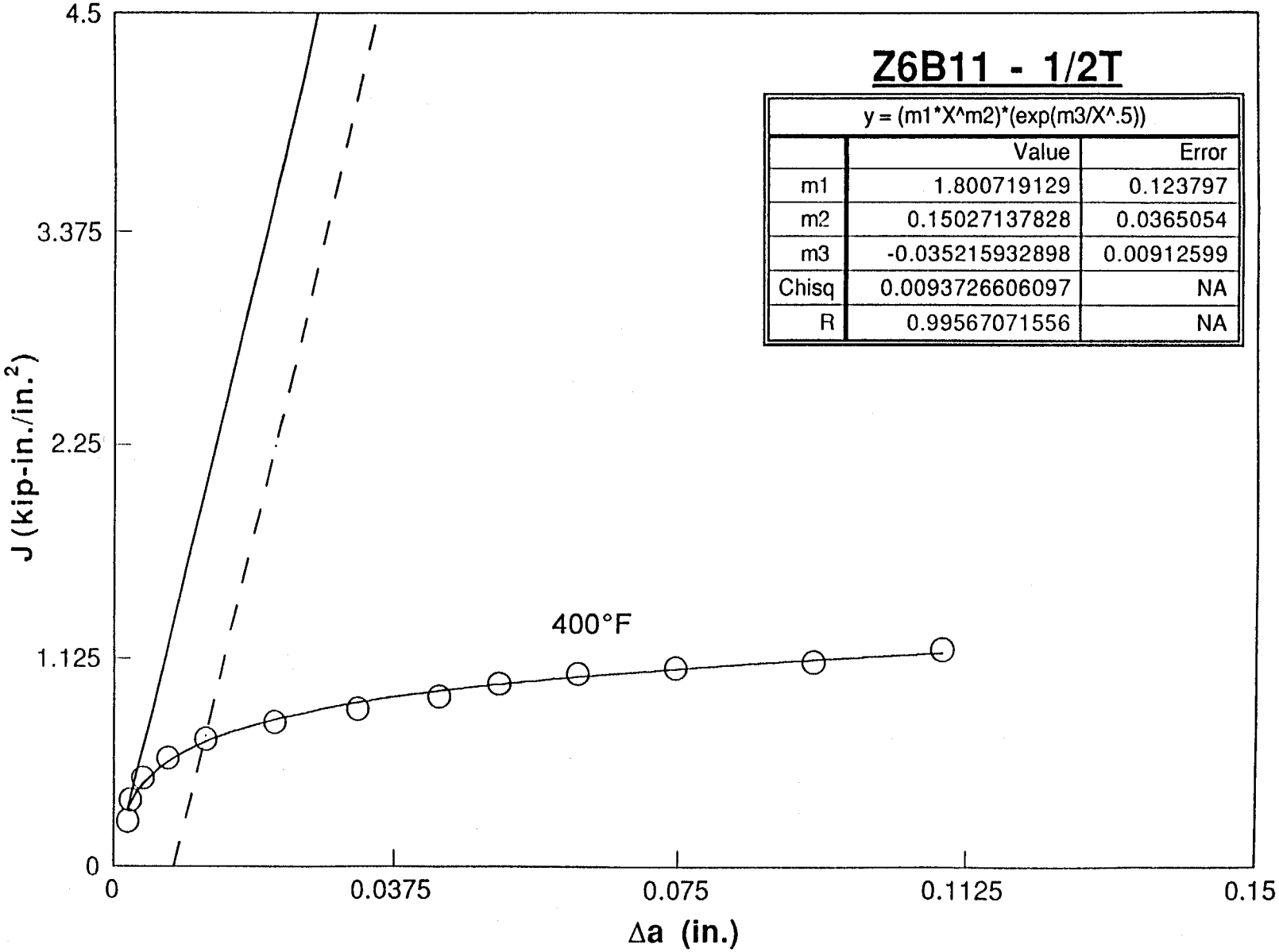
Z6B11 - 1/2T
y = (m1*X^m2)*(exp(m3/X^.5))
Value
Error
m1
1.800719129
0.123797
m2
0.15027137828
0.0365054
m3
-0.035215932898
0.00912599
Chisq
0.0093726606097
NA
R
0.99567071556
NA
400°F
J (kip-in./in.²)
Δa (in.)
4.5
3.375
2.25
1.125
0
0
0.0375
0.075
0.1125
0.15

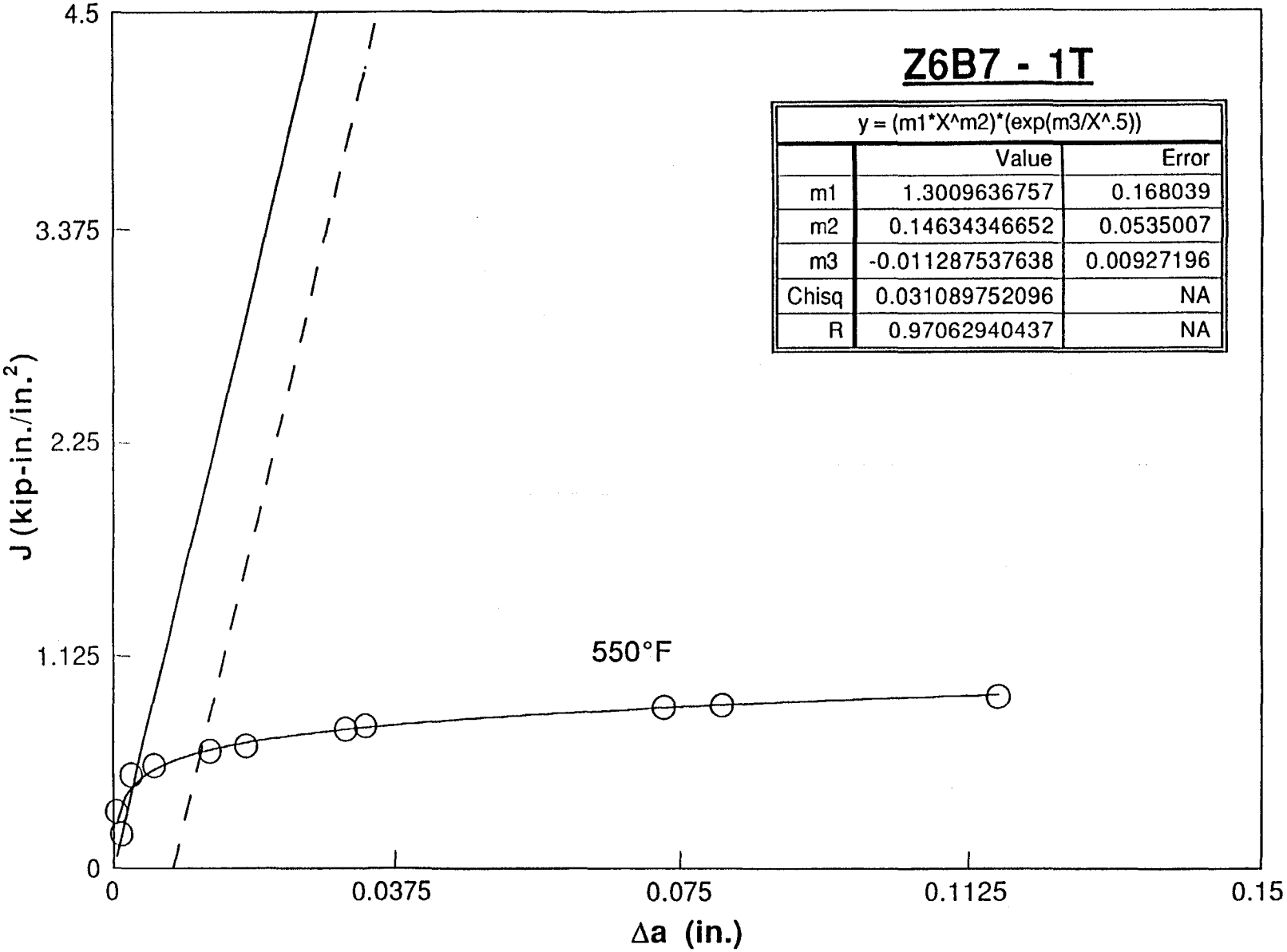
Z6B7 - 1T
y = (m1*X^m2)*(exp(m3/X^.5))
Value
Error
m1
1.3009636757
0.168039
m2
0.14634346652
0.0535007
m3
-0.011287537638
0.00927196
Chisq
0.031089752096
NA
R
0.97062940437
NA
550°F
J (kip-in./in.2)
Δa (in.)
4.5
3.375
2.25
1.125
0
0
0.0375
0.075
0.1125
0.15

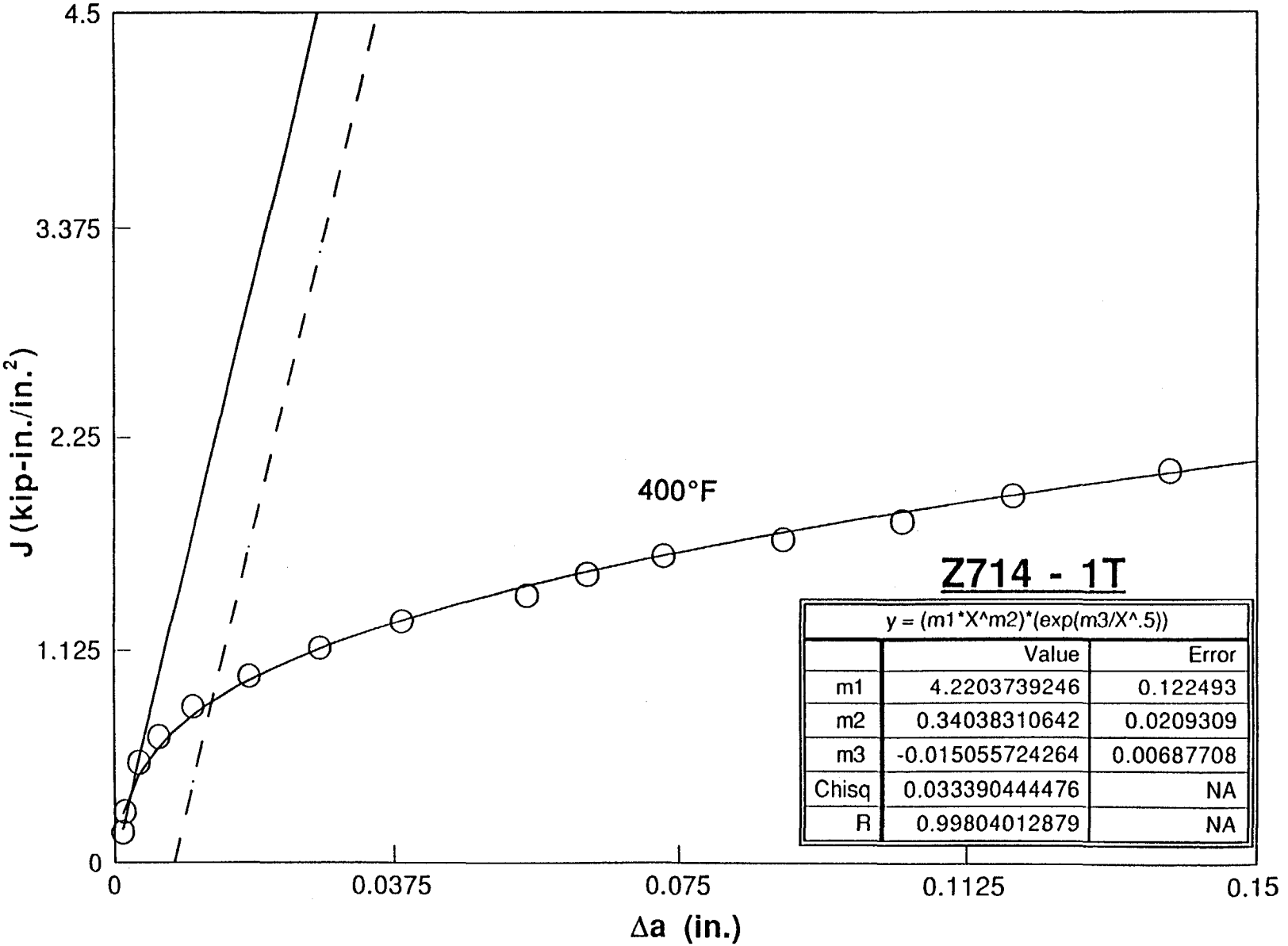

y = (m1*X^m2)*(exp(m3/X^.5))		
	Value	Error
m1	4.2203739246	0.122493
m2	0.34038310642	0.0209309
m3	-0.015055724264	0.00687708
Chisq	0.033390444476	NA
R	0.99804012879	NA

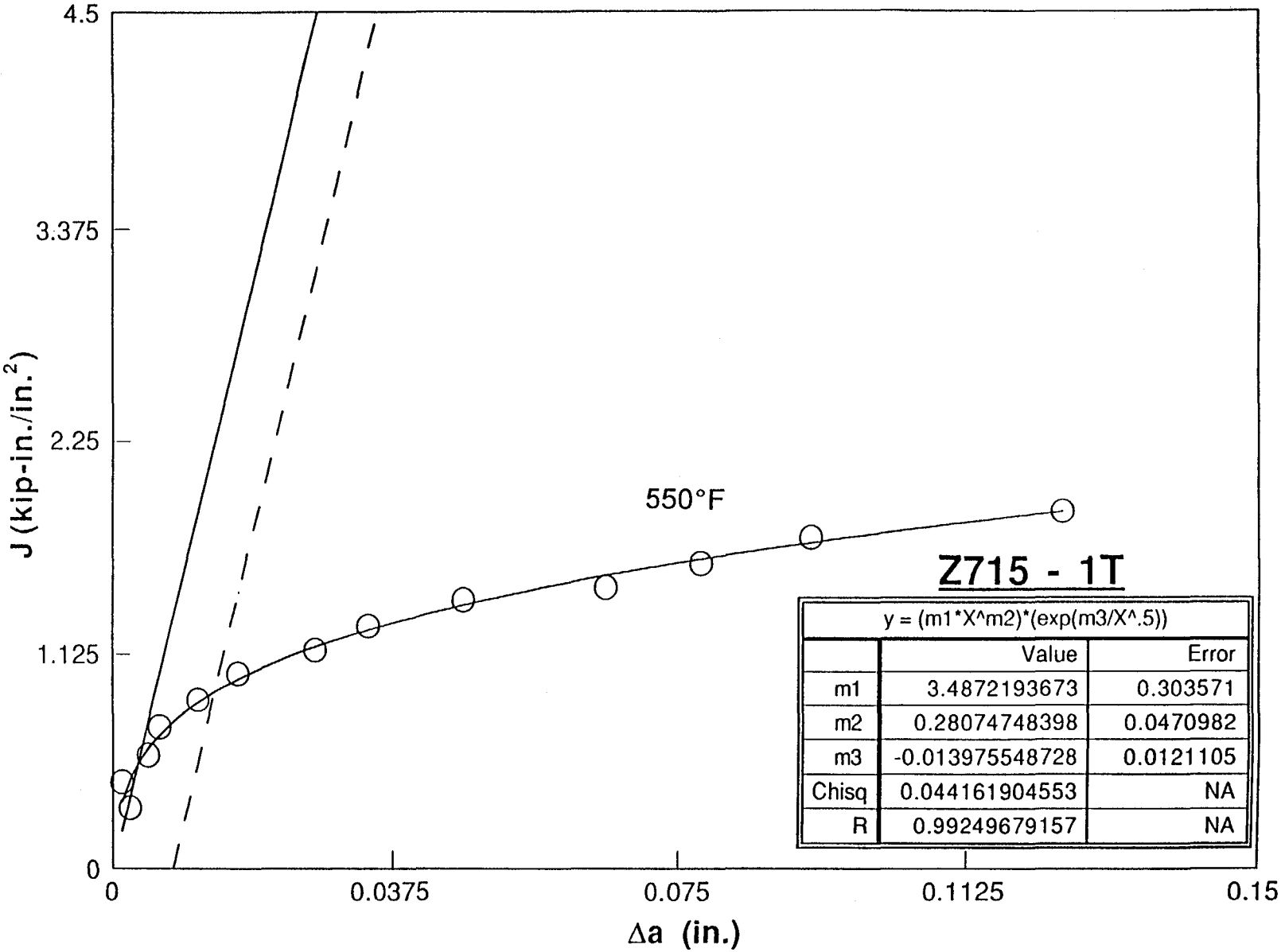
4.5
3.375
2.25
1.125
0
J (kip-in./in.^{2})
0
0.0375
0.075
0.1125
0.15
Δa (in.)
550°F
Z715 - 1T
y = (m1*X^m2)*(exp(m3/X^.5))
Value
Error
m1 3.4872193673 0.303571
m2 0.28074748398 0.0470982
m3 -0.013975548728 0.0121105
Chisq 0.044161904553 NA
R 0.99249679157 NA

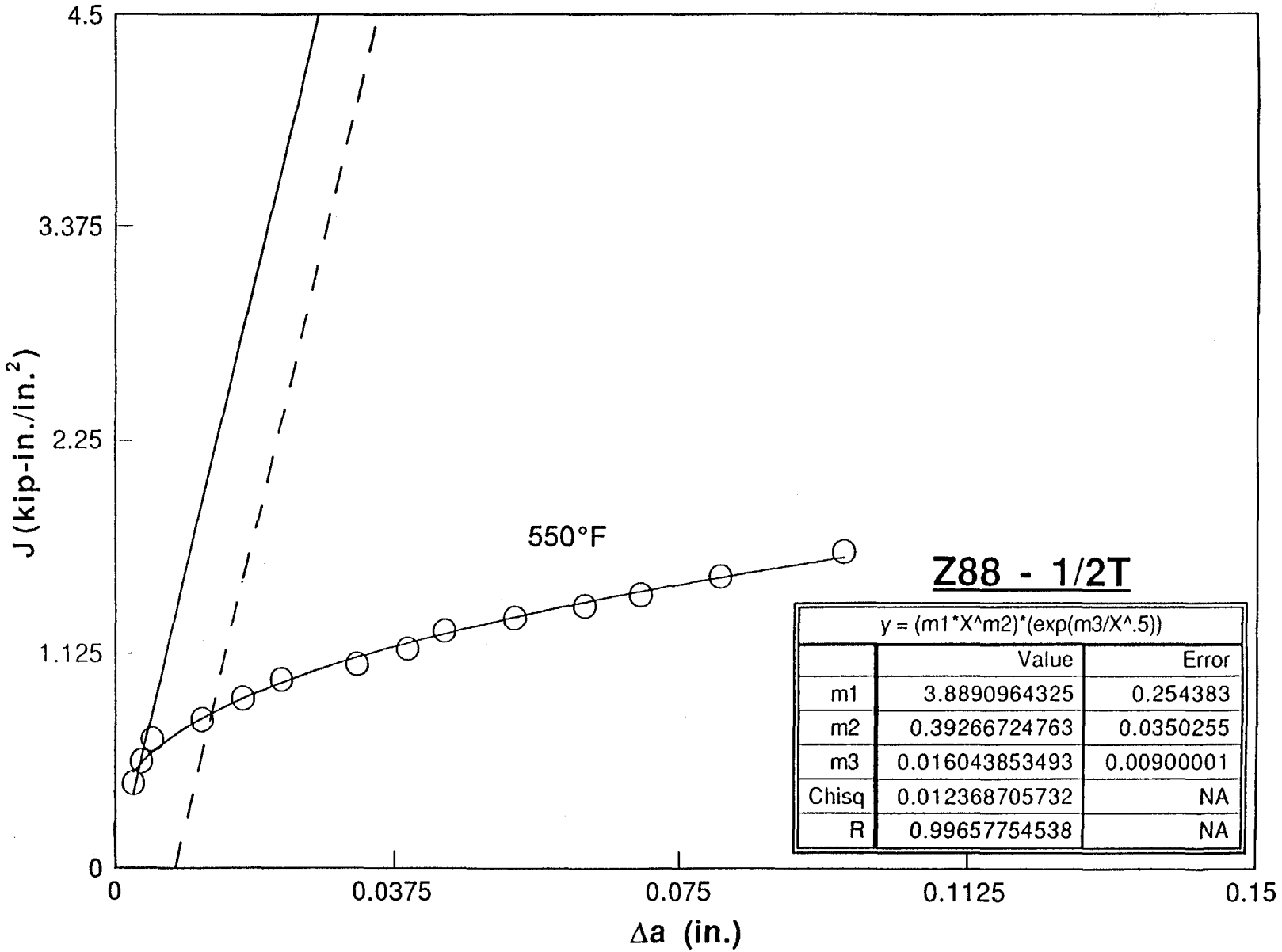
4.5
3.375
2.25
1.125
0
J (kip-in./in.^{2})
0
0.0375
0.075
0.1125
0.15
Δa (in.)
550°F
Z88 - 1/2T
y = (m1*X^m2)*(exp(m3/X^.5))
Value
Error
m1
3.8890964325
0.254383
m2
0.39266724763
0.0350255
m3
0.016043853493
0.00900001
Chisq
0.012368705732
NA
R
0.99657754538
NA

Internal Distribution

1. D. J. Alexander
2. B. R. Bass
3. J. W. Bryson
4. W. R. Corwin
5. W. G. Craddick
6. D. F. Craig
7. T. L. Dickson
8. E. C. Fox
9. H. W. Hayden, Jr.
10. J. J. Henry, Jr.
11. S. K. Iskander
12. W. F. Jackson
13. J. A. Keeney
14. R. L. Klueh

15-19. E. T. Manneschmidt
20. W. J. McAfee
21-25. D. E. McCabe
26. J. G. Merkle
27-29. R. K. Nanstad
30. D. J. Naus
31-33. W. E. Pennell
34. C. E. Pugh
35. M. A. Sokolov
36. R. E. Stoller

37-41. R. L. Swain
42. R. W. Swindeman
43. ORNL Patent Section
44. Central Research Library
45. Document Reference Section

46-47. M&C Records Office
48-49. Laboratory Records
50. Laboratory Records - RC

External Distribution

51. R. D. Thompson, Office of Administration, Division of Contracts, U. S. Nuclear Regulatory Commission, Mailstop T7 I2, Washington, DC, 20555-0001
52. B. J. Elliot, Division of Engineering, Office of Nuclear Reactor Regulation, Mailstop O7 D4, U.S. Nuclear Regulatory Commission, Washington, DC 20555-0001
53. J. R. Strosnider, Division of Engineering, Office of Nuclear Reactor Regulation, Mailstop O7 D4, U.S. Nuclear Regulatory Commission, Washington, DC 20555-0001
54. K. R. Wichman, Division of Engineering, Office of Nuclear Reactor Regulation, Mailstop O7 D4, U.S. Nuclear Regulatory Commission, Washington, DC 20555-0001
55. M. A. Mitchell, Division of Engineering Technology, Office of Nuclear Reactor Regulation, Mailstop O7 D4, U.S. Nuclear Regulatory Commission, Washington, DC 20555-0001
56. E. M. Hackett, EMMEB/DET/RES, Mailstop T10 E10, U.S. Nuclear Regulatory Commission, Washington, DC 20555-0001
57. R. E. Johnson, EMMEB/DET/RES, U.S. Nuclear Regulatory Commission, Mailstop T10 E10, Washington, DC 20555-0001
58-59. S. N. Malik, EMMEB/DET/RES, U.S. Nuclear Regulatory Commission, Mailstop T10 E10, Washington, DC 20555-0001
60. M. E. Mayfield, EMMEB/DET/RES, U.S. Nuclear Regulatory Commission, Mailstop T10 E10, Washington, DC
61. G. C. Millman, Division of Engineering Technology, U.S. Nuclear Regulatory Commission, Mailstop T10 E10, Washington, DC 20555-0001
62. L. C. Shao, Division of Engineering Technology, U.S. Nuclear Regulatory Commission, Mailstop T10 D20, Washington, DC 20555-0001
63. M. G. Vassilaros, EMMEB/DET/RES, U.S. Nuclear Regulatory Commission, Mailstop T10 E10, Washington, DC 20555-0001
64. J. W. Dally, Department of Mechanical Engineering, University of Maryland, College Park, Maryland 20742
65. E. Eason, Modeling and Computing Services, Suite 105, 6400 Lookout Road, Boulder, Colorado 80301
66. J. D. Landes, University of Tennessee, Engineering Science and Mechanics, 310 Perkins Hall, Knoxville, Tennessee 37996-2030
67. R. E. Link, U.S. Naval Academy, Mechanical Engineering Department, Mailstop 11C, 590 Hollway Road, Annapolis, Maryland 21402

68. J. A. Joyce, U.S. Naval Academy, Mechanical Engineering Department, MS 11C, 590 Hollway Road, Annapolis, Maryland 21402
69. T. Caine, General Electric Nuclear Energy, Mail Code 747, 175 Curtner Avenue, San Jose, California 95125
70. M. L. Hamilton, Battelle Pacific Northwest National Laboratory, Structural Materials Research Section, MS P8-15, Battelle Boulevard, P. O. Box 999, Richland, Washington 99352
71. W. A. Van der Sluys, Babcock and Wilcox, R&D Division, 1562 Beeson Street, Alliance, Ohio 44601
72. G. R. Irwin, Department of Mechanical Engineering, University of Maryland, College Park, Maryland 20742
73. L. A. James, Westinghouse Bettis Lab., P. O. Box 79, ZAP 13A, 814 Pittsburgh McKeesport Blvd., West Mifflin, Pennsylvania 15122
74. C. F. Shih, Box D, Division of Engineering, Brown University, Providence, Rhode Island, 02912
75. R. Dodds, 3140 Newmark Laboratory, 205 North Matthews, Urbana, Illinois 61801
76. R. Fields, National Inst. of Standards and Technology, Bldg. 223, B144, Gaithersburg,, Maryland 20899
77. W. L. Fourney, Department of Mechanical Engineering, University of Maryland, College Park, Maryland 20742
78. S. R. Martin, DOE-ORO, P. O. Box 2008, Oak Ridge, Tennessee 37831-6269
79. S. T. Rolfe, The University of Kansas, Lawrence, Kansas 66045-2235
80. A. R. Rosenfield, Battelle Columbus Division, Columbus, Ohio 43201
81. C. W. Schwartz, Department of Civil Engineering, University of Maryland, College Park, Maryland 20742
82. E. T. Wessel, 312 Wolverine, Lake Region Mobile Home Village, Haines City, Florida 33844
83. R. L. Tregoning, Code-614, Fatigue and Fracture Branch, NSWC-CD, 9500 McArthur Blvd., Bethesda, MD 20817
84. R. O. Hultgren, ORNL Site Manager, Office of Energy Research and Development, DOE–OR, P. O. Box 2008, Oak Ridge, TN 37831-6269

85-86. Office of Scientific and Technical Information, P. O. Box 62, Oak Ridge, Tennessee 37831

NRC FORM 335 (2-89) NRCM 1102, 3201, 3202

U.S. NUCLEAR REGULATORY COMMISSION

BIBLIOGRAPHIC DATA SHEET

(See instructions on the reverse)

1. REPORT NUMBER (Assigned by NRC, Add Vol., Supp., Rev., and Addendum Numbers, if any.)
NUREG/CR-6426
ORNL-6892
Vol. 1

2. TITLE AND SUBTITLE
Ductile Fracture Toughness of Modified A 302 Grade B Plate Materials, Data Analysis

3. DATE REPORT PUBLISHED
MONTH: January
YEAR: 1997

4. FIN OR GRANT NUMBER
B0119

5. AUTHOR(S)
D. E. McCabe, E. T. Manneschmidt, and R. L. Swain

6. TYPE OF REPORT

7. PERIOD COVERED *(Inclusive Dates)*

8. PERFORMING ORGANIZATION – NAME AND ADDRESS *(If NRC, provide Division, Office or Region, U.S. Nuclear Regulatory Commission, and mailing address; if contractor, provide name and mailing address.)*
Oak Ridge National Laboratory
Oak Ridge, Tennessee 37831-6285

9. SPONSORING ORGANIZATION – NAME AND ADDRESS *(If NRC, type "Same as above"; if contractor, provide NRC Division, Office or Region, U.S. Nuclear Regulatory Commission, and mailing address.)*
Division of Engineering Technology
Office of Nuclear Regulatory Research
U.S. Nuclear Regulatory Commission
Washington, DC 20555-0001

10. SUPPLEMENTARY NOTES
S. N. M. Malik, NRC Project Manager

11. ABSTRACT *(200 words or less)*

The objective of this work was to develop ductile fracture toughness data in the form of J-R surves for modified A 302 grade B plate materials typical of those used in fabricating reactor pressure vessels. A previous experimental study at Materials Engineering Associates, Lanham, Maryland, on one particular heat of A 302 grade B plate showed decreasing J-R curves with increased specimen thickness. This characteristic has not been observed in numerous tests made on the more recent production mterials of A 533 grade B and A 508 class 2 pressure vessel steels. It was unknown if the departure from norm for the MEA material was a gneric characteristic for all heats of A 302 grade B steels or just unique to that one particular plate.

12. KEY WORDS/DESCRIPTORS *(List words or phrases that will assist researchers in locating the report.)*
J-R Crack-Growth Resistance Curves
Ductile Fracture
A 302 Grade B Steel Plate
Reactor Pressure Vessel Steel
Charpy Low Upper Shelf Energy
ASTM E 813-87 and E 1152-89 Test Standards

13. AVAILABILITY STATEMENT
Unlimited

14. SECURITY CLASSIFICATION
(This Page)
Unclassified
(This Report)
Unclassified

15. NUMBER OF PAGES

16. PRICE